

**INVESTIGATION OF DIESEL STEAM
REFORMING OVER Ni BASED
CATALYSTS**

BY

MUHAMMAD NAEEM YOUNIS

A Thesis Presented to the
DEANSHIP OF GRADUATE STUDIES

KING FAHD UNIVERSITY OF PETROLEUM & MINERALS

DHAHRAN, SAUDI ARABIA

1963 1434

In Partial Fulfillment of the
Requirements for the Degree of

MASTER OF SCIENCE

In

CHEMICAL ENGINEERING

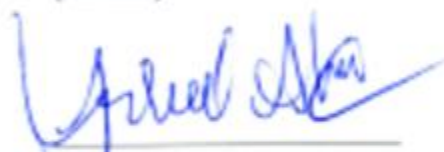
OCTOBER, 2014

KING FAHD UNIVERSITY OF PETROLEUM & MINERALS
DHAHRAN- 31261, SAUDI ARABIA
DEANSHIP OF GRADUATE STUDIES

This thesis, written by **Muhammad Naeem Younis** under the direction of his thesis advisor and approved by his thesis committee, has been presented and accepted by the Dean of Graduate Studies, in partial fulfillment of the requirements for the degree of **MASTER OF SCIENCE IN CHEMICAL ENGINEERING.**



Dr. Zuhair O. Malyabari
(Advisor)



Dr. Shakeel Ahmed
(Member)



Dr. Mohammed Saleh Ba-Shammakh
(Department Chairman)



Dr. Salam A. Zammo
(Dean of Graduate Studies)



Dr. Mohammad M. Hossain
(Member)

Date: 11/1/15



©MUHAMMAD NAEEM YOUNIS

2014

I dedicate my work to my parents and siblings.

ACKNOWLEDGMENTS

“In the name of Allah, The Most Merciful and The Most Gracious”

All praise and thanks to the Almighty, the Creator of all worlds for giving me the courage to accomplish this work sincerely and successfully. May there be every peace and blessings upon the holy prophet Muhammed (PBUH), his family and his companions.

I wish to express my appreciation to the Chemical Engineering Department of King Fahad University of Petroleum & Minerals, for providing me an opportunity to continue my study. I am also grateful to the Center for Refining and Petrochemical at KFUPM and Saudi Aramco for its support during this research. Also, I am grateful to all the faculty members, staff members and technicians of CRP for their support.

I would like to express my sincere gratitude to my thesis advisor Dr. Zuhair Omar Malaibari for his unlimited guidance, assistance and encouragement. I acknowledge the sincere efforts of Dr. Shakeel Ahmed, for teaching me the philosophy of research and providing me the understanding of catalyst and its working. My special thanks to Uwais Baduruthamal for technical support, all accessibility of labs. Special thanks to Ateeq ur Rahman for SEM, EDX and TEM analysis and evaluation. I must also extend my deep sense of gratitude to my other thesis committee member Dr. Mohammad Mozahar Hossain for his immense contribution and suggestions throughout the period of this work.

I would like to thank all of my colleagues, students and friends from the Chemical Engineering department and Center for Refining and Petrochemical for giving me remarkable company and for making my stay memorable. I am also grateful for support of Pakistani Community during my stay in KFUPM.

Finally, but very important, special thanks to my parents, brother and sisters for their encouragement, moral support, continuous prayers and enduring missing me among them.

TABLE OF CONTENTS

ACKNOWLEDGMENTS	v
TABLE OF CONTENTS	vi
LIST OF TABLES	x
LIST OF FIGURES	xii
LIST OF ABBREVIATIONS	xvi
ABSTRACT	xvii
ABSTRACT (ARABIC)	xviii
CHAPTER 1. INTRODUCTION	1
CHAPTER 2. LITERATURE REVIEW	8
2.1 Mechanism of liquid Hydrocarbon steam reforming	9
2.2 Categorization of various types of catalysts and Promoters used for DSR	11
2.2.1 DSR Based on Promoters for Active Metal	12
2.2.2 Effect of Active Metal Loading	13
2.2.3 Effect of the method of preparation of catalyst	15
2.2.4 Ni supported on some special Supports	19
2.2.5 Nobel Metal Catalyst	20
2.2.6 Catalyst summery	23

2.3	Catalyst Deactivation	24
2.3.1	Deactivation by Sintering and Sulfur	25
2.3.2	Deactivation by Coking.....	26
2.3.3	Kinetic study on catalyst deactivation.....	30
CHAPTER 3. RESEARCH OBJECTIVES		34
CHAPTER 4. EXPERIMENTAL SECTION.....		35
4.1	Materials	35
4.2	Catalyst Design and Synthesis.....	37
4.2.1	Synthesis of Ni Supported Catalysts	38
4.2.2	Synthesis of Ni based catalyst with different promoters.....	40
4.3	Evaluation of the Catalyst.....	43
4.3.1	Coke formation study on Ni-based catalyst	47
4.4	Characterization of the Catalyst.....	47
4.4.1	X-Ray Diffraction (XRD)	48
4.4.2	SEM and EDX.....	48
4.4.3	Thermo Gravimetric Analysis (TGA).....	49
4.4.4	Temperature Programmed Reduction (TPR)	49
4.4.5	Carbon, Hydrogen, Nitrogen Sulfur Analyzer (CHNS).....	50
4.4.6	Transmission Electron Microscopy (TEM).....	50

4.4.7	BET Surface Area and the Pore Volume.....	51
CHAPTER 5. RESULTS AND DISCUSSION.....		52
5.1	Physical Characterization.....	52
5.1.1	X-ray Diffraction Analysis (XRD).....	52
5.1.2	Scanning Electron Microscope (SEM)/ (EDX).....	59
5.1.3	N ₂ adsorption / desorption Isotherms Analysis	63
5.1.4	TPR of Promoted and non-Promoted Catalysts	67
5.1.5	Transmission Electron Microscopy (TEM).....	73
5.2	Performance Evaluation of Synthesized Catalysts	78
5.2.1	Blank Runs	83
5.2.2	Diesel Steam Reforming in a Gibbs free Reactor in Aspen HYSYS®.....	83
5.2.3	Diesel Steam Reforming over the non-promoted Ni/γAl ₂ O ₃ Catalyst	84
5.2.4	Diesel Steam Reforming over Lanthanide promoted Ni/γAl ₂ O ₃ Catalyst	86
5.2.5	Thermo Gravimetric Analysis (TGA).....	95
5.2.6	Effect of Temperature on Diesel Steam Reforming over 5%Pr-12%Ni/γAl ₂ O ₃ Catalyst.....	99
Chapter 6. CONCLUSION AND RECOMMENDATIONS.....		106
6.1	Conclusion	106
6.2	Recommendations.....	107

REFERENCES	108
Appendix A.....	117
Appendix B.....	128
VITAE	132

LIST OF TABLES

Table 1-1: Types of Fuel Cells [16]	7
Table 2-1: Formulation of different Ni supported catalysts [19]	14
Table 2-2 The comparison of fresh and used catalysts prepared by different methods [26].	17
Table 2-3: Ni particle diameters after TPR (temperature-programmed reduction) [27].	18
Table 2-4: Comparison of characterization results obtained before and after the reaction [23]	19
Table 2-5: Different Catalysts used for DSR and Respective Supports	23
Table 2-6: Carbon deposition rates for Commercial and promoted catalysts [22]	28
Table 2-7 The CO chemisorption capacity, n-dodecane conversion, turnover rates, and the amount of deposited carbon for La-Ni/ γ -Al ₂ O ₃ catalysts with different La content [35]	30
Table 4-1: Materials used for the synthesis of catalysts.	36
Table 4-2: Catalysts synthesized in this work and their compositions	37
Table 4-3: Reaction conditions for the diesel steam reforming experiments.	45
Table 5-1: Ni (111), Ni (200), Ni (220) phases in different promoted and non-promoted catalysts.	56
Table 5-2: XRD data analysis of promoted and non-promoted catalysts	58
Table 5-3: EDX analysis of Ni based catalysts and Ni based catalysts, impregnated with Lanthanide series.	62
Table 5-4: Surface properties of the Alumina, non-promoted and promoted catalysts.	66
Table 5-5: The average particle diameter of promoted and non-promoted catalysts obtained from TEM images.	74
Table 5-6: Boiling point distribution of Diesel used in Diesel Steam Reforming by SimDis GC-MS .	80
Table 5-7: Conversion and selectivity of 6%Ni/ γ Al ₂ O ₃ , 12%Ni/ γ Al ₂ O ₃ and 18%Ni/ γ Al ₂ O ₃ (Time = 10h, S/C = 3.0, GHSV = 5800 h ⁻¹ , pressure = 1bar, Temperature = 620 °C)	86
Table 5-8: Conversion and selectivity of 5%La-12%Ni/ γ Al ₂ O ₃ (Time = 40h, S/C = 3.0, GHSV = 5800 h ⁻¹ , pressure = 1atm, Temperature = 620 °C)	87

Table 5-9: Conversion and selectivity of 5%Ce-12%Ni/ γ Al ₂ O ₃ (Time = 40h, S/C = 3.0, GHSV = 5800 h ⁻¹ , pressure = 1atm, Temperature = 620 °C)	88
Table 5-10: Conversion and selectivity of 5%Eu-12%Ni/ γ Al ₂ O ₃ (Time = 40h, S/C = 3.0, GHSV = 5800 h ⁻¹ , pressure = 1atm, Temperature = 620 °C)	89
Table 5-11: Conversion and selectivity of 5% Pr-12%Ni/ γ Al ₂ O ₃ (Time = 40h, S/C = 3.0, GHSV = 5800 h ⁻¹ , pressure = 1atm, Temperature = 620 °C)	90
Table 5-12: Conversion and selectivity of 5% Gd-12%Ni/ γ Al ₂ O ₃ (Time = 40h, S/C = 3.0, GHSV = 5800 h ⁻¹ , pressure = 1atm, Temperature = 620 °C)	91
Table 5-13: Comparison of selectivities of different products over Lanthanide promoted bimetallic and non-promoted monometallic Ni-based catalysts at 620 °C, 1 atm, S/C = 3.0, GHSV of 5800 h ⁻¹ and sulfur in fuel = 6 ppm.	95
Table 5-14: %Weight loss results of all the spent catalysts from TGA.	98

LIST OF FIGURES

Figure 1-1: Visual representation of fuel cell system with: (a) Partial oxidation reformer (POX), (b) Steam Reformer (SR), and (c) Auto-thermal Reformer (ATR) [1]	3
Figure 1-2: The Working principle of a PEM fuel cell [13]	6
Figure 2-1: The effect of variation in temperature on H ₂ yields over La, Ce, Yb promoted and non-promoted Ni-based catalysts [22]	12
Figure 2-2: The effect on composition of product gas stream with change in metal loading and support in diesel steam reforming experiments (GHSV = 25,000 cm ³ g ⁻¹ h ⁻¹ , T = 700 °C) [20].....	15
Figure 2-3: Dispersion of active metal over the alumina support in catalysts prepared by coprecipitation and impregnation method [27].	16
Figure 2-4: The product gas composition at different temperatures during steam reforming of n-hexadecane at S/C = 3.0 [21].....	21
Figure 2-5: Conversion of n-hexadecane and %H ₂ Yield at different temperature at S/C ratio = 3.0 and no sulfur contents. [21]	22
Figure 2-6: Activity of Pd/Zr ₂ catalyst in terms of %H ₂ yield during steam reforming of n -hexadecane at T = 750 °C, S = 0ppm and S = 50ppm and S/C = 3. [21]	26
Figure 2-7: A conceptual model of fouling, crystallite encapsulation and pore plugging of a supported metal catalyst due to carbon deposition. [30].....	27
Figure 2-8: H ₂ yield as a function of TOS for steam reforming of n-dodecane on La-Ni/γ-Al ₂ O ₃ catalysts with different amounts of La (773 K, LHSV: 40ml ⁻¹ C ₁₂ H ₂₆ (l)g ⁻¹ h ⁻¹ (Low SV: 20 ml-C ₁₂ H ₂₆ (l)g ⁻¹ h ⁻¹), S/C=3.5, 101 kPa). [35]	29
Figure 2-9: First order kinetics of deactivation mechanism during the steam reforming of n-hexadecane at 750 °C and S/C=3 with no sulfur contents [21].	31
Figure 2-10: Summary of rate of reaction for n-hexadecane steam reforming over Pd/Zr ₂ O catalyst at different temperatures, S/C ratios and sulfur contents in fuel [21].....	32
Figure 2-11: Summary of rate of deactivation constants obtained from regression analysis of the results obtained from steam reforming of n-hexadecane over Pd/Zr ₂ O catalysts at different temperatures, S/C ratios and sulfur contents in fuel . [21].....	32

Figure 4-1: Procedure for impregnation of Ni on γ -Al ₂ O ₃ using the incipient wet impregnation method.....	39
Figure 4-2: Procedure for impregnation of Lanthanum (La), Cerium (Ce), Europium (Eu), Praseodymium (Pr) and Gadolinium (Gd) on γ -Al ₂ O ₃ using the incipient wet impregnation method.....	41
Figure 4-3: Procedure for impregnation of Ni on an already Lanthanide series promoted γ -Al ₂ O ₃ using the incipient wet impregnation method	42
Figure 4-4: Process Flow Diagram of The Testing Unit (Fixed bed reactor Unit).....	46
Figure 5-1: XRD pattern showing the (111), (200) and (220) reflections of Ni in alumina supported nickel catalysts.....	54
Figure 5-2 : XRD patterns of support, non-promoted and promoted prepared catalysts (a) γ -Al ₂ O ₃ support (b) 12% Ni/ γ -Al ₂ O ₃ (c) \blacklozenge La (012), (110), (300) (d) \blacklozenge Ce (111), (110), (311) (e) \blacktriangle Eu(1,0,1), (1,0,2), (2,0,1) (f) \bullet Pr (013) (200), (401) (g) \bullet Gd (002), (100), (114).....	57
Figure 5-3: EDX images of (A) 6% Ni/ γ -Al ₂ O ₃ (B) 12% Ni/ γ -Al ₂ O ₃ (C) 18% Ni/ γ -Al ₂ O ₃	60
Figure 5-4: EDX images of (A) 5%Ce-12% Ni/ γ -Al ₂ O ₃ (B)5%Eu-12% Ni/ γ -Al ₂ O ₃ (C) 5%Pr-12% Ni/ γ -Al ₂ O ₃ (D) 5%Gd-12% Ni/ γ -Al ₂ O ₃ (E) 5%La-12% Ni/ γ -Al ₂ O ₃	61
Figure 5-5: N ₂ adsorption-desorption isotherm of 12%Ni ₃ , 18%Ni, Ni-Ce, Ni-Eu, Ni-Pr and Ni-Gd and γ Al ₂ O ₃	65
Figure 5-6: BJH pore size distribution of 12%Ni, 18%Ni, Ni-Ce, Ni-Eu, Ni-Pr and Ni-Gd and γ Al ₂ O ₃	65
Figure 5-7: TPR profiles of 6%, 12% and 18% nickel impregnated over alumina support.	69
Figure 5-8: TPR profiles of non-promoted and promoted catalysts of La-Ni, Ce-Ni, Eu-Ni, Pr-Ni and Gd-Ni.	72
Figure 5-9: TEM image of non-promoted 12%Ni/ γ -Al ₂ O ₃ catalyst sample.....	75
Figure 5-10: TEM image of La-Ni catalyst sample	75
Figure 5-11: TEM image of Ce-Ni catalyst for DSR.....	76
Figure 5-12: TEM image of Eu-Ni catalyst sample.....	76
Figure 5-13: TEM image of Pr-Ni catalyst sample.....	77
Figure 5-14: TEM image of Gd-Ni catalyst sample	77

Figure 5-15: SimDis GC-MS results of Diesel used in Diesel Steam Reforming.....	79
Figure 5-16: Diesel steam reforming, the effect of temperature on an equilibrium product composition at, S/C = 3.0, P = 1 atm.	84
Figure 5-17: Diesel Steam reforming on the surface of Ni/Al ₂ O ₃ catalyst with different Ni metal loading of 6% to 18% in 10 hours; at 620 °C, 1 atm, S/C = 3.0, GHSV of 5800 h ⁻¹ and sulfur in fuel = 6 ppm.	85
Figure 5-18: Conversion of Diesel during a 40h run over Lanthanide promoted bimetallic and non-promoted monometallic Ni-based catalysts at 620 °C, 1 atm, S/C = 3.0, GHSV of 5800 h ⁻¹ and sulfur in fuel = 6 ppm	92
Figure 5-19: % Yield of H ₂ during a 40h run over Lanthanide promoted bimetallic and non-promoted monometallic Ni-based catalysts at 620 °C, 1 atm, S/C = 3.0, GHSV of 5800 h ⁻¹ and sulfur in fuel =6 ppm.....	94
Figure 5-20: Reforming efficiency during a 40h run over Lanthanide promoted bimetallic Ni-based catalysts at 620 °C, 1 atm, S/C = 3.0, GHSV of 5800 h ⁻¹ and sulfur in fuel = 6 ppm.	94
Figure 5-21: TGA results of non-promoted and promoted catalysts. Zone 1 represents gasification of polymerized carbon, zone 2 represents weight loss due to carbon whiskers and the zone 3 represents weight loss due to gasification of encapsulated carbon.	97
Figure 5-22: CHNS results of Coke formed (%) on non-promoted and promoted catalysts.	98
Figure 5-23: The effect of temperature on conversion of Diesel during a 40h run over Pr-Ni bimetallic and non-promoted monometallic Ni-based catalysts at 1 atm, S/C = 3.0, GHSV of 5800 h ⁻¹ and sulfur in fuel = 6 ppm.....	100
Figure 5-24: The effect of temperature on the reforming efficiency of Diesel during a 40h run over Pr-Ni bimetallic Ni-based catalysts at 1 atm, S/C = 3.0, GHSV of 5800 h ⁻¹ and sulfur in fuel = 6 ppm.....	101
Figure 5-25: The effect of temperature on the % Yield of H ₂ during a 40h run over Pr-Ni bimetallic and non-promoted monometallic Ni-based catalysts at 620 °C, 1 atm, S/C = 3.0, GHSV of 5800 h ⁻¹ and sulfur in fuel = 6 ppm	101
Figure 5-26: The effect of temperature on conversion of Diesel and water, selectivity of H ₂ , CO, CO ₂ and CH ₄ after 10h of reaction, over Pr-Ni catalysts at 1 atm, S/C = 3.0, GHSV of 5800 h ⁻¹ and sulfur in fuel = 6 ppm	102
Figure 5-27: Comparison of the %H ₂ Yield at three different temperatures for data obtained at equilibrium conversion with results from Pr-Ni catalyst, at 1 atm and S/C = 3.0.....	102

Figure 5-28: TGA results of Pr-Ni catalyst (the effect of temperature on coke formation).....	104
Figure 5-29: CHNS results of Pr-Ni catalyst (the effect of temperature on coke formation).....	105

LIST OF ABBREVIATIONS

Ni	Nickel	MCFC	Molten Carbonate Fuel Cell
La	Lanthanum	Ce	Cerium
BET	Brunauer–Emmett–Teller	Eu	Europium
BJH	Barrett-Joyner-Halenda	Pr	Praseodymium
TPR	Temperature Programmed Reduction	Gd	Gadolinium
CHNS	Carbon Hydrogen Nitrogen Sulfur	γ -Al ₂ O ₃	Gamma Alumina
DSR	Diesel Steam Reforming	PEM	Proton Exchange Membrane
FBR	Fixed Bed Reactor	GHSV	Gas Hourly Space Velocity
TGA	Thermo Gravimetric Analysis	SEM	Scanning Electron Microscopy
XRD	X-ray Diffraction	SOFC	Solid Oxide Fuel Cells
EDX	Energy Dispersive X-ray Spectroscopy	TEM	Transmission Electron Microscopy

ABSTRACT

Full Name : Muhammad Naeem Younis

Thesis Title : Investigation of Diesel Steam Reforming over Ni Based Catalysts.

Major Field : Chemical Engineering

Date of Degree : October 2014

In this thesis, an investigation of the diesel steam reforming over Ni based catalyst was carried out. The lanthanide series (La, Ce, Eu, Pr and Gd) promoted Ni/ γ -Al₂O₃ catalysts were prepared by wetness incipient impregnation method. Catalyst activity and coke formation resistance of monometallic and bimetallic lanthanide promoted prepared catalysts were investigated for diesel steam reforming.

TEM, XRD, SEM, EDX and N₂ adsorption/desorption isotherms were used to characterize the physico-chemical properties of all the prepared catalysts. TEM analyses show that lanthanide promoted catalysts exhibited uniform metal dispersion. Performance evaluation of all promoted and non-promoted catalysts were conducted in a Fixed Bed Reactor system for 40 h.

The praseodymium promoted catalyst showed the highest activity and carbon formation resistance among all other prepared catalysts. Pr-Ni/Al₂O₃ catalyst was further evaluated at three different temperatures, the highest conversion was achieved at 600°C. TPR suggested a better interaction of metal and support in Pr-Ni/Al₂O₃ catalyst. TGA and CHNS analysis of spent catalyst showed the capability of each promoter to resist the coke formation.

ملخص الرسالة

الاسم الكامل: محمد نعيم يونس

عنوان الرسالة: التحقيق في تحول بخار الديزل على المحفزات المبنية على النيكل.

التخصص: الهندسة الكيميائية

تاريخ الدرجة العلمية: أكتوبر 2014

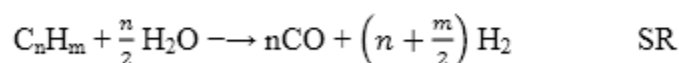
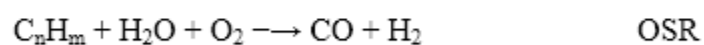
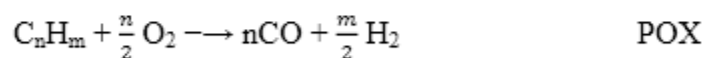
في هذه الأطروحة، أُجري التحقيق على إصلاح بخار الديزل على محفز النيكل. تم تحضير سلسلة العوامل الحفازة $Ni/\gamma-Al_2O_3$ المحسنة بمركبات اللانثانيدات (La, Ce, Eu, Pr and Gd) بطريقة التحميل التسريبي. تعزيز النشاط المحفز ومقاومة تشكيل فحم الكوك للعوامل الحفازة المجففة تمت دراستها و التحقق منها.

استخدمت طرق TEM، XRD، SEM، EDX وامتزاز N_2 لتوصيف الخصائص الفيزيائية والكيميائية لجميع المحفزات المعدة. تحليل TEM أظهر أن يحل تبين أن تعزيز المحفزات بواسطة اللانثانيدات ساهم في الحصول على تشبنت موحد للمعادن. وأجري تقييم أداء جميع المحفزات وغير المعززة في نظام مفاعل ثابت لمدة 40 ساعة. أظهر المحفز المعزز بربراسيوديميوم نشاط حفزي و أعلى مقاومة لتشكيل الكربون بين جميع المحفزات المعدة الأخرى. تم تقييم العامل الحفاز Pr-Ni مرة أخرى في ثلاث درجات حرارة مختلفة؛ وقد تحقق أعلى تحويل في درجة حرارة 600 مئوية. أظهر TPR وجود تداخل أفضل بين المعدن والداعم في حالة العامل الحفاز Pr-Ni. أظهر تحليل TGA و CHNS للمواد الحفازة المستهلكة قدرة المعززات لمقاومة تشكيل فحم الكوك

CHAPTER 1

INTRODUCTION

Interest in clean, a versatile environmental friendly and reliable source of fuel is growing. Conversion of conventionally available fossil fuel (especially liquid hydrocarbon) into hydrogen using steam reforming is the topic of interest. Solid oxide fuel cells, which can operate with mixtures of H₂ and CO, are more appropriate for the steam reforming product of both fossil and biodegradable fuel sources as compare to proton exchange membrane (PEM) fuel cells. Similarly, use of synthetic diesel is a compelling opportunity. There are three modes of catalytic reforming of hydrocarbons namely as: partial oxidation (POX), steam reforming (SR), and Auto thermal steam reforming or oxidative steam reforming (OSR). Above mentioned types of reactions comprises partial or full oxidation of hydrocarbon fuels to produce a hydrogen-rich mixture of gases or synthesis gas [1]. These are the types of reactions as shown below:



POX: In this configuration, fuel or hydrocarbon reacts with a calculated amount of oxygen to produce a mixture of carbon monoxide and hydrogen.

OSR: In this type of reaction, yield of hydrogen is amplified to maximum by adding water. Addition of water also reduces chances of catalyst deactivation. However water is optional in this case representing one design option. In this system excess steam can be further condensed and recycled using a separate gas cleanup setup that further boosts the overall thermodynamic efficiency of the system.

ATR is a special case of OSR, its reaction involves steam, air (or O_2) and fuel and it works in such a way that the net heat of reaction is zero. It is also called the combination of POX and SR [1].

In catalytic steam reforming oxygen in water reacts with hydrocarbon to produce a mixture of hydrogen and carbon monoxide as shown in Figure 1-1. The reaction is carried out in the absence of oxygen or inert environment. This reaction is highly endothermic as lots of energy is required to break water molecules hence need an external heat source. The amount of energy required to carry out this endothermic reaction is generally on the order of 22% of LHC (lower heat of combustion) of fuel [2].

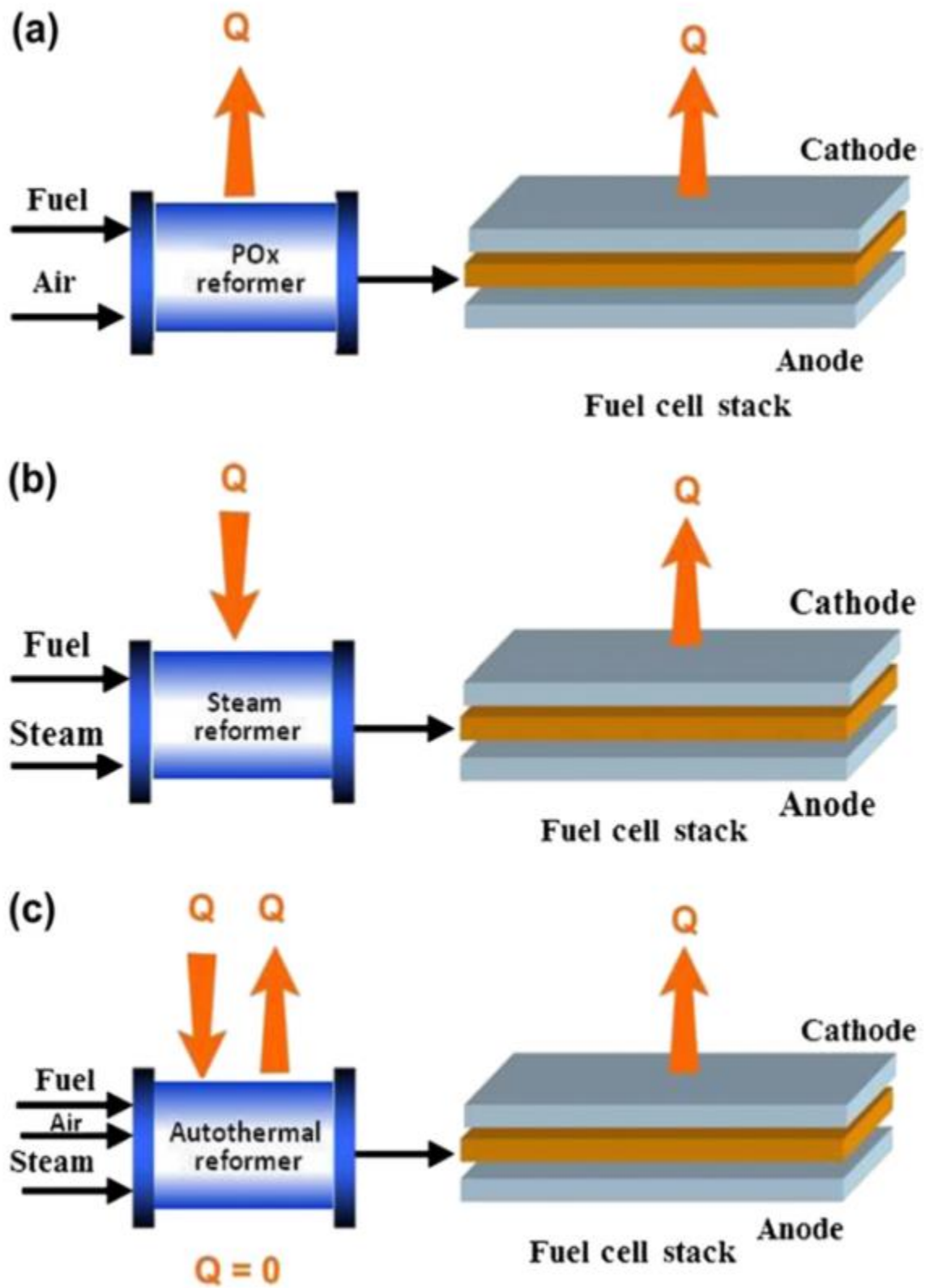


Figure 1-1: Visual representation of fuel cell system with: (a) Partial oxidation reformer (POX), (b) Steam Reformer (SR), and (c) Auto-thermal Reformer (ATR) [1]

These reactions shown contain H_2 and CO as the products, However CO_2 and water are essential part of the product gas, but are not shown here for the sake of simplicity. Hydrogen is main fuel for the fuel cells, however in some types of fuel cells mixture of both CO and H_2 are also used [3]. In the OSR reaction type, it is not possible to balance the stoichiometry of reaction equation; however in ATR the stoichiometric equation is balanced and net heat of reaction is zero [1].

Type of reaction not only effects the overall efficiency of the whole system as presented in Figure 1-1 but it also change the operating conditions of a fuel cell system. In each of the system presented, either catalytic or non-catalytic thermal reactions are going on. Temperatures for catalytic system ranges $600\text{ }^\circ\text{C}$ to $1000\text{ }^\circ\text{C}$, depending on type of fuel, method of reforming, and catalyst type [2]. Most of the non-catalytic reactions work at higher temperatures and results into coke formation or unwanted oxides of nitrogen. [4] Non-catalytic reformers are not widely used because they requisite more costly materials of construction, and result in to lower system efficiency due to the larger temperature difference between the fuel cell and reformer.

One of the most critical challenges facing the world is the development of clean, reliable, and efficient energy conversion processes. Hydrogen is a clean, efficient and versatile energy carrier for the future, it is ideal fuel for fuel cells and power generation units [5] [6] [7]. The growing world needs environmental friendly energy source to fulfill its energy demands. Several renewable and biodegradable technologies are available to fulfill this challenge such as wind, solar, hydroelectric, photovoltaic, and others. In comparison to other available eco-friendly technologies the most propitious are those based on fuel cells. Fuel cells are one of the best techniques to convert chemical energy

into electrical energy with higher efficiencies and less environmental hazards. Economics of fuel cell systems are mostly studied for various applications and these cells could be useful to fulfill energy demands for both stationary (central and remote area power stations) and mobile units (transportation system) [8] [9].

Combustion of fossil fuels like petroleum, coal, and natural gas are currently fulfilling most of the world's energy demand. . Combustion of fossil fuels emits greenhouse gases which led to the drastic climatic change [10]. As a consequence of tremendous increase in energy demand of world, fossil fuels are being consumed at a brisk pace. This has led to the uncertainty about their long term availability so the renewable sources are increasingly seen as a viable option. Solar and wind are proposed to be the most important form of renewable energy sources. They are intermittent in nature so they are required to be stored for perpetual use. One of many most elegant ways to store energy is to produce hydrogen or other materials using solar or wind energy and harness their chemical energy using fuel cell to produce green electrical energy [11]. Fuel cells are the devices which convert chemical energy stored in fuels (hydrogen and other small chain organic molecules) into electrical energy [12]. Figure 1-2 shows the schematics of a generic PEM Fuel cell [13]. Therefore, Fuel cells are promising and convenient energy source.

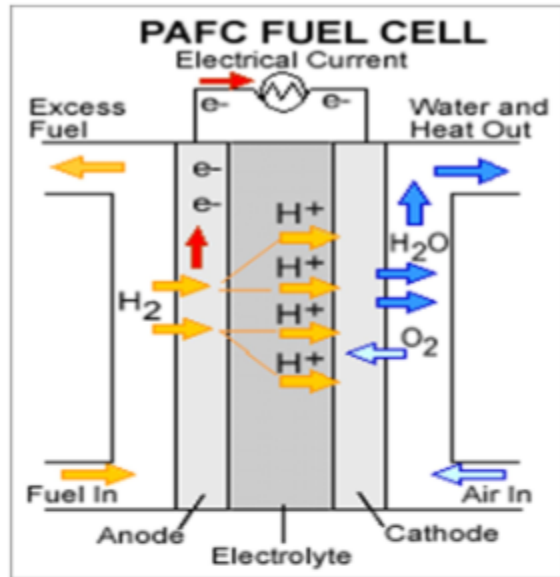


Figure 1-2: The Working principle of a PEM fuel cell [13]

There are different types of fuel cells available as shown in Figure 1-2 [14]. Out of them, the polymer electrolyte membrane (PEM) is the most promising especially for the power generation, for portable applications. Different types of feed can be used in the anode side of the PEM fuel cell. Apart from hydrogen, methanol and ethanol; formic acid has been explored with success. PEMFCs using formic acid as anode feed are called the direct formic acid fuel cells (DFAFCs) [15]. According to available literature, there are different types of fuel cells as mentioned in the Table 1-1 [16].

Table 1-1: Types of Fuel Cells [16]

Fuel Cell Class	Operating Temp.	Mobile ion	Dynamics	Tolerance to Poison			Cost	Power density
				CO	CO ₂	S		
Alkaline (AFC)	60-120 °C	OH ⁻	High	Low	Low	Low	Med.	Med.
Molten Carbonate (MCFC)	600-1000 °C	CO ₃ ²⁻	Low	Med.	High	High	Med.	Low
Polymer Electrolyte (PEFC)	50-100 °C	H ⁺	High	Low	High	Low	High	High
HT-Polymer Electrolyte (HT-PEFC)	150-200 °C	H ⁺	High	High	High	Med.	High	High
Phosphoric Acid (PAFC)	175-220 °C	H ⁺	Med.	Med.	High	High	High	Med.
Solid Oxide (SOFC)	600-1000 °C	O ²⁻	Low	High	High	Med.	Med.	High

CHAPTER 2

LITERATURE REVIEW

The classical hydrogen fuel cell suffers from several drawbacks. First and foremost being safety. Hydrogen as fuel has highest energy contents in comparison of other conventional energy sources; hence its safety is an important issue in the development of this technology and according to some authors there is a possibility for a large scale incident [17]. Consequently, two major problems related to use of hydrogen as a fuel are observed, first is its storage and second is its transportation.

Hydrogen is not naturally available fuel source, so it must be extracted from other compounds using certain technology which itself requires energy. Hydrogen mostly comes from reforming of methane. This process in addition requires energy which comes from burning of the fossil fuels. Cost of hydrogen production could be minimized if the energy required for this process comes from renewable sources, and if the conversion of fuel is very high. This would require energy stations that would have to power the extraction process without using more energy resources than are being produced and catalysts that could convert maximum fuel into products. First issue can be done by using natural energy sources in key areas [18], however, catalyst which provide maximum conversion needs extensive research.

2.1 Mechanism of liquid Hydrocarbon steam reforming

PEM fuel cells required pure hydrogen source, however Solid oxide fuel cells (SOFCs) can work at sever conditions. SOFC's could be useful in case of IC (internal combustion) engines; hence would not only decrease the fuel demand but also reduce the greenhouse gas emissions. Feed of SOFC comprised of a gaseous mixture of H₂ and CO [19]. Steam reforming of hydrocarbon fuels especially diesel to produce such mixtures has considerable advantages:

- (1) Direct hydrogen is not required.
- (2) Selection of diesel fuel came from the fact that its volume density is high.
- (3) The Availability of diesel is not an issue as its distribution infrastructure already exists.

As described earlier there are three methods to produce hydrogen from diesel:

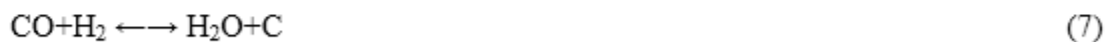
- (1) Steam reforming (SR) (Eq. (1))
- (2) Catalytic partial oxidation
- (3) Auto thermal reforming.

Steam reforming is a well-established and cost effective industrial method to produce hydrogen [20] [21]. Steam reforming could double the energy efficiency then that of conventional methods by increasing volumetric density of hydrogen in the product stream

[22]. Steam reforming of liquid hydrocarbons is a chemical reaction taking place between steam and liquid fuel i.e. Diesel at an elevated temperature. This is basically a reversible process that forms products such as hydrogen, carbon dioxide, water and carbon mono oxide as an intermediate product but due to incompleteness of a sub reaction carbon mono oxide is usually observed in the products as well. The chemical equations defining the reaction are as given below [23]



Most of the coke formed due to following reactions. (Equations 5–7)



Carbon deposition reactions (reactions from 5 to 7) should be stopped to prevent heavy carbon deposition that cause the pressure drop in the system and is also a major cause of catalyst deactivation.

2.2 Categorization of various types of catalysts and Promoters used for

DSR

Diesel steam reforming is an endothermic reaction and requires very high activation energy that's why different catalysts are used to overcome this barrier earlier and easily. There are a large number of catalysts used for steam reforming and can be found easily in literature available. As here the aim is to categorize these catalysts. So, in the following section few properties of the catalysts will be highlighted upon which we can categorize these catalysts.

DSR Based on active metal

When we search into literature, we will come about a catalyst that had basically two types of active metals.

- Ni based catalyst
- Noble metals based catalyst

One type that had nickel (Ni) as their active metal is used commercially and a lot of research had been carried out for Ni based catalyst and they can give a reasonable production under specific condition. Moreover they are easily available and cost effective. On the other hand the catalysts bearing noble metals as their active metals can give higher production than the nickel catalyst especially at the low temperature which is the focal point of the current research agenda in the energy sector. But the catalyst

containing noble metals are expensive and a lot of extensive work is required to commercialize these catalysts [3].

Normally nickel, based catalysts being used are NiAl_2O_4 , $\text{Ni-Al}_2\text{O}_3$, NiZrO_2 and NiSiO_2 etc.

2.2.1 DSR Based on Promoters for Active Metal

Promoters are basically used to enhance the interaction of support and active metal. Rare-earth such as La, Ce, Yb etc. promoted $\text{Ni}/\gamma\text{-Al}_2\text{O}_3$ catalysts [24] and Co, La, Mn promoted $\text{Rh}/\text{CeO}_2\text{-ZrO}_2$ catalysts have [25] been used so far for reforming of diesel or diesel surrogates. Yb-Ni catalyst presented a high hydrogen yield at the temperature range of 650 to 700°C when, tested for various reaction conditions with other promoted catalysts [22].

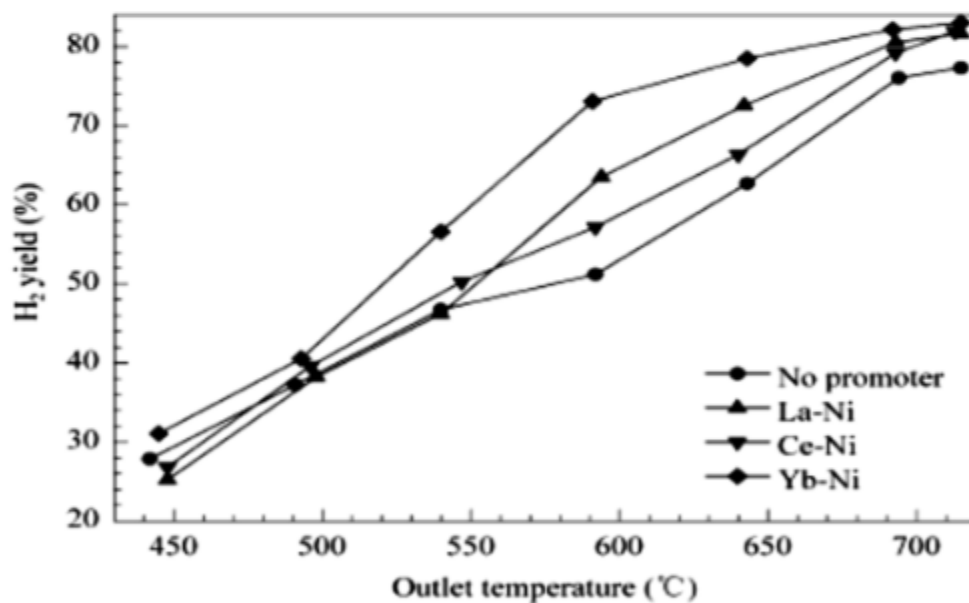


Figure 2-1: The effect of variation in temperature on H_2 yields over La, Ce, Yb promoted and non-promoted Ni-based catalysts [22]

Figure 2-1 shows the effect of variation in temperature when different promoted and non-promoted Ni-based catalysts were tested. When steam reforming was performed at lower temperature ($<500\text{ }^{\circ}\text{C}$), no significant difference in the hydrogen yield of La, Ce and Yb promoted and non-promoted catalysts were observed. Yb promoted catalysts was reported with extraordinary results at high temperatures. Rare earth promoted catalysts not only increase the conversion and hydrogen yield but also increases life of catalyst by increasing its resistance against carbon formation, however there were still significant differences among promoted catalysts. [22].

2.2.2 Effect of Active Metal Loading

It's a well-established fact that a catalyst takes part chemically in the reaction but at the end it separates as it was originally. So the rate of reaction does depend on the available surface area of the active metal for the reaction. The surface area of active metal could be increased by increasing the percentage weight of the active metal. Similarly, the surface area could increase the productivity but only up to a certain extent. Most of the authors related this fact to the mass transfer limitations on the catalyst surface [25]. The effect of variation in percentage weight of Ni metal over ZrO_2 support has been discussed and Ni loading of 2.5%, 5%, and 10%, studied. An $\text{Al}_2\text{O}_3/\text{YSZ}$ -supported NiAl_2O_4 catalyst was tested efficiently for diesel steam reforming. When diesel steam reforming of Ni-spinal catalyst was performed for 15 hours at high GHSV, no deactivation or coke formation was observed, however a Ni based catalyst under similar conditions was reported with deactivation because of severe whisker carbon formation. The variation in quantity of nickel metal affects the overall conversion and hydrogen yield. It was concluded that no significant effect of YSZ presence on conversion was observed and conversion with

catalyst containing >2% Ni was very low [19]. Although NiAl₂O₄ supported on Al₂O₃-YSZ support, prepared by wet-impregnation method, presented good resistance towards carbon formation, even at low steam to carbon ratios (S/C), but still the phenomenon behind to understand the interactions between the active metal and support is unknown [26].

Table 2-1: Formulation of different Ni supported catalysts [19]

Catalyst	Ni content and form	Alumina type	Zirconia type	Calculated ratio Ni/Al ₂ O ₃ (%)
05SpAlYSZ	5%–Spinel from (NiAl ₂ O ₄)	γ-Amorphous, 40 μm	ZrO ₂ -Y ₂ O ₃ (7%); <20	10.53
05SpAl	5%–Spinel from (NiAl ₂ O ₄)	γ-Amorphous, 40 μm	No	5.26
10SpAl	10%–Spinel from (NiAl ₂ O ₄)	γ-Amorphous, 40 μm	No	11.1
2.5SpAl	2.5%–Spinel from (NiAl ₂ O ₄)	γ-Amorphous, 40 μm	No	2.56
05MeAlYSZ	5%– Metallic Ni	α, 1 μm	ZrO ₂ -Y ₂ O ₃ (7%); <20	10.53

Graphical representation of Ni metal loading in terms of conversion for a specific set of conditions is shown in Figure 2-2.

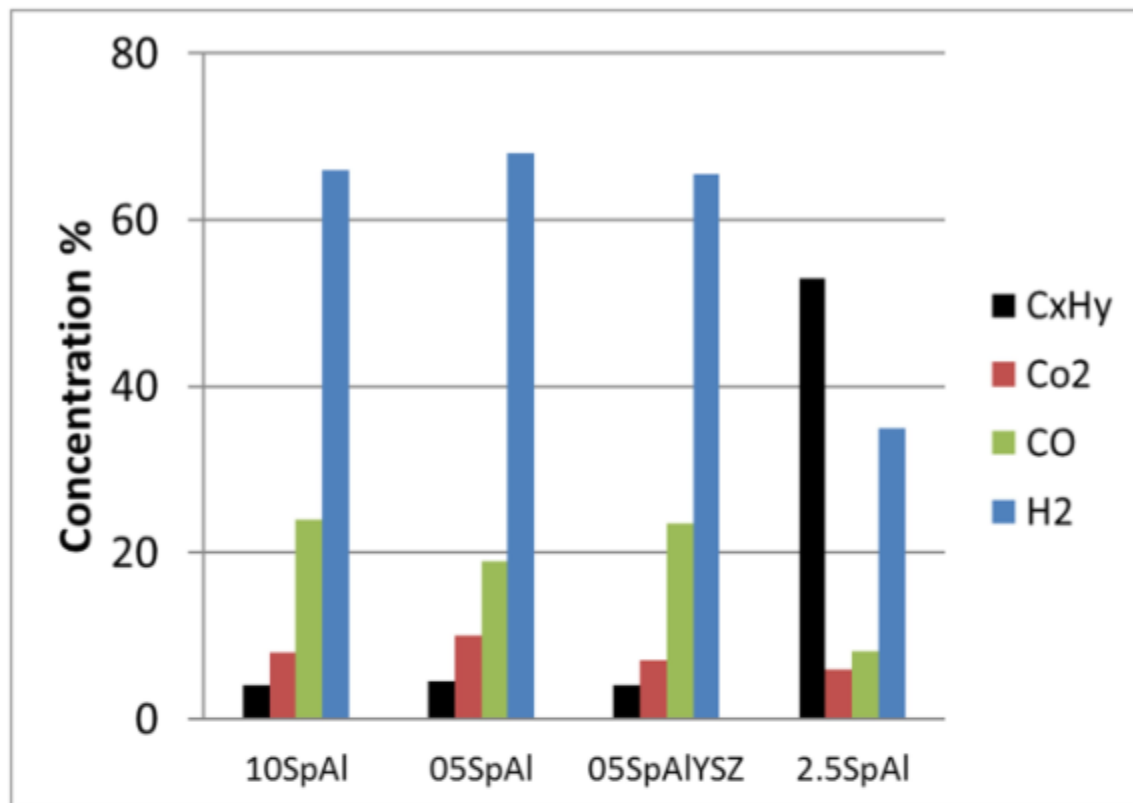


Figure 2-2: The effect on composition of product gas stream with change in metal loading and support in diesel steam reforming experiments (GHSV = 25,000 cm³ g⁻¹ h⁻¹, T = 700 °C) [20]

2.2.3 Effect of the method of preparation of catalyst

Catalyst could be prepared by any of these; impregnation method or Co-precipitation method. In former catalyst pellets are continuously dipped into a solution containing active metals and in later catalytic agent precipitates along with the base metal from a solution in which catalytic agent is soluble under normal conditions. It was seen that same catalyst prepared with different methods gives different results.

Diesel steam reforming experiments performed separately on Ni–Al spinel catalysts prepared by co-precipitation and wet impregnation method resulted into different catalyst stability times and product compositions. These experiments were performed in a fixed-

bed reactor setup, at 760 °C and conditions were kept constant for both catalysts [3]. The catalyst produced by the co-precipitation method (Copr) experienced rapid deactivation due to coke formation and the amount of methane formed was five times the amount formed from the catalyst prepared by the wet impregnation method (Impr). Similarly the hydrogen production was very low in case of Copr-catalyst (co-precipitation method). The Impregnated catalyst was evaluated for 12 hours and no signs of carbon formation or loss in catalyst activity were observed. The major dissimilarity between both catalysts was Ni-aluminates dispersion. Figure 2-3 shows the effect on dispersion induced by the preparation method. In the catalyst prepared by the Impr method (impregnation method), more active metal surface area is available and that was confirmed by characterization performed before and after steam reforming tests, using X-ray diffraction, scanning electron microscopy, and temperature programmed reduction [26].

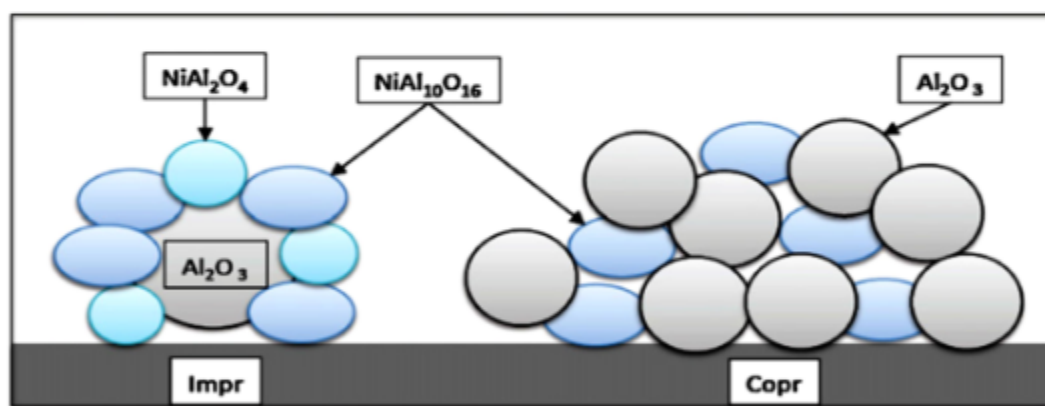


Figure 2-3: Dispersion of active metal over the alumina support in catalysts prepared by coprecipitation and impregnation method [27].

Table 2-2 The comparison of fresh and used catalysts prepared by different methods [26].

Catalyst	F-Impr	F-Copr	U-Impr	U-Copr
XRD	NiAl ₁₀ O ₁₆ ; NiAl ₂ O ₄	NiAl ₁₀ O ₁₆	Ni; NiAl ₁₀ O ₁₆ ; NiAl ₂ O ₄	Ni; NiAl ₁₀ O ₁₆
	γ-Al ₂ O ₃ ;κ-Al ₂ O ₃	γ-Al ₂ O ₃	γ-Al ₂ O ₃ ; κ-Al ₂ O ₃	γ-Al ₂ O ₃ .
SEM/EDXS	Aluminate phase	NiAl ₁₀ O ₁₆ particles	Unchanged surface. No carbon detected	Rough surface
	identification; phase homogeneously distributed at the surface.	obvious.		Carbon deposition (CNF)
BET	79 m ² g ⁻¹	134 m ² g ⁻¹	--	--
Reforming	Stable activity for 12 h.	Unstable activity: Deactivated in 7h.	--	--
SD	Homogeneous around 80 m	Large distribution: 10–800 m	--	--
TGA	--	--	Mass loss at 600 °C: CNFOxidation	No significant mass loss at 600 °C

Table 2-2 shows the comparison of results obtained from different characterization techniques for catalysts prepared by both impregnation and co-precipitation methods before and after steam reforming. The metastable 'NiAl₁₀O₁₆' phase is present in both catalysts supported on alumina. The reason of better activity and resistance towards carbon formation is due to growth of a second active spinel 'NiAl₂O₄' phase in catalyst prepared by impregnation method. Though the co-precipitation method resulted in to more surface area than Impr method catalyst but surface area is not always the reason of better activity and stability. [26]

In another study (Guohui Li et. al.) three Ni–Al₂O₃ catalysts were prepared with varying nickel metal loading (10-13%) on alumina support with different preparation methods. Alumina support used for this study was either commercial or prepared by sol-gel method and preparation methods used were co-precipitation and impregnation methods to synthesize Ni–Al co-precip, Ni/sol–gel Al₂O₃ and Ni/ γ -Al₂O catalysts. The catalyst characterization showed that Ni-particles size, its reduction kinetics and surface area depends on the preparation method. NiAl₂O₄ species were present in all prepared catalysts, however NiO phase was only found in Ni/ γ -Al₂O₃ catalyst. TPR of both catalysts revealed that reduction of Ni/ γ -Al₂O₃ catalyst was the easiest compared to other catalysts. XRD and TEM were used to find the Ni metal particle sizes and dispersion of metal in all the prepared catalysts. It was concluded that formation NiAl₂O₄ spinel phase during calcination increased the Ni dispersion, Ni metal particle size and available active sites in the reduced catalyst. However increase in calcination temperature reduced the surface area of all the prepared catalysts [27].

Table 2-3: Ni particle diameters after TPR (temperature-programmed reduction) [27].

Ni particle diameter (nm)	After TSR*			After TPR
	XRD	TEM	H ₂ uptake	XRD
Ni–Al co-precip	11	10	16	15
Ni/sol–gel Al ₂ O ₃	12	10–20	17	15
Ni/ γ -Al ₂ O ₃	15	30	40	15

* Temperature Staged Reduction

2.2.4 Ni supported on some special Supports

There are a lot of different supports in literature that had been tested and most of them had given satisfactorily results. Following is the testing of diesel steam reforming results of Ni supported on Rh-Ni/MgAl. The temperature range was also relatively low for this testing and ranging from 700°C to 950°C. The results are shown in Table 2-4 for the S/C ratio of 3.0 and atmospheric pressure.

Table 2-4: Comparison of characterization results obtained before and after the reaction [23]

Catalyst ^a	BET (m ² /g) ^b		Before the reaction		
			Dispersion (%) ^c		Active metal particle
	Before	After	Ni	Ni + Rh	size (nm) ^c
spc-Ni/MgAl	197.7	42.3	7.12	–	6.33
Rh-Ni/MgAl-A	105.4	–	–	12.16	8.34
Rh-Ni/MgAl-B	107	–	–	13.53	7.5
Rh-Ni/MgAl-C	106.2	–	–	13.8	7.37

Catalyst ^a	BET (m ² /g) ^b		After the reaction ^b		
			Dispersion (%) ^c		Active metal particle size (nm) ^c
	Before	After	Ni	Ni + Rh	
spc-Ni/MgAl	197.7%	42.3	0.25		401.73
Rh-Ni/MgAl-A	105.4	–	–	1.04*	93.23*
				1.54	66.03
Rh-Ni/MgAl-B	107.0	–	–	2.75	36.89
Rh-Ni/MgAl-C	106.2	–	–	3.13	32.41 [†]

2.2.5 Nobel Metal Catalyst

Noble metals such as Pt, Ir, Pd, Rh and Ru are also used for steam reforming and showed very good stability and coke formation resistance [28]. The performance evaluation of Pd.ZrO₂ catalyst (coated on a metal foil) was investigated in a tubular reactor for the steam reforming of n-hexadecane at various temperatures (T), steam to carbon ratios (S/C), and sulfur content (S) of the fuel. A reduction in hydrogen yield was observed with time on stream (TOS), which suggest catalyst deactivation and coke formation [21].

Catalyst testing was performed between the temperature ranges of 600 to 900 °C to determine the effect of temperature on product yield and results are shown in Figure 2-4. Maximum conversion during the steam reforming of n-hexadecane was observed at 750°C; however, hydrogen yield was found highest at 900°C. It was observed that the formation of C1+ (ethane, ethane, propane, propene etc.) gases were maximum at 700°C

a) Catalyst was tested for steam reforming of n-hexadecane at 950 °C and GHSV = 10,000 h⁻¹.

resulted into minimum hydrogen yield. Conversion of n-hexadecane was observed higher at high temperatures because of higher activity of the catalyst. Conversion between 750 and 900 °C, was approximately 80%, but hydrogen yield increased enormously as shown in Figure 2-4 and Figure 2-5 [21].

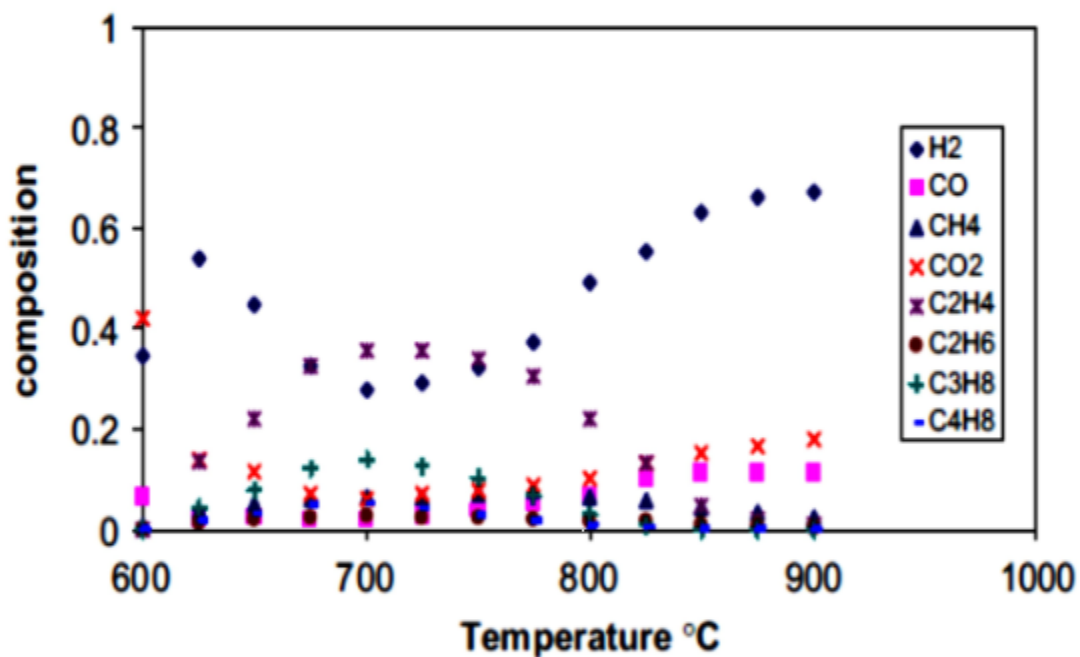


Figure 2-4: The product gas composition at different temperatures during steam reforming of n-hexadecane at S/C = 3.0 [21]

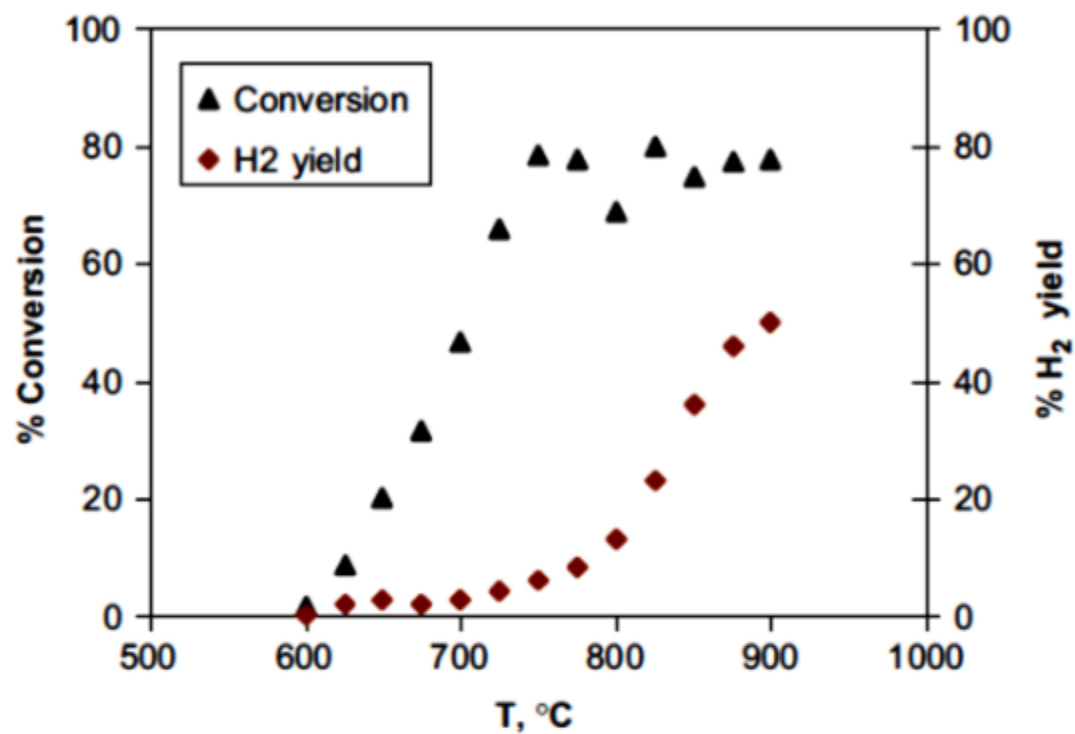


Figure 2-5: Conversion of n-hexadecane and %H₂ Yield at different temperature at S/C ratio = 3.0 and no sulfur contents. [21]

2.2.6 Catalyst summery

Brief summary of the different catalyst reported in literature along with their respective supports and conversions are tabulated in Table 2-5.

Table 2-5: Different Catalysts used for DSR and Respective Supports

Author	Feed	Catalyst	Temp	S/C	Conv
			(°C)		(%)
Clémence et al. (2011)	n-hexadecane	Ni/Zr+Y	695	1.9	80
		/ γ -Al ₂ O ₃			
Achouri et al. (2012)	Diesel/Biodiesel	Ni	760	1.9	Unstable (Copr)
		/ γ -Al ₂ O ₃			
	Diesel/Biodiesel	Ni	760	1.9	Stable (Impr)
		/ γ -Al ₂ O ₃			
Goud et al. (2007)	n-hexadecane	Pd	600-900	3	80
		/ZrO ₂			
Lihao et al. (2011)	n-hexadecane	Yb-Ni	645	3	95
		Ce-Ni			93
		La-Ni			87
		/ γ -Al ₂ O ₃			
Lakhaptri et al. (2009)	n-hexadecane	Rh-Ni/ γ -Al ₂ O ₃	800	3	NR
Kim et al.	n-hexadecane	Rh-Ni/MgAl	700-950	3	65% H ₂ (NR)
Sugisawa et al. -2011	n-dodecane	La/Ni/Al ₂ O ₃	500	3.5	45%
Fauteux-Lefebvre et al. (2010)	Propane, hexadecane and tetralin	NiAl ₂ O ₄ /Al ₂ O ₃ -YSZ	700-750	3	NR
Granlund et al. (2014)	MK1	Co, La, Mn-Rh/CeO ₂ -ZrO ₂	700-950 (ATR)	2.5 [O ₂ /C=0.45]	70-95%

2.3 Catalyst Deactivation

Deactivation of catalyst is still one of the biggest challenge for the successful and continuous supply of hydrogen from liquid fuel steam reforming and requires rigorous research. Catalysts have need of reactivation or regeneration due to coke formation and decline in available active site for the reaction, which ultimately increases the cost of catalyst. Furthermore regeneration of catalyst further results in to less catalytic activity after regeneration due to loss in active sites. Development of cheap, poison and coke formation resistance of catalyst is necessary for higher fuel conversion. Noble-metal-based catalysts (Pt, Rh, Pd) are also active for steam reforming, but these metals are normally too expensive to be used in conventional industrial reformers [29]. Nickel-based catalysts turn up as a good alternative but due to heavy coke formation and sulfur poisoning results into catalyst deactivation. There are three ways of how coke formed:

(a) Carbon that diffuses into active metal and separate metal from its crystal is called whisker carbon. In this type of coke formation carbon filament grow further from the detached metal.

(b) Carbon formation due to pyrolysis or cracking of fuel (hydrocarbon) at high temperatures in the absence of air is called pyrolytic carbon.

(c) Polymerization of hydrocarbons that results into carbon encapsulation, further forms graphite [30] [31] [32]. Coke also sometime formed due to the large nickel particle size, e.g. particle size greater than 12 μm [33].

2.3.1 Deactivation by Sintering and Sulfur

One of the many reasons of deactivation of Ni based catalyst is deactivation by sintering. Catalyst preparation significantly affects the metal dispersion at the surface of its support. Precisely, better metal dispersion over support results into lower chances of metal sintering. Another reason for catalyst deactivation is the presence of contaminants in diesel. Sulfur quickly deactivates the metal particles forming metal sulfides during catalytic reforming. Sulfur is poisonous for catalyst as it starts occupying the active metal sites and catalysts starts losing their activity, hence cracking of diesel starts at acidic support, that further increases rate of deactivation due to coke formation [30]. Deactivation of catalyst due to sulfidation reaction decreases at high temperatures in an oxidizing atmosphere. Regeneration of the catalyst due to sulfur poisoning is very difficult is possible at high temperatures that results in specific surface loss. Bimetallic catalysts usually offer better activity and coke formation resistance and they often have a longer lifespan. Noble metal modified catalysts (Pd–Pt on CeO or Ni–Pt on CeO) showed better resistance towards deactivation caused by sulfur in fuel, however, a mono-metallic catalyst (Pt/CeO) was deactivated within 30 h during ATR [34]. Steam reforming of isooctane (containing 500 ppm of sulfur) showed activity for 160 h; however the Ni based catalyst lost its activity after 8 h [19]. Similarly, the catalyst Ni hexa-aluminate $[\text{Ni}_{0.4}\text{Al}_{11.6}\text{O}_{19-5}]$ (A = Ba, La or Sr) used for auto thermal reforming of n-tetradecane (with 50 ppm of sulfur) lasted only for 2 h. [26]

Figure 2-6 shows that, after only 10 hours of operation, %H₂ yield reduced to less than 5% with only 50 ppm of sulfur in fuel [21].

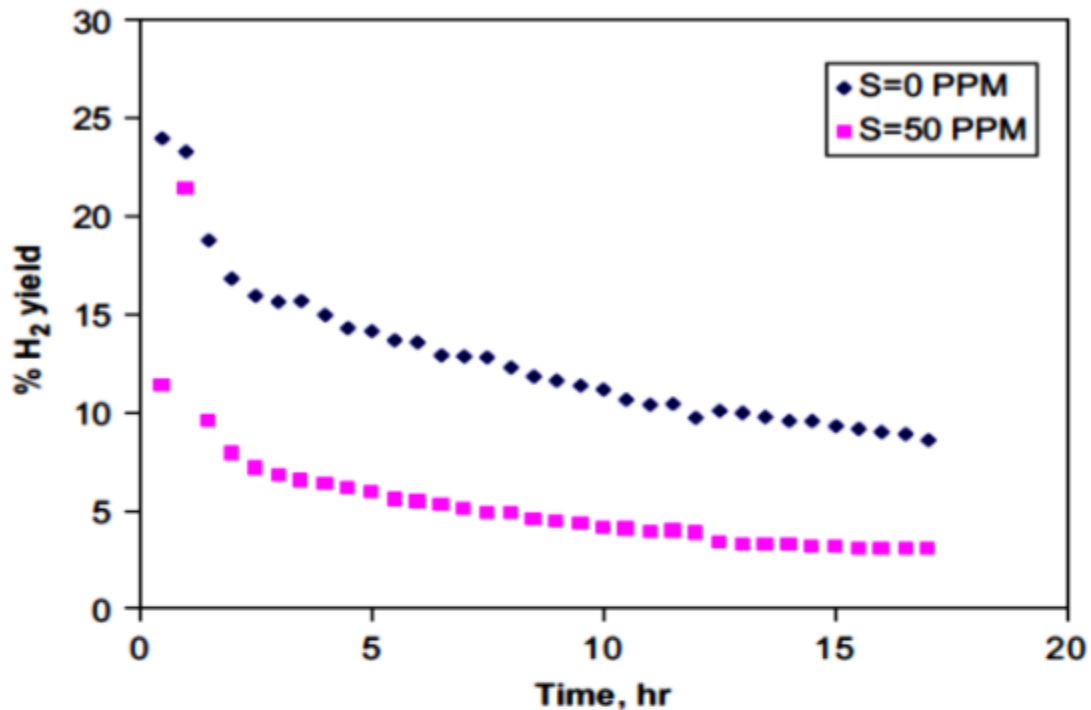


Figure 2-6: Activity of Pd/Zr₂ catalyst in terms of %H₂ yield during steam reforming of n -hexadecane at T = 750 °C, S = 0ppm and S = 50ppm and S/C = 3. [21]

2.3.2 Deactivation by Coking

As described earlier the major problem with nickel-based catalysts are deactivation due to carbon formation. Different types of coke formed are already described in earlier section 2.3.1 in detail.

These two coking mechanisms whisker and pyrolytic carbon are favored at high temperatures activated in diesel steam reforming. Commercial diesel is usually a mixture of different liquid hydrocarbons, such as paraffin, olefins, aromatics and cycloalkanes. Kinetics of steam reforming reaction is governed by the type of reformed chemicals.

Figure 2-7: A conceptual model of fouling, crystallite encapsulation and pore plugging of

a supported metal catalyst due to carbon deposition. Coking is also caused by the polymerization of heavy hydrocarbons in the case of diesel reforming. There is a difference in the coking mechanism of Ni and for noble metals. Carbon whiskers as described formed after diffusion of coke into Ni metal, however noble metals presents very good resistance towards coke formation and do not dissolve carbon. Ni catalysts are also more susceptible to coking as they help breaking the C-C bond present in hydrocarbon chain. Presence of radical carbon ($\text{CH}_{0.3}$) at the surface further increases the rate of coke formation [19].

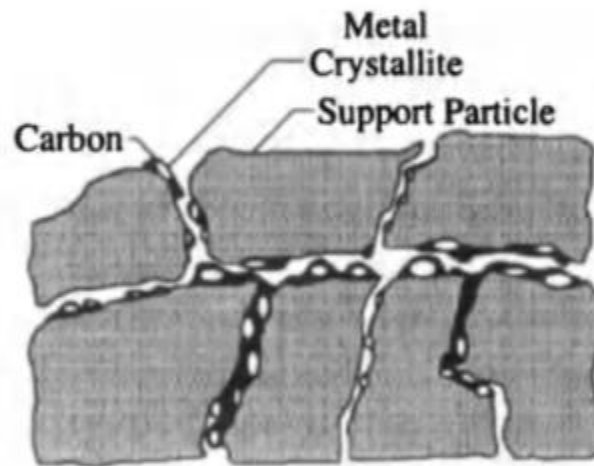


Figure 2-7: A conceptual model of fouling, crystallite encapsulation and pore plugging of a supported metal catalyst due to carbon deposition. [30]

Evaluation of Carbon Formation

Amount of carbon deposited can easily be calculated by using the following equation:

[22]

$$C (\%) = \frac{M_C}{M_{\text{Cat}}} \times 100 \quad (13)$$

Where, M_C is the amount of carbon deposited on the catalyst (g), and M_{Cat} is the weight of the catalyst (g) used.

Addition of promoters increases the catalyst activity and suppresses the amount of carbon deposited. The amount of carbon deposited after 6h of steam reforming reaction with $LHSV = 0.25 \text{ h}^{-1}$ and $S/C = 1.5$ at different promoted and non-promoted catalysts are listed in **Table 2-6**.

Table 2-6: Carbon deposition rates for Commercial and promoted catalysts [22]

Catalysts	No Promoter	La-Ni	Ce-Ni	Yb-Ni	S-1	G-1	G-2
C %	5.8	2.4	1.5	1.3	1.9	4.7	1.1

It's clear from the results presented that some of the promoters are very good career of oxygen and their addition enhances coke formation resistance of Ni-based catalysts [34]. It has also been concluded that promoter like Yb increases the dispersion of active metal and strengthen the interaction between the support and active metal. It also inhibits the transportation and reduces the phenomenon of sintering of active metal [22].

In a study (carried out by Masanori et. al. 2011) the effect of La promoter in $Ni/\gamma-Al_2O_3$ catalyst was observed at a relatively low temperature (773 K). The addition of lanthanum to the $Ni/\gamma-Al_2O_3$ suppresses the carbon deposition and results are shown in Figure 2-8. Lanthanum supported bimetallic catalyst initially enhanced the %yield of hydrogen, however, the catalyst deactivated with increased time-on-stream at a high steam-to-carbon ratio of 3.5, because of oxidation of the active Ni metal. The effect of promoter loading on n-dodecane conversions, after 1.5 h time-on-stream and the amount of

deposited carbon are also listed in Table 2-6. However, the CO chemisorption capacity decreased after La addition (metal dispersion: <1%) [35]

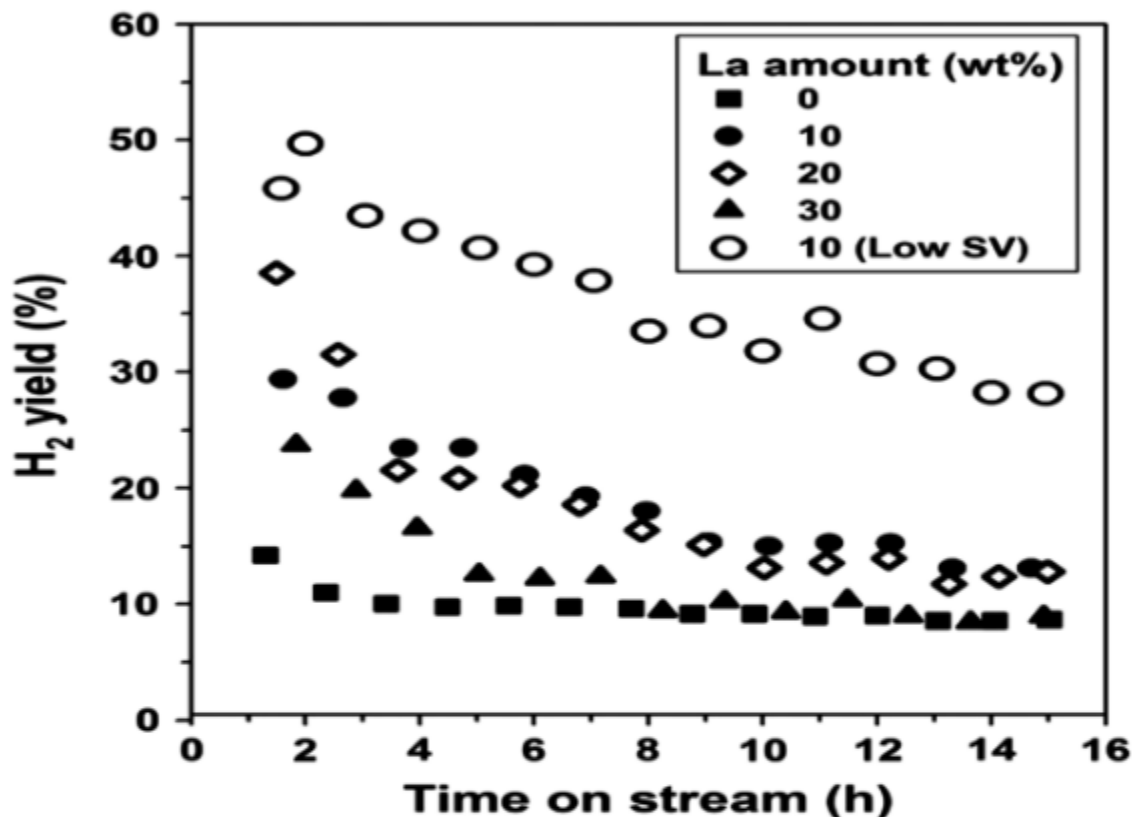


Figure 2-8: H₂ yield as a function of TOS for steam reforming of n-dodecane on La-Ni/γ-Al₂O₃ catalysts with different amounts of La (773 K, LHSV: 40ml⁻¹ C₁₂H₂₆(l)g⁻¹ h⁻¹ (Low SV: 20 ml-C₁₂H₂₆(l)g⁻¹ h⁻¹), S/C=3.5, 101 kPa). [35]

Presumably because, of the blockage of Ni sites by La species, The addition of La beyond 10 wt.% did not change the CO chemisorption capacity drastically within these small values as tabulated in Table 2-7. However, the addition of La, in Ni/γ-Al₂O₃ completely suppressed carbon formation on the catalyst during steam reforming.

Table 2-7 The CO chemisorption capacity, n-dodecane conversion, turnover rates, and the amount of deposited carbon for La-Ni/ γ -Al₂O₃ catalysts with different La content² [35]

La content (wt. %)	CO adsorbed ($\mu\text{mol g}^{-1}$)	n-dodecane conversion [§] (%)	Turnover rate ^a (s^{-1})	Coke deposited ^b (wt.%)
0	92	11	0.059	8
10	15	35.1	1.14	0
20	21	40.4	0.94	0
30	20	26.8	0.66	0

2.3.3 Kinetic study on catalyst deactivation

Kinetics of liquid hydrocarbon fuels (diesel, Naphtha and gasoline) has not been studied intensely as compare to methane. Published kinetic data for steam reforming reactions of long chain liquid hydrocarbons is limited [36]. Nobel metal based catalysts also face sever deactivation issues such as Pd/Zr₂O catalyst deactivated during the steam reforming of n-hexadecane [21]. Steam reforming reactions are carried out in the absence of air and deficiency of oxygen increase the rate of cracking of long chain hydrocarbon fuels. Similarly decomposition of carbon oxides formed also leads to coke formation [37]. Thermo gravimetric analysis (TGA) of spent commercial (Ni/Al₂O₃) showed an increase in catalyst weight with time on stream [38]. Studies made (by Depeyre et al. 1985) suggested coke formation due to cracking might be modeled as first order kinetics [39].

^a Determined using n-dodecane conversion and the amount of CO adsorbed.

^b Measured after 15 h-reaction time using thermogravimetric analysis.

[§] 1.5 h time-on-stream

The mass balance equation given below provides the relationship between time on stream (TOS) and conversion for a plug flow reactor [21].

$$-\ln(1 - X) = k_0 \tau \exp(-k_d t) \quad (14)$$

A plot of time on stream vs $\ln(-\ln(1 - x))$ results into a straight line. The slope of straight line is $-k_d$ or the deactivation rate constant and the intercept is $\ln(k_0)$.

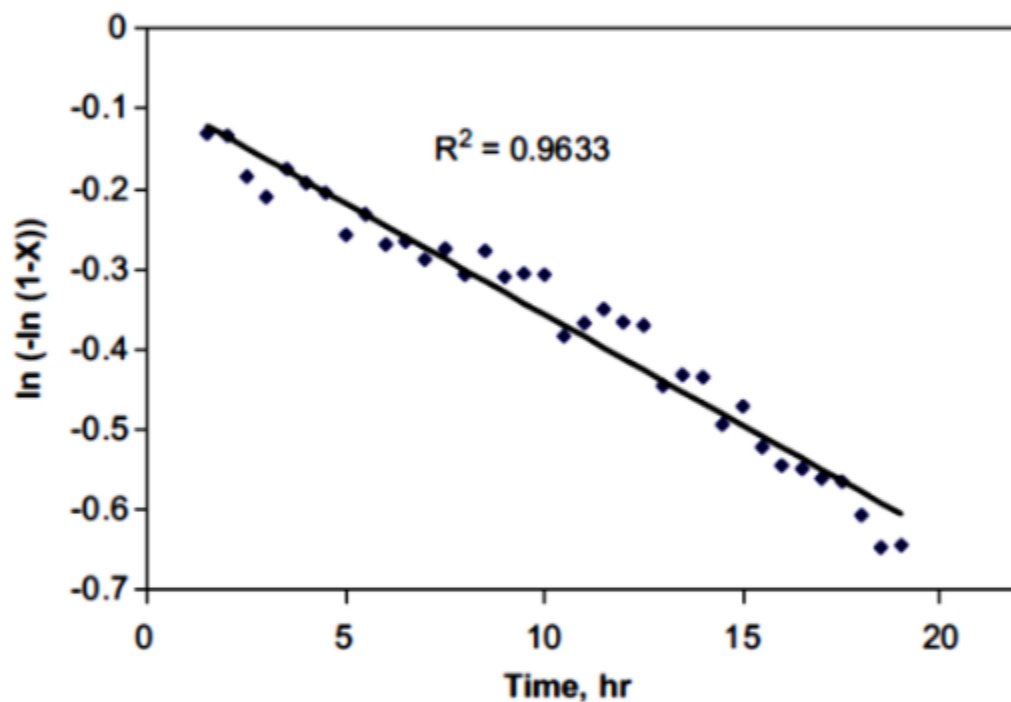


Figure 2-9: First order kinetics of deactivation mechanism during the steam reforming of n-hexadecane at 750 °C and S/C=3 with no sulfur contents [21].

This result, shown in Figure 2-9 for n-hexadecane steam reforming, shows a good fit ($R^2=0.9633$) proposing that results obtained from model are close to experimental results. Similar model was employed to calculate the constants for rate of deactivation at various reaction conditions and sulfur contents of fuel. All the constants obtained during steam reforming at different S/C ratios, reaction temperatures and sulfur contents in fuel are summarized in Figure 2-10 and Figure 2-11 [21].

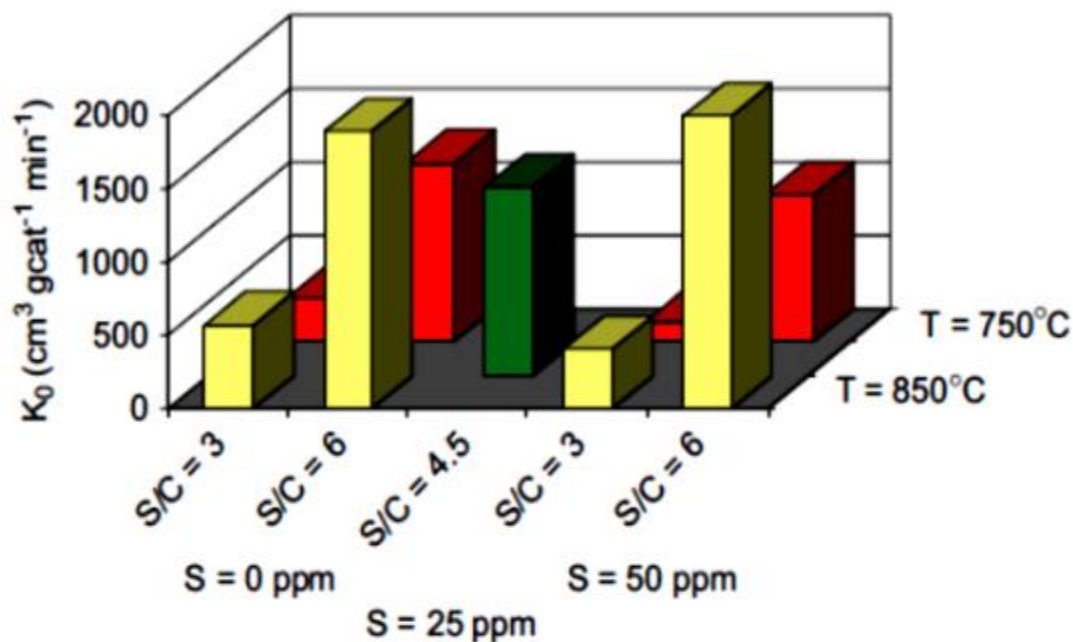


Figure 2-10: Summary of rate of reaction for n-hexadecane steam reforming over Pd/Zr₂O catalyst at different temperatures, S/C ratios and sulfur contents in fuel [21]

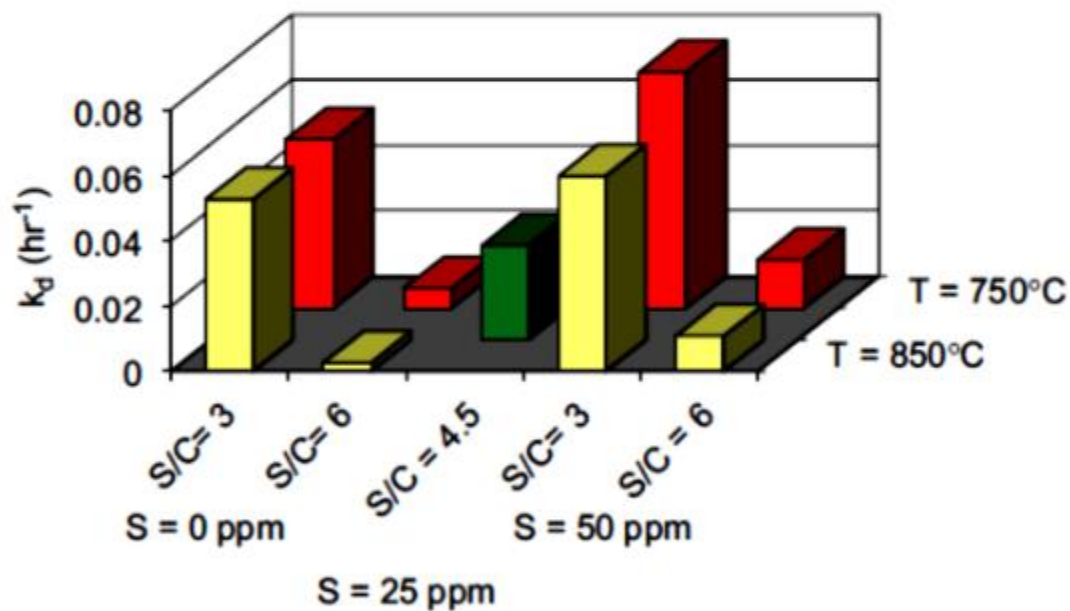


Figure 2-11: Summary of rate of deactivation constants obtained from regression analysis of the results obtained from steam reforming of n-hexadecane over Pd/Zr₂O catalysts at different temperatures, S/C ratios and sulfur contents in fuel . [21]

It was reported for this particular catalyst that coke formation was not suppressed by higher temperatures, however increase in S/C ratio decrease the rate of coke formation.

The values of k_0 and k_d depend on T, S/C and sulfur concentration in fuel. [21]

In most of the literature found on diesel fuel steam reforming, the fuels used were surrogates of diesel instead of commercial diesel with varying sulfur contents. Different surrogates either contain one specific type of hydrocarbon or a mixture of two or three known contents, which are not representative of real commercial diesel. Therefore, most of the reported catalysts showed rapid deactivation when checked for commercial diesel fuel.

The addition of promoters, not only enhanced the metal and support interaction hence suppressed the chances of catalyst deactivation [26]. Similarly, transition metals were found successful in terms of stability, but they are very expensive [3]. Ni catalysts escalate the dissociation of C-C bonds and further accumulation of radical carbon species at the catalyst surface. Ni catalysts also habitually break and forms carbon whiskers [40].

According to literature, different types of promoters have been used so far [34] [35] [24] [38]. In this research it has been planned to impregnate different promoters from lanthanide series including, La, Ce, Eu, Pr, Gd to investigate the deactivation by coke formation and to increase the catalyst activity.

CHAPTER 3

RESEARCH OBJECTIVES

The overall objective of this study is to investigate the activity and stability of Ni-based steam reforming catalysts for diesel conversion to produce hydrogen rich gas.

However, the specific objectives are as follows:

1. Preparation of Ni supported steam reforming catalysts with different Ni metal loadings.
2. Modification to improve the overall efficiency of Ni-based SR catalysts using Lanthanides series (La, Ce, Gd, Eu, and Pr) as promoters.
3. Characterization of prepared catalysts by XRD, TPR, TGA TEM, CHNS and BET Surface area.
4. Testing of catalysts for diesel steam reforming in the fixed bed reactor and calculation of coke formed using TGA and CHNS.

CHAPTER 4

EXPERIMENTAL SECTION

In this section two series of Ni-based catalysts were prepared using the wetness incipient impregnation method. Different characterization techniques were employed to understand the behaviors of catalysts prepared. However, performance evaluations of synthesized catalysts were further carried out in a fixed bed reactor system.

4.1 Materials

Catalysts used during the study were synthesized using the materials mentioned in Table 4-1 with addresses of companies from where these materials were acquired.

Table 4-1: Materials used for the synthesis of catalysts.

Material	Name of Company
Al ₂ O ₃ support	Axens IFP group technologies, ProCatalyse Catalysts and Adsorbents, USINI De Salindres, 30430-France
Ni(NO ₃) ₂ ·6H ₂ O	Aldrich Chemical Company, Inc, MILWAUKEE WI 53233 USA
La(NO ₃) ₃ ·6H ₂ O	REacton® from Alfa Aesar, A Johnson Matthey Company
Ce(NO ₃) ₃ ·6H ₂ O	Merck KGa A 64271, Darmstadt, Germany
Eu(NO ₃) ₃ ·6H ₂ O	REacton™, RARE EARTH PRODUCTS, Waterloo Road, Widnes, Cheshire, A Johnson Matthey Company, Alfa Aesar
Pr(NO ₃) ₃ ·6H ₂ O	SIGMA Aldrich
Gd(NO ₃) ₃ ·6H ₂ O	Alfa Aesar, A Johnson Matthey Company

4.2 Catalyst Design and Synthesis

All the catalysts used in this study were prepared using the wetness incipient impregnation method. Nominal catalyst composition has been outlined in the following table.

Table 4-2: Catalysts synthesized in this work and their compositions

Support Material	Active material (Wt. %)	Catalysts Prepared
γ -Al ₂ O ₃	6% Ni	6%Ni/ γ -Al ₂ O ₃
	12% Ni	12%Ni/ γ -Al ₂ O ₃
	18% Ni	18%Ni/ γ -Al ₂ O ₃
	12% Ni+ 5% La	5%La-12%Ni/ γ -Al ₂ O ₃
	12% Ni+ 5% Ce	5%Ce-12%Ni/ γ -Al ₂ O ₃
	12% Ni+ 5% Eu	5%Eu-12%Ni/ γ -Al ₂ O ₃
	12% Ni+ 5% Pr	5%Pr-12%Ni/ γ -Al ₂ O ₃
	12% Ni+ 5% Gd	5%Gd-12%Ni/ γ -Al ₂ O ₃

4.2.1 Synthesis of Ni Supported Catalysts

The catalysts are prepared by wetness incipient impregnation method. The detailed procedure of preparation is as follows.

Al₂O₃ support (of size between 2 to 3mm) was dried at 250 °C for 2 hours to remove the absorbed moisture. After that nickel was impregnated on the alumina support using nickel nitrate solution [Ni(NO₃)₂•6H₂O] according to Figure 4-1. The contents of active metal impregnated on alumina support were 6%, 12% and 18 wt%. The nickel impregnated alumina support was dried in the air in a furnace, first up to 60°C with the temperature ramp of 0.3°C/min and was kept under this temperature for 15 minutes. Later it was heated upto 120°C with the temperature ramp of 1.0°C/min. Once desired temperature of 120°C achieved, it was then heated up to 240°C with the temperature ramp of 1.4°C/min.

The nitrate was removed by calcining the catalyst in a special fixed bed reactor with a dilute hydrogen flow of 170ml/min and a heating rate of 3.3°C/min from room temperature to 450°C and then heating at a rate of 5°C/min from 450°C to 750°C and then cooled to room temperature. The performance evaluation of the nickel impregnated catalyst series was further accomplished to find the best nickel metal loading, in terms of diesel and water conversion.

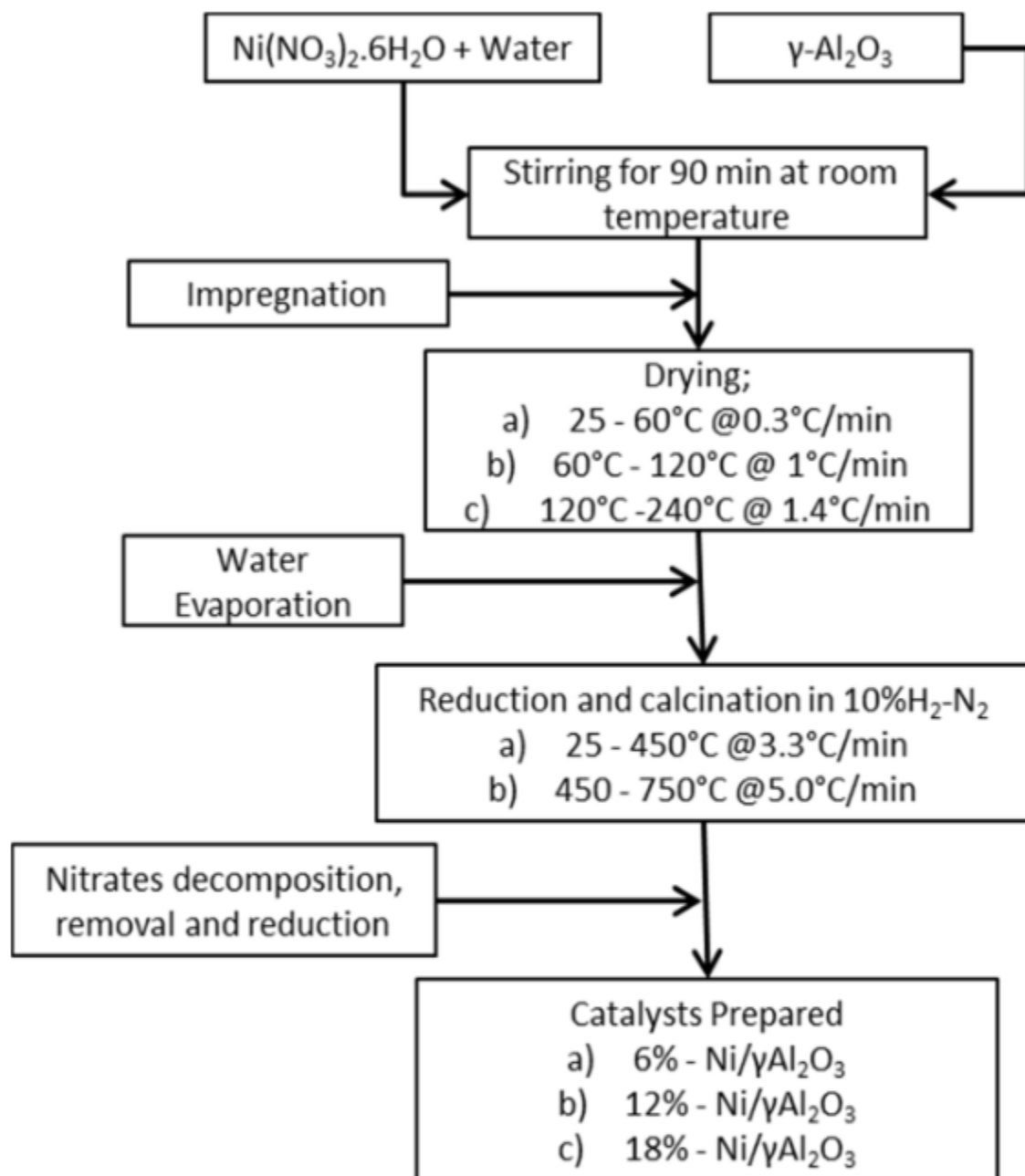


Figure 4-1: Procedure for impregnation of Ni on $\gamma\text{-Al}_2\text{O}_3$ using the incipient wet impregnation method.

4.2.2 Synthesis of Ni based catalyst with different promoters

All promoted catalysts were prepared by the wetness incipient impregnation method. In this context, Al_2O_3 support was dried at 250°C for 2 h to remove the absorbed moisture. Then it was impregnated with lanthanide series, one by one; using nitrate solutions of lanthanum nitrate $[\text{La}(\text{NO}_3)_3 \cdot 6\text{H}_2\text{O}]$, cerium nitrate $[\text{Ce}(\text{NO}_3)_3 \cdot 6\text{H}_2\text{O}]$, europium nitrate $[\text{Eu}(\text{NO}_3)_3 \cdot 6\text{H}_2\text{O}]$, praseodymium nitrate $[\text{Pr}(\text{NO}_3)_3 \cdot 6\text{H}_2\text{O}]$ and gadolinium nitrate $[\text{Gd}(\text{NO}_3)_3 \cdot 6\text{H}_2\text{O}]$ as shown in Figure 4-2. The lanthanide series impregnated on γ -alumina support was later dried in the presence of air in a furnace at 110°C overnight. The catalyst was then calcined in a muffle furnace at a heating rate of $5^\circ\text{C}/\text{min}$ from room temperature to 450°C and then cooled to room temperature.

Then nickel was impregnated on each of the lanthanide series catalyst, following the same procedure as in section 4.2.1.

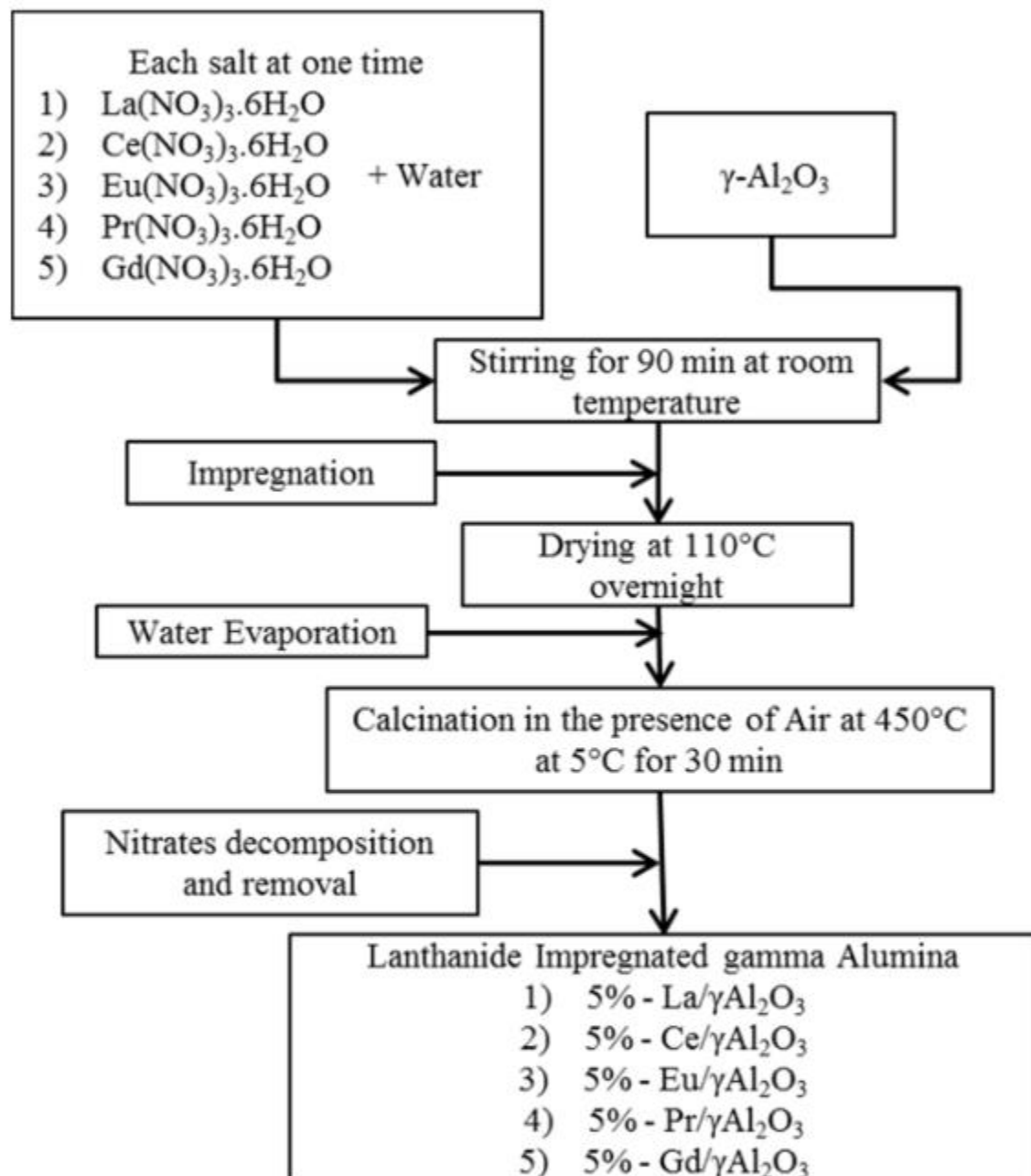


Figure 4-2: Procedure for impregnation of Lanthanum (La), Cerium (Ce), Europium (Eu), Praseodymium (Pr) and Gadolinium (Gd) on $\gamma\text{-Al}_2\text{O}_3$ using the incipient wet impregnation method.

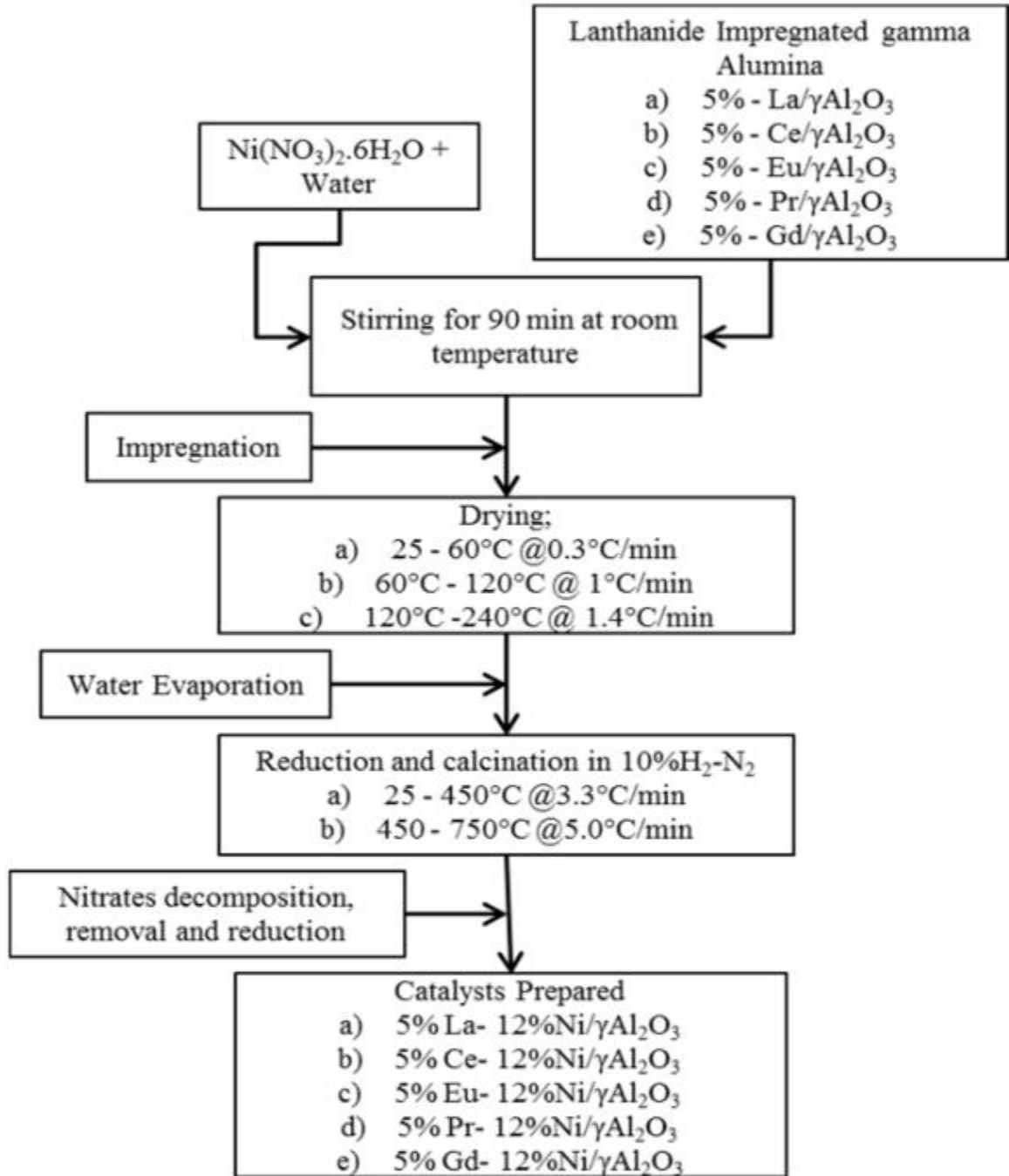


Figure 4-3: Procedure for impregnation of Ni on an already Lanthanide series promoted γ - Al_2O_3 using the incipient wet impregnation method

4.3 Evaluation of the Catalyst

All of the lanthanide series promoted catalysts were tested for 40hrs. Catalyst evaluation was carried out in a fixed-bed flow reactor system. Figure 4-4 shows a schematic of the fixed bed reactor unit. The reaction system consists of gas and liquid feed sections, preheating section, a reactor section and product collection section. Gases were fed through mass flow controllers (Brooks instruments Model SLA5840). Liquid feeds were pumped by precision pumps (Gilson, Inc.). The reactor tube with 17.5 mm internal diameter and 100 cm in length was made of a Haynes 230 alloy. The reactor was vertically installed in an electrical furnace. The volume of catalyst taken for reaction is 25ml and the catalytic bed height is approximately 11.5 cm in all experiments. The granules (size 2-3mm) of the catalyst were placed on an inert layer of silicon carbide and bed height of SiC is 1.5 cm. The system consists of a three-zone electric furnace. K-type thermo-couples were provided to measure, record, and control the inside temperature of the reactor.

Water was vaporized in a preheater and then mixed with a fine mist of diesel fuel produced by an ultrasonic generator in the presence of a very low nitrogen flow (10NL/h) before entering the reaction zone. The product collection section consists of a pressure control valve, a gas-liquid separator, a liquid level controller, gas wetness meter and a product tank installed on weighing scale. The product mixture was separated in a gas-liquid separator (at 4-7 °C) and the gaseous product was further passed through wetness meter to measure the flow rate of gas mixture.

A small part of product gas was withdrawn by an online gas chromatograph (Shimadzu GC-17) using Ar, as a carrier gas. GC was equipped with a TCD (Thermal conductivity detector) to measure the mole fraction of H₂, N₂, CH₄, CO₂ and CO at regular intervals (after every one hour).

A dilute flow of hydrogen in nitrogen gas (5% H₂-N₂) was provided during the heating process, to keep the catalyst in reduced form. The reactor was heated up to 620 °C at the start of the reaction and once the temperature of furnace and inside the catalyst bed were same, steam was introduced into the system. The temperature of the catalyst bed started decreasing once steam reached the surface of the catalyst bed and at that time a thin mist of diesel was introduced into the reactor through an ultrasonic injector. Once steady state conditions were achieved, a portion of the product stream was injected into online GC for gas analysis. However, due to endothermic reactions, the temperature measured inside the reactor (the catalyst bed) was always 220°C below the set point and furnace temperature. This means that the reaction was strongly endothermic in nature. In order to reduce the temperature increase at the end of catalyst bed, silicon carbide (SiC) particles were used at the end of the catalyst bed. The SiC served as a heat sink, thereby decreasing temperature gradients inside the reactor and hence reducing the coke formation of any unconverted diesel. SiC was tested in the blank run and was found to be inert.

Simulated Distillation (SimDis)analysis of diesel fuel (used in this study) shows 100% recovery at 427 °C, however Initial boiling point (IBP) was 57°C and sulfur contents

were 6 ppm. All the experiments were carried out at 620°C**, atmospheric pressure, a steam to carbon ratio (S/C) of 3.0 and gas hourly space velocity of 5800 h⁻¹. Diesel Steam Reforming (DSR) of all non-promoted (monometallic) catalysts were carried out continuously for 10 hours and in case of lanthanide promoted (bimetallic) catalysts, experiments were performed continuously 40 hours. In each experiment, the un reacted mixture of diesel and water was collected from the product tank at regular intervals of 10 hours. The unreacted mixture removed was further separated to find out the exact amount of diesel and water conversion.

Shut Down Procedure:

Reaction can be stopped at any time by stopping the diesel feed to the system, followed by water (steam), termination and introduction of nitrogen gas into the system.

Performance evaluation, efficiency and activity of catalysts, of La, Ce, Eu, Pr and Gd impregnated Ni/ γ -Al₂O₃ catalysts were found out by keeping the reaction conditions, S/C ratio, diesel and other feed compositions constant.

Table 4-3: Reaction conditions for the diesel steam reforming experiments.

Reaction Conditions	
Pressure	1 atm
Temperature	580 °C, 600 °C, 620 °C
GHSV	5800 h ⁻¹
S/C	3.0
Time on Stream	40 h

** Some reactions were performed at different temperatures and details will be provided in relevant sections.

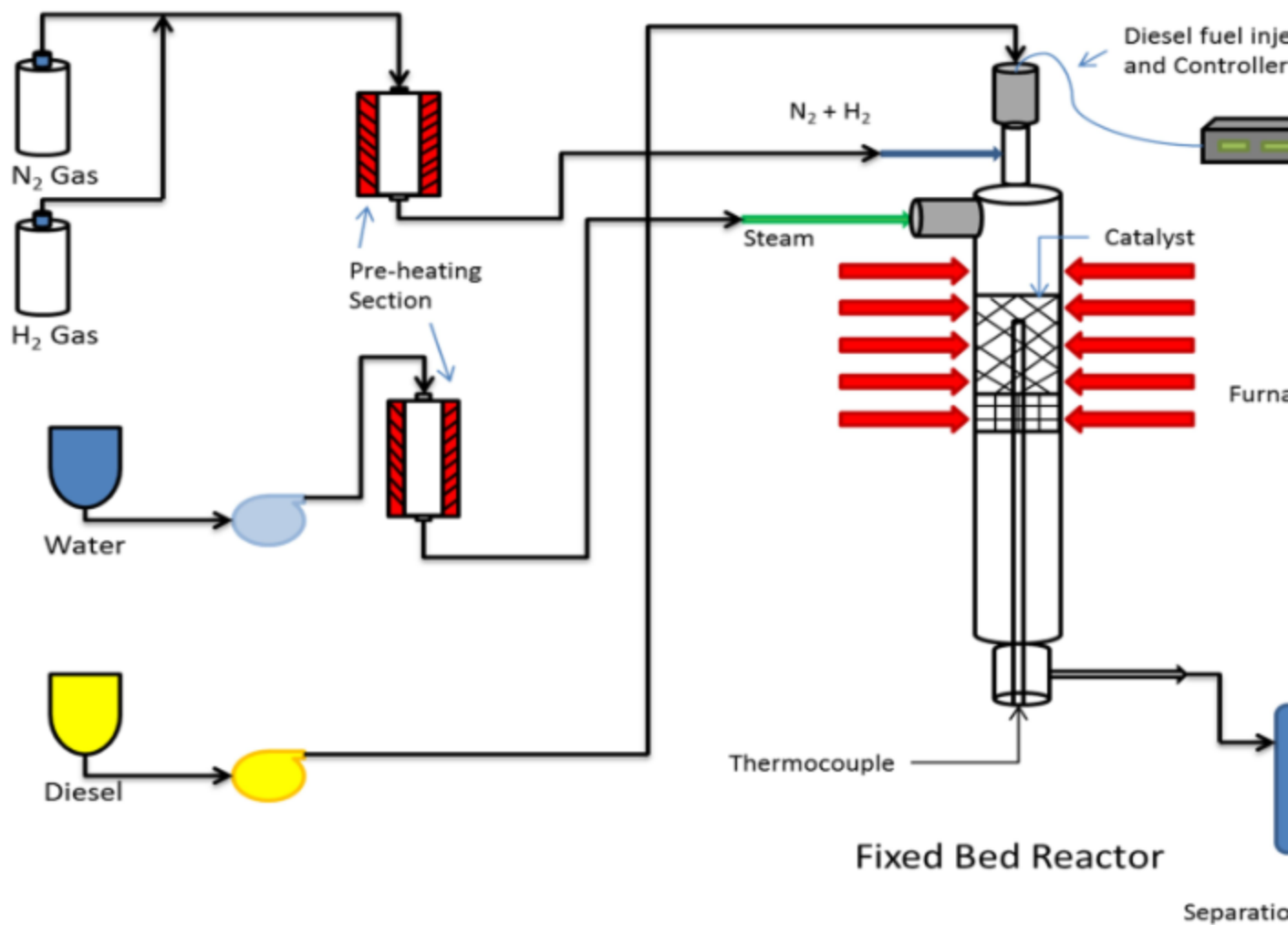


Figure 4-4: Process Flow Diagram of The Testing Unit (Fixed bed reactor Unit)

4.3.1 Coke formation study on Ni-based catalyst

Analysis of fresh and used catalyst was helpful to understand the coke formation during diesel steam reforming reaction. The amount of carbon deposited was measured using thermo gravimetric analysis and CHNS techniques.

4.4 Characterization of the Catalyst

Two series of catalysts were synthesized for diesel steam reforming experiments. The aim of the catalyst characterization was to investigate how does variation in Ni metal loading and lanthanide series impregnation in Ni based catalyst affects the surface and bulk properties of the Ni/Al₂O₃ catalyst. The benefits of the impregnating lanthanide series to Ni-based catalysts were driven by structural interaction between the two metals, or between the metals and the support within the new bimetallic catalyst. All these interactions maybe of structural or textural nature, that results into change in the physical properties of the catalyst such as the metal dispersion or metal crystal surface area or they may be chemical nature, affecting the adsorption and chemical interactions. Characterization studies of lanthanide promoted catalysts containing La, Ce, Eu, Pr and Gd reveal very important features of the catalysts. Following techniques have been used for the characterization of all the promoted and non-promoted catalysts:

1. X-ray Diffraction (XRD)
2. Energy Dispersive X-Ray Analysis (EDX)
3. Scanning Electron Microscope (SEM)
4. BET Surface area and pore volume

5. Temperature Program Reduction (TPR)
6. Transmission Electron Microscopy (TEM)
7. Thermo gravimetric Analysis (TGA)
8. Carbon, Hydrogen, Nitrogen, Sulfur Analyzer (CHNS)
- 9.

4.4.1 X-Ray Diffraction (XRD)

XRD is a most abundantly used technique to identify different chemical phases through the catalyst bulk and metal particle sizes of different identified metals in the catalyst. XRD patterns were measured on Rigaku MiniFlex II (30KV and 15mA) using Cu K α radiation of $\lambda= 1.5425 \text{ \AA}$. Spectra was collected for a 2θ range of 1.2 to 80° using a step size of 0.02° and a count time of 1 second. XRD measurements were done with catalysts that were calcined and further reduced. In addition to the non-promoted and lanthanide promoted catalysts, XRD patterns were measured for pure $\gamma\text{-Al}_2\text{O}_3$ that was also calcined at the same catalyst conditions, in order to distinguish patterns related to the support. All the obtained XRD patterns were compared with the patterns of International Center Diffraction Data (ICDD) or previously known as the Joint Committee on Powder Diffraction Standards (JCPDS). Rigaku MiniFlex uses PDXL software for XRD analysis that is based on database provided by ICDD.

4.4.2 SEM and EDX

Scanning Electron microscopy is a powerful visualization tool used to understand the morphology of catalyst, particle size of metal, composition of catalyst, structure and other

surface properties. EDX of all the prepared catalysts were also performed to find out the point and bulk surface composition of the catalyst.

The morphologies of the un-promoted and promoted catalysts were investigated by using a scanning electron microscope (JEOL JSM-6460LV) operated at 5 to 20 kV. SEM was also equipped with energy dispersive X-ray (EDX). For SEM-EDX analysis, 2–3 mg sample powder was dispersed on a copper tape which was mounted on the sample holder. The sample was then coated with gold to make it conductive for electron beam.

4.4.3 Thermo Gravimetric Analysis (TGA)

Thermo gravimetric analysis or thermal gravimetric analysis (TGA) is a type of analysis which records the change in weight of sample with change in temperature. TGA analysis helps studying the stability of catalyst. Approximately 40-45 mg of the spent catalyst sample was placed into an aluminum sample pan for TGA using an empty aluminum pan as a reference. All TGA were recorded on a Shimadzu TGA-60 between 25 °C and 1000°C at the heating rate of 10°C/min in an air atmosphere (100ml/min). TGA was used to find the carbon deposition on the catalyst surface after 40 hours testing.

4.4.4 Temperature Programmed Reduction (TPR)

Temperature-Programmed Reduction (TPR) reveals the temperature at which the reduction occurs, determines the number of reducible species present in the catalyst and the amount of hydrogen required completing reduction. The reducibility of metal supported catalysts in TPR profiles also explains the metal support interaction. All the catalysts were in reduced form, so first catalysts were heated at preparation port to 400°C with continuous air flow. In second step, the sample tube was switched from preparation

port to degasing port. Degasing was performed at a heating rate of 10 °C/min up to 400 °C in the presence of Ar gas at the flow rate of 20cc/min. Temperature programmed reduction (TPR) of catalysts were carried out using 10% hydrogen in N₂ at 20 mL min⁻¹. About 50 mg of the catalyst was loaded in a U-shaped quartz reactor and heated from room temperature to 1000 °C at 10 °C min⁻¹. A TCD detector was used to analyze the effluent gases. Micromeritics A2720 by Micromeritics Instrument Corporation was used to perform the TPR of catalyst samples.

4.4.5 Carbon, Hydrogen, Nitrogen Sulfur Analyzer (CHNS)

The quantity of coke formed was measured using Elementar Vario Micro Cube CHNS analyzer (Carbon, Hydrogen, Nitrogen Sulfur analyzer). This instrument helps to determine the elemental composition of the catalyst hence the percentage of carbon deposited on the surface or in the pores of catalysts.

4.4.6 Transmission Electron Microscopy (TEM)

TEM images were obtained with ultra-high resolution TEM (JEOL, JEM-2100F) at voltage of 200 kV. Very small amounts of finely grinded solid (catalyst) sample was first dissolved in 20 ml ethanol, solvent and ultrasonicated for 30 min. 5 µl of this solution was drawn in a micropipette and dropped on a carbon/formvar (3 mm diameter) substrate grid. The substrate grid was later placed in a desiccator for drying and further used for TEM.

4.4.7 BET Surface Area and the Pore Volume

Surface area and pore volume were evaluated by the Brunauer, Emmett and Teller (BET). Analysis of support and the synthesized catalysts were carried out using Micromeritics model ASAP 2010. Physical adsorption was done at the liquid nitrogen temperature of 77K.

CHAPTER 5

RESULTS AND DISCUSSION

In the first part of this section, physico-chemical characterization results of all the monometallic and bimetallic catalysts synthesized and γ - Al_2O_3 support are presented and discussed. In the second part of this section, performance evaluation results, including diesel and water conversion, hydrogen yield, diesel reforming efficacies and selectivity results were presented, discussed and compared.

5.1 Physical Characterization

5.1.1 X-ray Diffraction Analysis (XRD)

XRD of all the catalysts were performed to find the crystalline phase and crystallization degree of different identified metals in the catalyst. XRD patterns were measured on a Smart Lab (9kW) Rigaku XRD X-ray diffraction X-ray diffractometer, with a diffraction range $2\theta = 2-80^\circ$ using Cu $K\alpha$ radiation of $\lambda=1.5425 \text{ \AA}$.

XRD diffraction patterns for non-promoted 6%, 12% and 18% Ni/ γ - Al_2O_3 catalysts in addition to γ - Al_2O_3 are presented in Figure 5-1. The International Center of Diffraction Data (ICDD) was used to identify different phases in each chemical. γ -alumina support showed three major diffraction peaks; Al_2O_3 (311), Al_2O_3 (400) and Al_2O_3 (440) [41]. All three Ni XRD patterns shown are in reduced form and major peaks are attributed to Ni (111), Ni (200) and Ni (220). Ni (111) phase was observed at 44° , 43.05° and 42.9° in

6%, 12% and 18% Ni/ γ -Al₂O₃ catalysts respectively. Ni (200) phase was observed at 51.4°, 51.5° and 51.6° respectively in 6%, 12% and 18% Ni –alumina. Ni(220) phase was observed at 75.9°, 76.1° and 76° in 6%, 12% and 18% Ni-alumina non-promoted catalysts respectively.

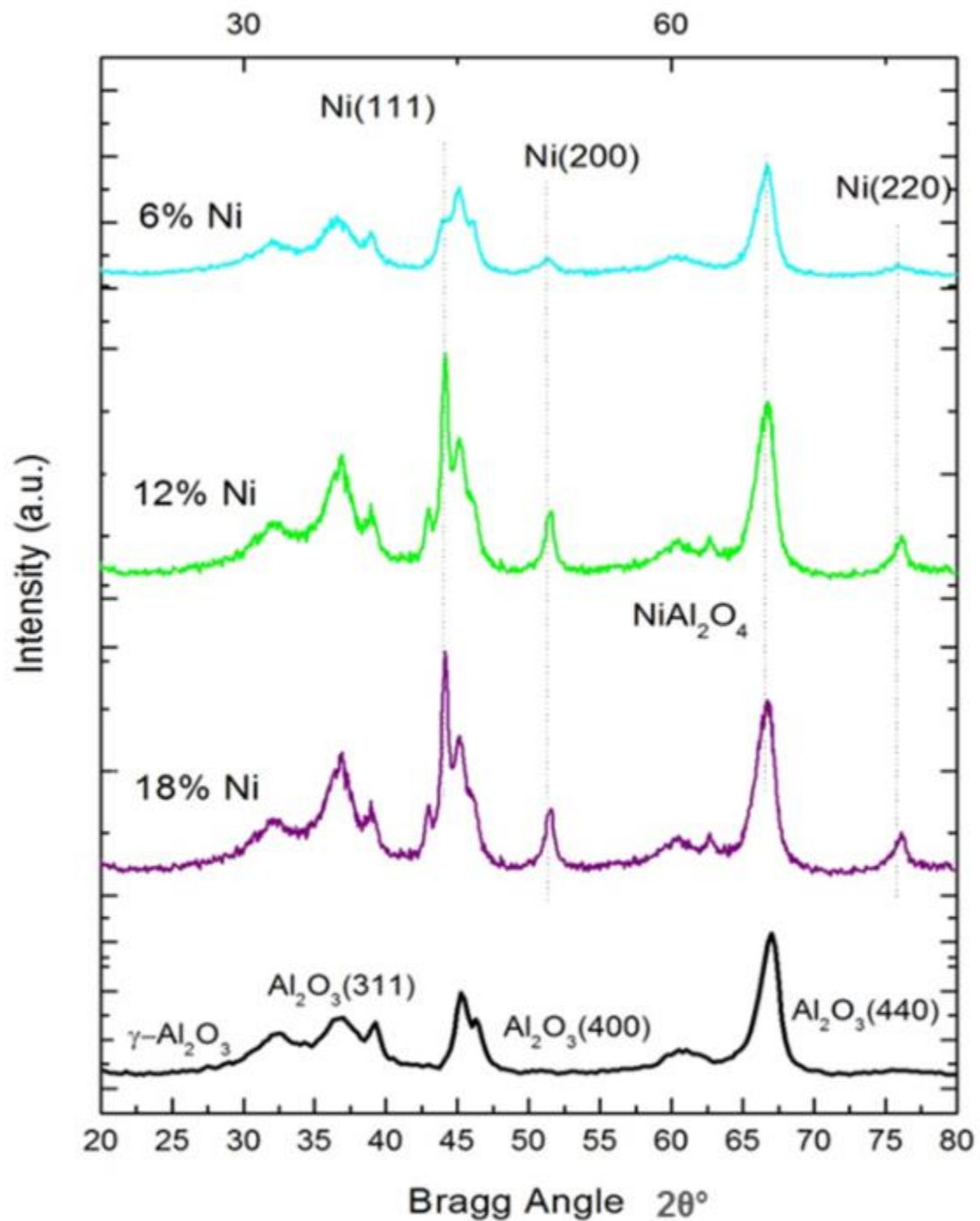


Figure 5-1: XRD pattern showing the (111), (200) and (220) reflections of Ni in alumina supported nickel catalysts.

Figure 5-2 shows the XRD results of non-promoted (12%Ni) and promoted catalysts of Ni-La, Ni-Ce, Ni-Eu, Ni-Pr and Ni-Gd and all the diffraction peaks are visible. Table 5-2 present the particle size comparison of all the promoted and non-promoted catalysts. Average particle sizes were calculated using scherrer's equation and not much variation in average Ni particle size found.

In Ni-La catalysts Ni phases (111), (200) and (220) were observed at 43°, 51° and 76° respectively. However, NiAl₂O₄ was observed at 66° in Ni-La catalyst. The NiAl₂O₄ phase that was previously merged in Al₂O₃ (440) is now giving a small peak separately. In Ni-La catalyst, La peaks were observed at 25°, 34° and 57°. Similarly, details of Ni phases observed at different angles and details are in Table 5-1. In Ce-Ni catalyst, Ce peaks were observed at 2θ = 26°, 35° and 57° with phases (111), (110) and (311) (JCPDS, Card No. 01-075-7749). XRD of Eu-Ni catalyst revealed Eu diffraction peaks at 26°, 35° and 58° with phases (101) and (201) (JCPDS, Card No. 01-077-6545). Different phases of Pr in Pr-Ni catalyst were detected at 25°, 35° and 57° with phases of (013), (200) and (401) (JCPDS, Card No. 00-039-0736). For Gd-Ni catalyst, the diffraction peaks of Gd were observed at 25°, 35° and 57° with phases (002), (100) and (114) (JCPDS, Card No. 01-071-4518).

The crystalline size of Ni, La, Ce, Eu, Pr and Gd crystals were calculated using Scherrer's equation

$$d = \frac{0.9 \lambda}{(\beta \cos \theta)} \quad 5-1$$

Where, 'd' is average particle size and β is the peak full width at half maxima (FWHM).

The crystallite size for the identified species was calculated and the values are summarized in Table 5-2. It was observed that there was slight variation in nickel crystal sizes in all the promoted and non-promoted catalysts. It can be seen that the size of Ni crystals in 12% Ni loading is almost twice the size of Ni crystals in 6% Ni loading and more than thrice in 18% Ni loading. This means that a part of the Ni metal is not supported at γ -Al₂O₃ but present as larger, unsupported crystals in 18% Ni/ γ -Al₂O₃. It can be seen that the crystals in lanthanide promoted catalysts are almost stable. The stability of the lanthanide promoted catalysts is most likely due to the fact that lanthanide promoters form a protecting layer around support particles, inhibiting crystal growth [28]. The increase in crystal size leads to considerably fewer active sites and a deactivation of the catalyst as a consequence.

Table 5-1: Ni (111), Ni (200), Ni (220) phases in different promoted and non-promoted catalysts.

Catalysts	Ni (111)	Ni (200)	Ni (220)
Non-promoted	43°	51.5°	76°
La-Ni	43°	51°	76°
Ce-Ni	44°	52°	77°
Eu-Ni	44°	52°	77°
Pr-Ni	43	52	77°
Gd-Ni	43°	52°	76°

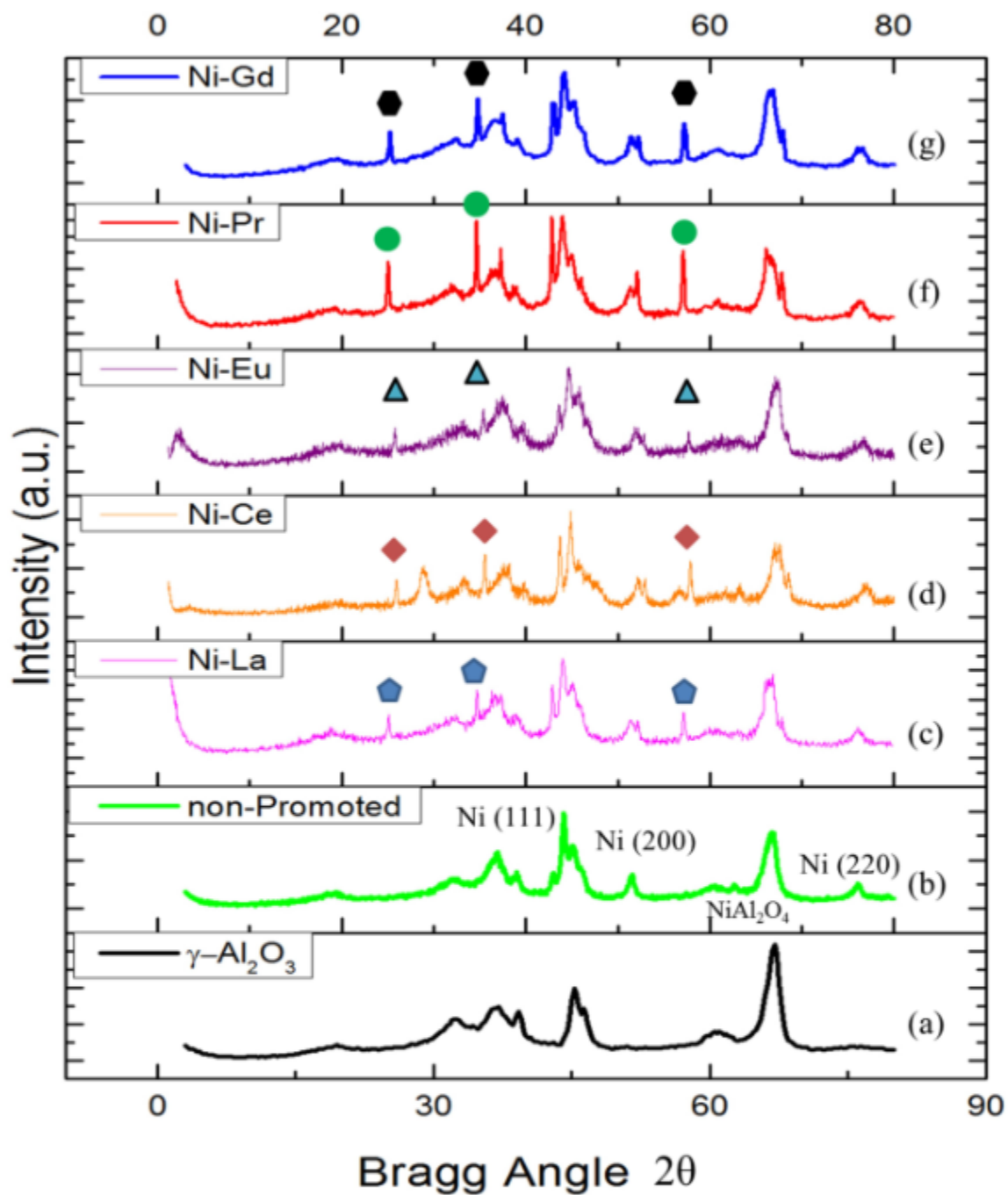


Figure 5-2 : XRD patterns of support, non-promoted and promoted prepared catalysts (a) γ - Al_2O_3 support (b) 12% Ni/ γ - Al_2O_3 (c) \blacklozenge La (012), (110), (300) (d) \blacklozenge Ce (111), (110), (311) (e) \blacktriangle Eu(1,0,1), (1,0,2), (2,0,1) (f) \bullet Pr (013) (200), (401) (g) \bullet Gd (002), (100), (114)

Table 5-2: XRD data analysis of promoted and non-promoted catalysts

Sample Catalyst	2θ angle (degree)	FWHM (degree)	Crystal size (nm)
6%Ni/Al ₂ O ₃	51.4	1.119	8.2
12%Ni/Al ₂ O ₃	51.4	0.834	11.1
18%Ni/Al ₂ O ₃	51.8	0.326	28.3
La-Ni/Al ₂ O ₃	51.2	1.105	8.3
Ce-Ni/Al ₂ O ₃	52.2	1.21	7.6
Eu-Ni/Al ₂ O ₃	52.0	0.96	9.6
Pr-Ni/Al ₂ O ₃	51.5	1.27	7.3
Gd-Ni/Al ₂ O ₃	51.6	1.40	6.6

5.1.2 Scanning Electron Microscope (SEM)/ (EDX)

Surface analyses of all the prepared catalysts were performed. Point and surface EDX clearly shows that alumina and nickel particles form a single solid phase. It was further confirmed by TPR that Ni is exclusively associated with alumina particles in all the catalyst. The point EDX when performed at different spots in all the lanthanide series promoted catalysts, it showed a very good interaction of Ni, alumina and promoters. The results obtained suggested the presence of active metal and promoter on alumina at every point in all the catalysts.

The EDX analysis (in Figure 5-3) of 6%, 12% and 18% Ni/ γ -Al₂O₃ catalysts, confirmed the presence of Nickel and Alumina in the respective samples. JEOL JSM-6460 LV machine was used to find out the composition and presence of desired metal in relevant catalyst samples. Presence of metal elements such as Ni, La, Ce, Eu, Pr and Gd in all catalyst samples reveals the successful deposition of metals on γ -Al₂O₃. The composition of Ni, La, Ce, Eu, Pr and Gd in all catalyst samples are shown in Table 5-3. To confirm the composition of the lanthanide series and nickel metal in all the catalysts, EDX was carried out at different points and also at the whole surface.

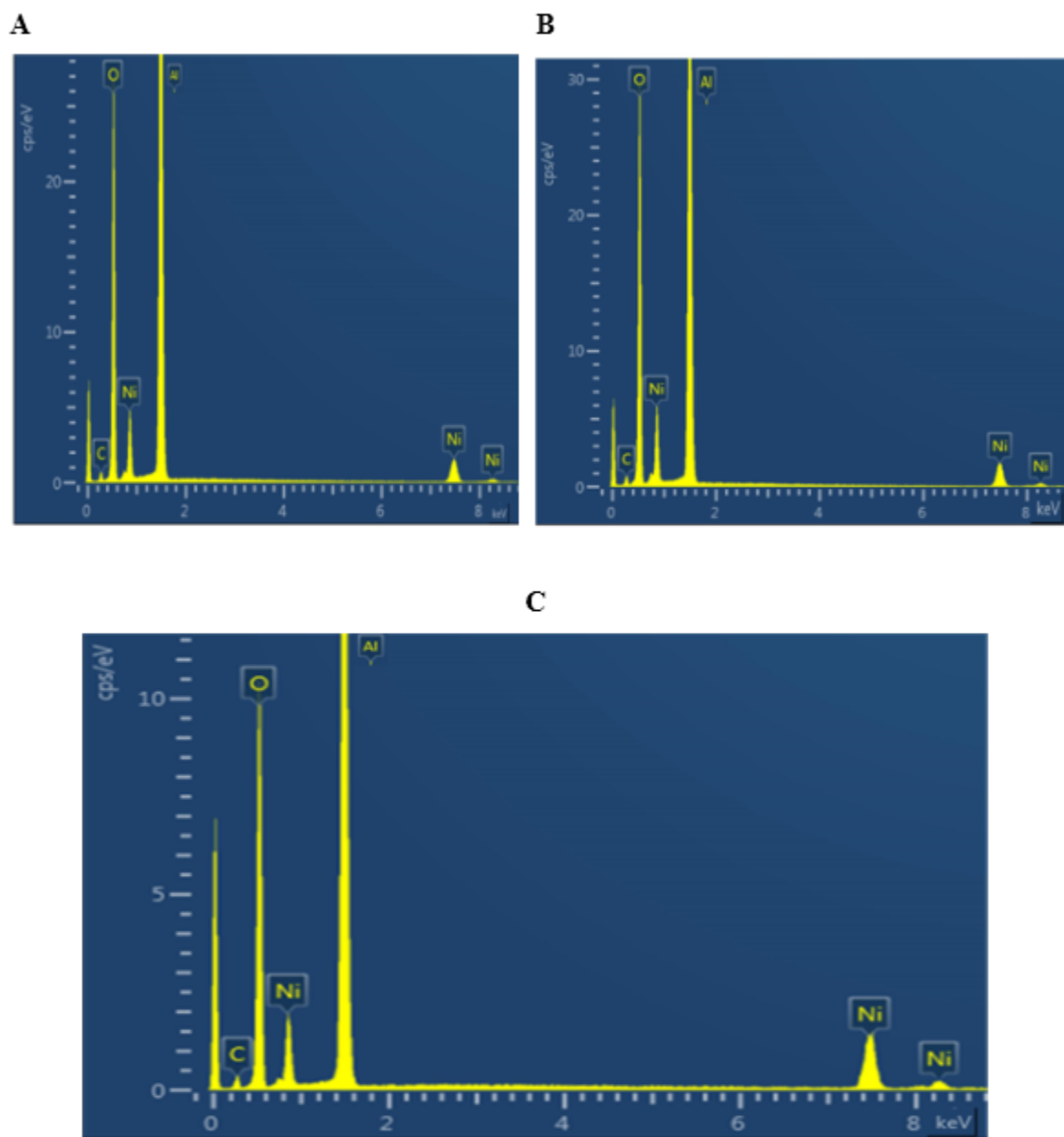


Figure 5-3: EDX images of (A) 6% Ni/ γ -Al₂O₃ (B) 12% Ni/ γ -Al₂O₃ (C) 18% Ni/ γ -Al₂O₃

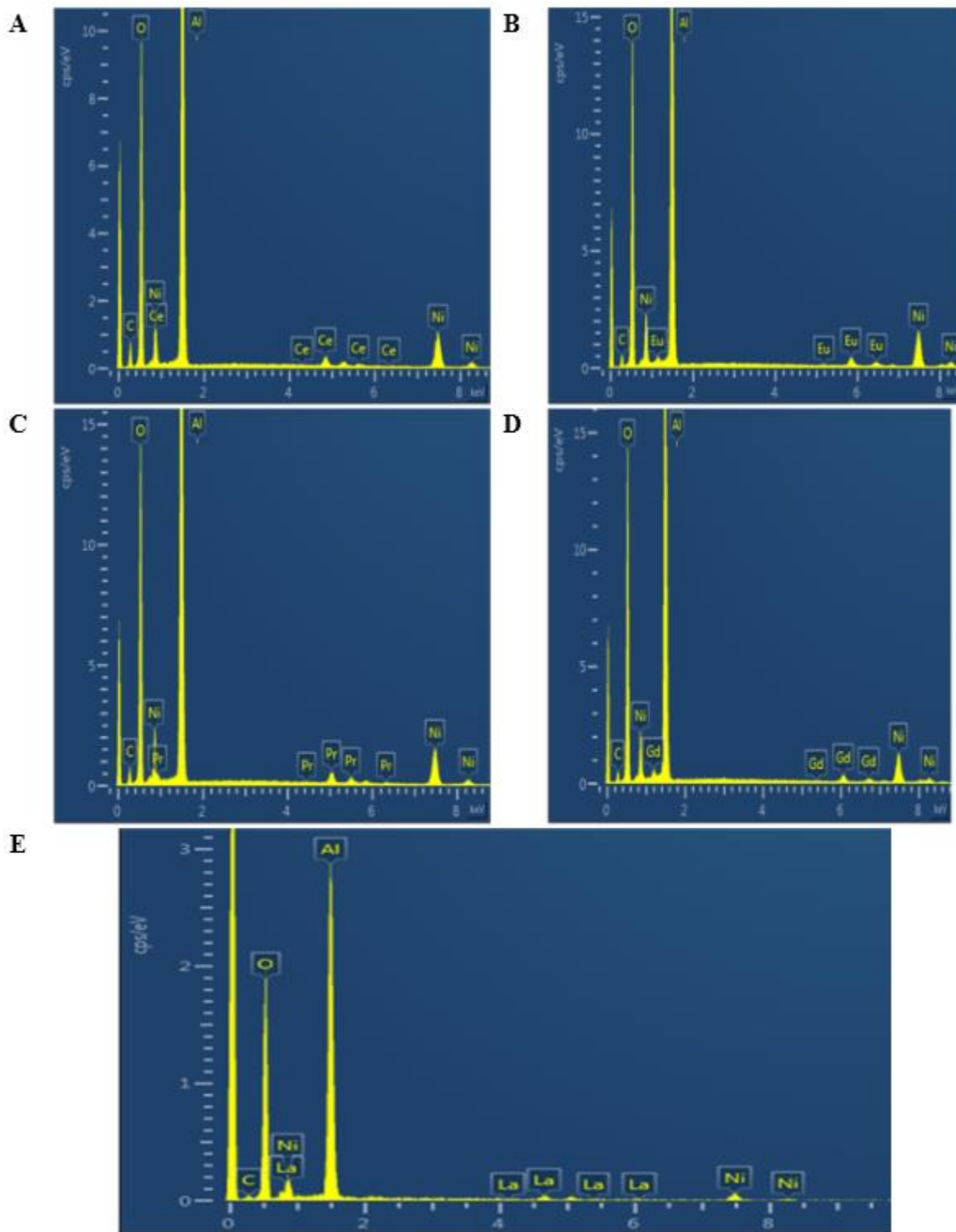


Figure 5-4: EDX images of (A) 5%Ce-12% Ni/ γ -Al₂O₃ (B)5%Eu-12% Ni/ γ -Al₂O₃ (C) 5%Pr-12% Ni/ γ -Al₂O₃ (D) 5%Gd-12% Ni/ γ -Al₂O₃ (E) 5%La-12% Ni/ γ -Al₂O₃

Table 5-3: EDX analysis of Ni based catalysts and Ni based catalysts, impregnated with Lanthanide series.

Catalyst	Weight %					
	Ni	La	Ce	Eu	Pr	Gd
6% Ni/ γ -Al ₂ O ₃	5.8	--	--	--	--	--
12% Ni/ γ -Al ₂ O ₃	11.9	--	--	--	--	--
18% Ni/ γ -Al ₂ O ₃	18.3	--	--	--	--	--
5%La-12% Ni/ γ -Al ₂ O ₃	11.9	4.9	--	--	--	--
5%Ce-12% Ni/ γ -Al ₂ O ₃	12.2	--	4.9	--	--	--
5%Eu-12% Ni/ γ -Al ₂ O ₃	12.1	--	--	5.0	--	--
5%Pr-12% Ni/ γ -Al ₂ O ₃	12.0	--	--	--	5.1	--
5%Gd-12% Ni/ γ -Al ₂ O ₃	12.5	--	--	--	--	4.7

5.1.3 N₂ adsorption / desorption Isotherms Analysis

Figure 5-5 shows the N₂ adsorption–desorption isotherms and corresponding BJH (Barret-Joyner-Halenda) pore size distribution curves of monometallic Ni over γ -Al₂O₃, and lanthanide series promoted bimetallic catalyst samples. Monolayer–multilayer adsorption, a capillary condensation, and a multilayer adsorption on the outer particles surface are the three phases which can be distinguished from the figure in all samples. Non-promoted and the lanthanide promoted samples exhibited a type IV isotherm. N₂-adsorption–desorption isotherms of type IV were related typically to mesoporous materials with a H₂ class of hysteresis loops characterizing ink bottle type of pores [42]. BET surface area, pore size and the total volume of 12%Ni/ γ -Al₂O₃, Ce, Eu, Pr and Gd based catalysts were calculated from the nitrogen adsorption isotherm data and summarized in Table 5-4. The measured BET surface area of γ -Al₂O₃ is 83 m²/g. BET surface area results of 12% and 18% Ni catalysts advocates a considerable difference in the surface area.. The high peak in 18% Ni in XRD results can be attributed to the presence of larger Ni, caused by agglomeration of the Ni species of the catalyst. This is in line with the results from BET specific surface area measurements where it is significantly smaller than for the other samples. The sample promoted with Eu and Gd had the lowest specific surface area. But the Eu-Ni catalyst resulted into higher activity compared to other evaluated materials (La, Ce, and Gd). Ce-Ni catalyst showed the highest surface area compared to other promoted catalysts but showed the lowest conversion of diesel at the same time, as shown in Figure 5-18. This indicates that the specific surface area might not be one of the main characteristics important for a good steam reforming catalyst. It is also reasonable to argue that the main part of the reactions

takes place primarily on the outer surface of the material or close to the pore mouth, due to high reaction temperatures, implying that large specific surface areas might not be one of the key characteristics in steam reforming catalysts.

There are slight variations observed in the total pore volume of all the promoted and non-promoted catalysts. The BJH pore size of monometallic and bimetallic catalysts is measured between 17.4 and 18.5 nm, which suggest a minor variation. From BJH, the pore size distribution curve, it is quite clear that the pore sizes of all the catalysts are very consistent and results are between 17.4 and 18.5 nm. The average pore diameters of all the promoted and non-promoted catalysts are comparable. It could be beneficial for the catalysts to have a larger average pore diameter since the diesel molecules are large and bulky. However, there is no direct trend between catalytic activity and the average pore diameter, so the parameter cannot be considered as a key characteristic of the catalytic material for diesel steam reforming.

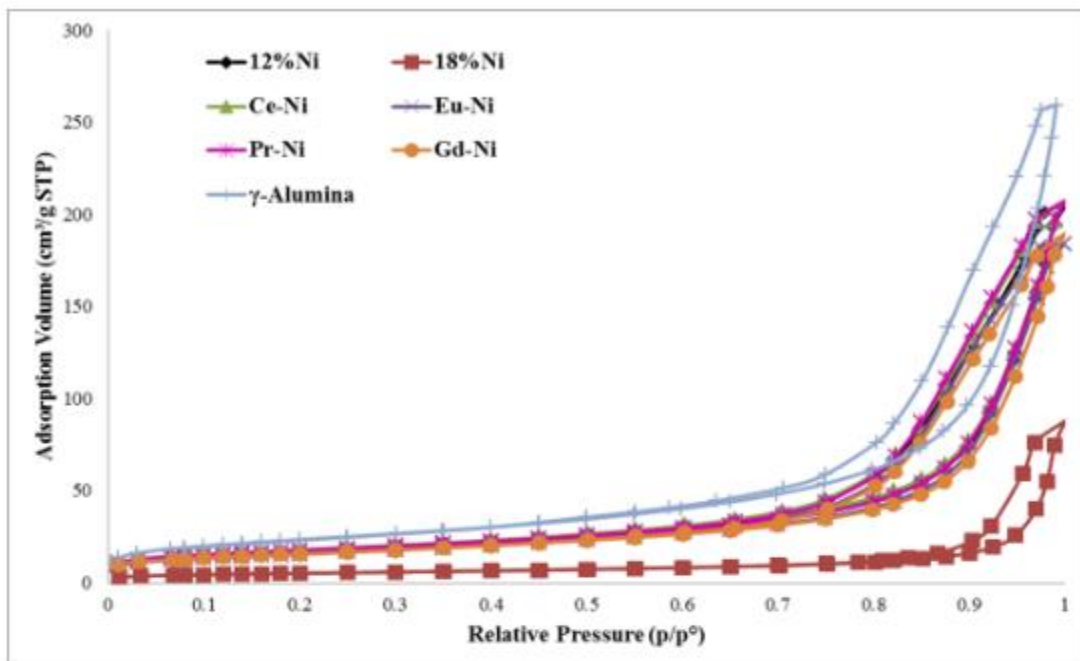


Figure 5-5: N₂ adsorption-desorption isotherm of 12%Ni₃, 18%Ni, Ni-Ce, Ni-Eu, Ni-Pr and Ni-Gd and γ Al₂O₃.

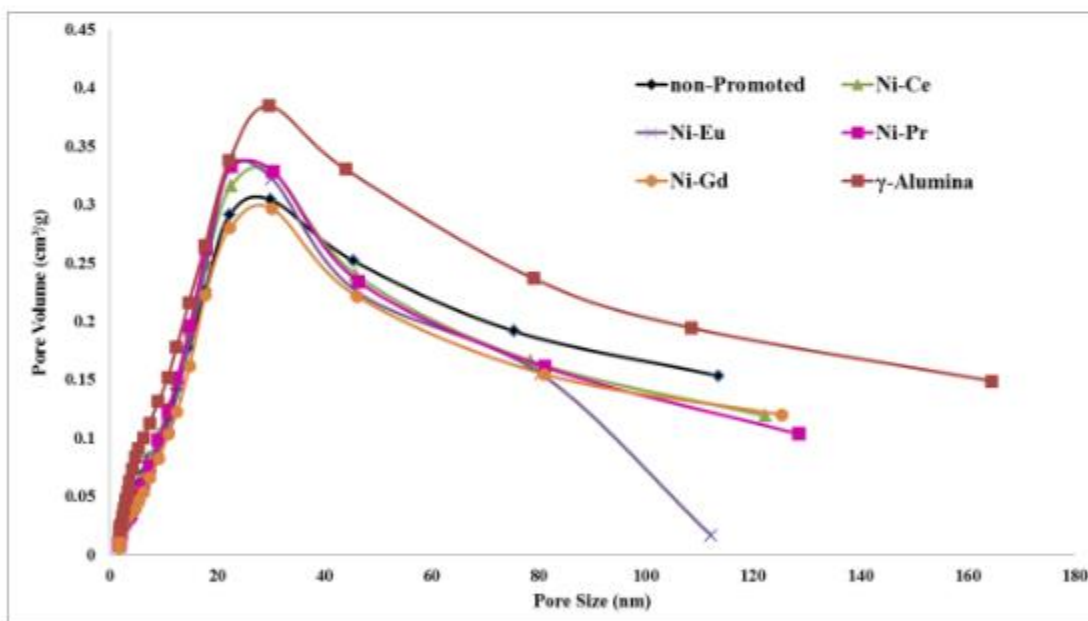


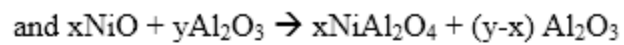
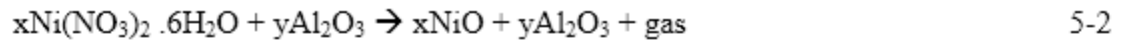
Figure 5-6: BJH pore size distribution of 12%Ni, 18%Ni, Ni-Ce, Ni-Eu, Ni-Pr and Ni-Gd and γ Al₂O₃.

Table 5-4: Surface properties of the Alumina, non-promoted and promoted catalysts.

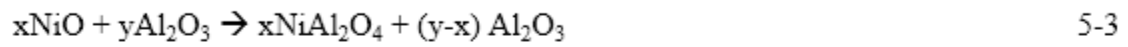
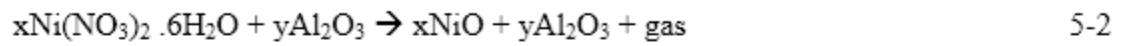
Sample	S _{BET} (m ² g ⁻¹)	d _{BJH} (nm)	V _{total} (cm ³ g ⁻¹)
γ-Al ₂ O ₃	83	17.6	0.63
12%Ni/γ-Al ₂ O ₃	62.54	17.6	0.30
18%Ni/γ-Al ₂ O ₃	18.34		
Ce-Ni/γ-Al ₂ O ₃	63.57	17.9	0.31
Eu-Ni/γ-Al ₂ O ₃	56.29	18.1	0.28
Pr-Ni/γ-Al ₂ O ₃	62.0	18.5	0.31
Gd-Ni/γ-Al ₂ O ₃	56.04	18.14	0.28
La-Ni/γ-Al ₂ O ₃	58.61	17.4	0.29

5.1.4 TPR of Promoted and non-Promoted Catalysts

Temperature Programmed Reduction (TPR) of Non-promoted Catalysts The reduction H₂-TPR measurements were performed on fresh non-promoted catalytic materials, the support and support impregnated with La, Ce, Eu, Pr and Gd. The resulting H₂-TPR profiles are shown in Figure 5-7 and Figure 5-8. The temperature programmed reduction (TPR) profiles of 6%Ni/ γ Al₂O₃, 12%Ni/ γ Al₂O₃ and 18%Ni/ γ Al₂O₃ are shown in Figure 5-7. It is evident from the figure that in all non-promoted catalysts, three main reduction peaks were observed. The first peak observed was due to the reduction of free NiO particles [24]. In 6% Ni catalyst NiO reduction peak was observed at 381 °C, however, in 12% and 18% Ni catalysts peaks were observed at 355 °C and 335 °C respectively. It is also evident that hydrogen consumption in 12% Ni was twice the consumption in 6% Ni and consumption in 18% Ni was thrice the consumption in 6% Ni. The broad peak at low temperature in 18%Ni also suggests most of the nickel is freely available and it has weak interaction with support that is also in accordance with the results obtained from BET and XRD. The second peak observed represents the reduction of dispersed NiO non-crystalline species, and that has strong interaction with support. The reduction peaks at higher temperature are due to the reduction of nickel species strongly interacted with alumina support [43]. In 6%Ni catalyst, second peak was merged in the first bigger peak and is apparent at 585 °C in 12% Ni. In 18% nickel catalyst 2nd peak does not seem to be visible due to the first bigger peak. The third peak around 830 °C is the reduction peak of NiAl₂O₄ and that is irreversible and shows very strong interaction with support. The route to build NiAl₂O₄ in the catalyst included a NiO formation step, as shown in equation.



5-3.



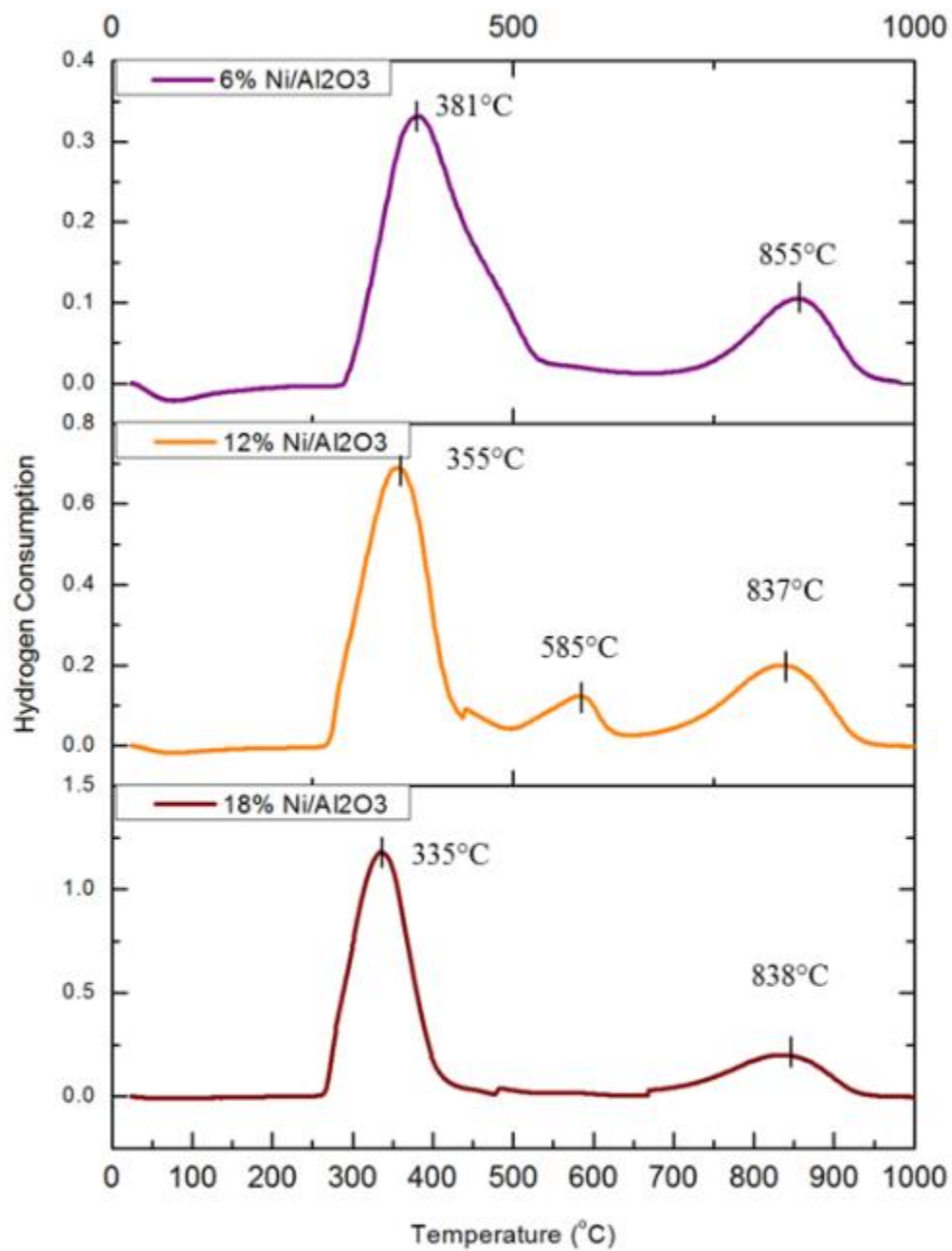


Figure 5-7: TPR profiles of 6%, 12% and 18% nickel impregnated over alumina support.

Temperature Programmed Reduction (TPR) of Promoted Catalysts

Figure 5-8 represent the comparison of TPR profiles of non-promoted and promoted catalyst synthesized in the study. In La-Ni, a new reduction peak at 290 °C appeared, representing the more active metal species in the catalyst, however, the low temperature peak shifted slightly towards higher temperature. Similarly, in case of the Ce-Ni catalyst LT (Low Temperature) reduction peak was found with a slight shift towards higher temperature. For the Eu-Ni, Pr-Ni and Gd-Ni samples, the temperature of the LT peak slightly shifts to higher temperatures compared to that of non-promoted (12%Ni/ γ -Al₂O₃) catalyst, presenting also higher hydrogen consumption. This feature can be related to structural modifications induced in the Ni lattice. The impregnation with lanthanide series suggests an increase in oxygen vacancies in support structure, hence increase the oxygen ion conductivity. This phenomenon was also confirmed by reduction at higher temperature, hence higher H₂ consumption [28]. The shift of 30 °C, 50 °C and 70 °C was observed for Pr-Ni, Gd-Ni and Eu-Ni respectively. The Pr, Gd and Eu promoter strengthens the interaction between active metal and support; however, new low temperature reduction peak in case of Gd promoted catalyst at 321 °C indicates that adding Gd could increase active metal species. The major issue of catalyst deactivation was due to coke formation and the coke formation of the catalyst would be mainly due to transfer of the active metal and further agglomeration on the support surfaces [44]. The weak interactions between support and active metals lead to transfer of active metal, which is not favorable to the sintering resistance ability of the catalyst [45]. However, strengthening the interaction between the active metal and support further improves the sintering and carbon resistance, and inhibit the transfer of active metal and agglomeration

[46]. On the other hand, the high temperature (HT) peak that appeared at 585°C in case of non-promoted catalyst disappeared in case of Pr-Ni and Gd-Ni catalysts, which suggest decreases in its hydrogen consumption compared to non-promoted catalyst. As can be expected, the presence of the dopant cations leads to a lower lattice strain and higher free volume in the oxide network, and then facilitates the equilibrium between surface and bulk oxygen atoms [47]. The Pr promoted, Ni-based catalyst exhibit much higher H₂ uptake than the other materials (much broader peak compared to others), that suggests one possible explanation for Pr-Ni having such high activity might be that more oxygen can be stored, which reduces the coke formation and better steam reforming.

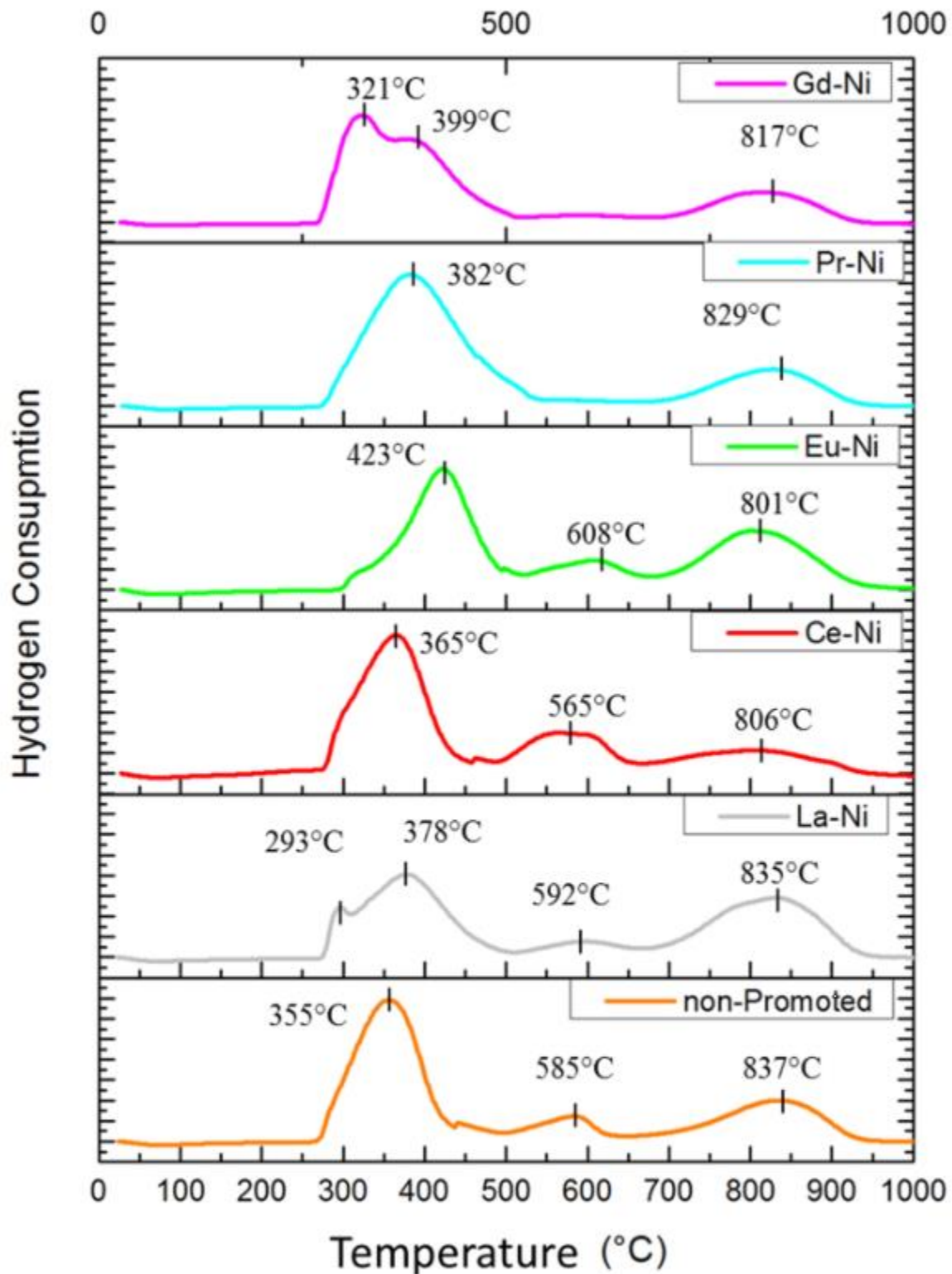


Figure 5-8: TPR profiles of non-promoted and promoted catalysts of La-Ni, Ce-Ni, Eu-Ni, Pr-Ni and Gd-Ni.

5.1.5 Transmission Electron Microscopy (TEM)

Transmission Electron Microscopy or TEM of all the non-promoted and promoted catalysts were performed to find out the particle size and dispersion of metal particles on the surface of alumina support. The representative TEM images of promoted and non-promoted catalyst samples in the reduced form are shown in Figure 5-9. The TEM image of non-promoted catalyst shows that Ni nano-particles are uniformly dispersed on the surface of γ -Al₂O₃ support. Analyses of TEM images suggests uniform dispersion of metal particles (no agglomeration) and other micrographs revealed that grain size is in the range of 9–12nm that support the observations made from XRD measurements. From several TEM images acquired for each sample, the particle size distributions were determined from measurements of several particles. From the particle size distributions, as shown in TEM images, the number averaged particle sizes of all the prepared catalysts were calculated and are shown in the Table 5-5 TEM of Figure 5-10 reveals the uniform dispersion of metal on La-Ni catalyst and average particle size was close to 10.5 nm. The average particle size of Ce-Ni, Eu-Ni, Pr-Ni and Gd-Ni was found to be 9.5nm, 11.7nm, 11.5nm and 10.9nm (from Figure 5-11, Figure 5-12, Figure 5-13 and Figure 5-14). The dispersion of metal particles was improved when non-promoted catalyst was impregnated with the lanthanide series.

Table 5-5: The average particle diameter of promoted and non-promoted catalysts obtained from TEM images.

Sample	Avg. Particle Size (nm) \pm 0.5
Ni/γ-Al₂O₃	11.2
Ce-Ni	9.5
La-Ni	10.5
Gd-Ni	10.9
Pr-Ni	11.5
Eu-Ni	11.7

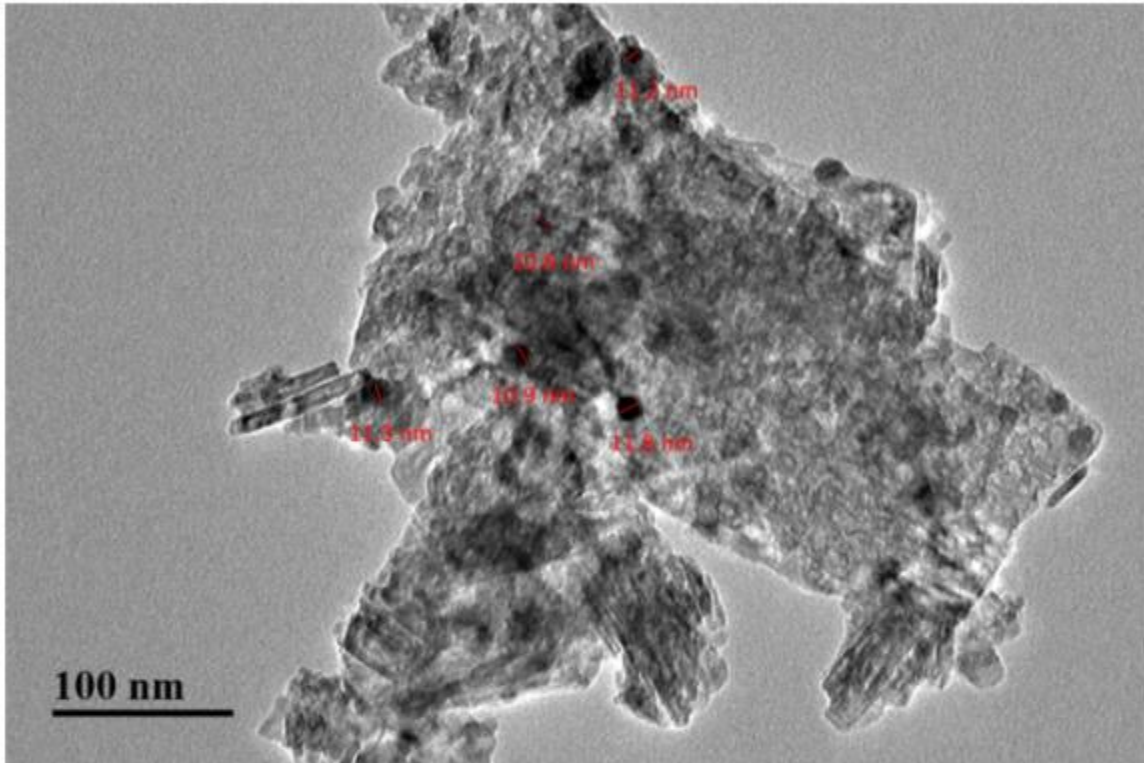


Figure 5-9: TEM image of non-promoted 12%Ni/ γ -Al₂O₃ catalyst sample

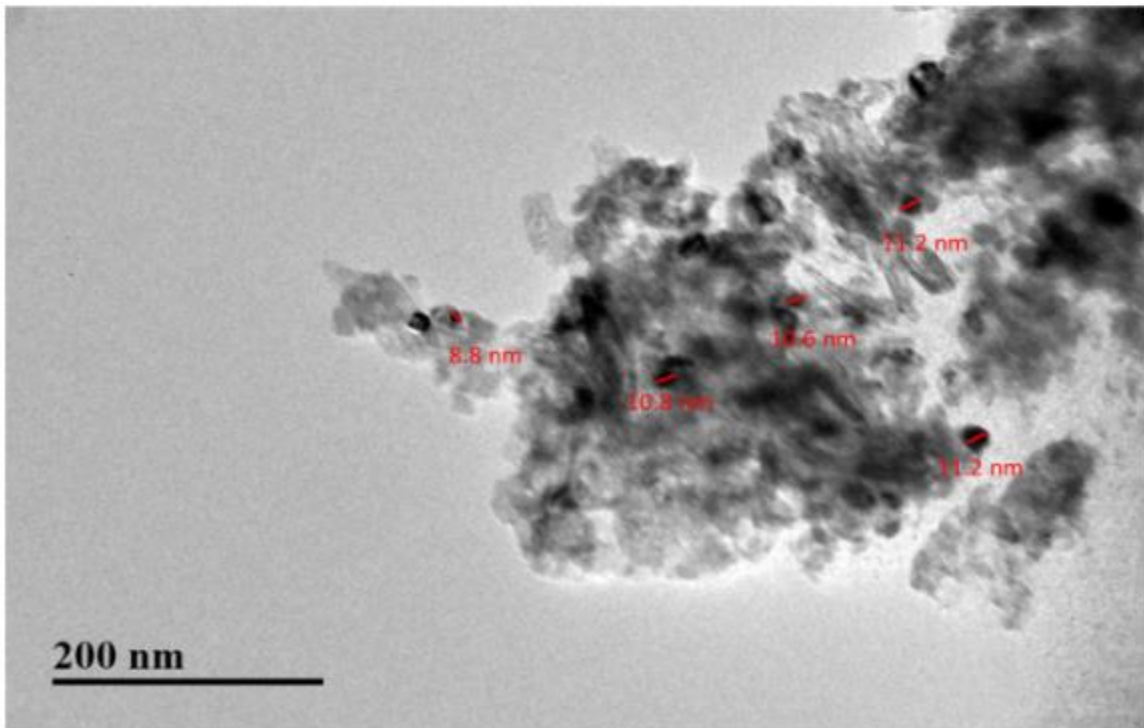


Figure 5-10: TEM image of La-Ni catalyst sample

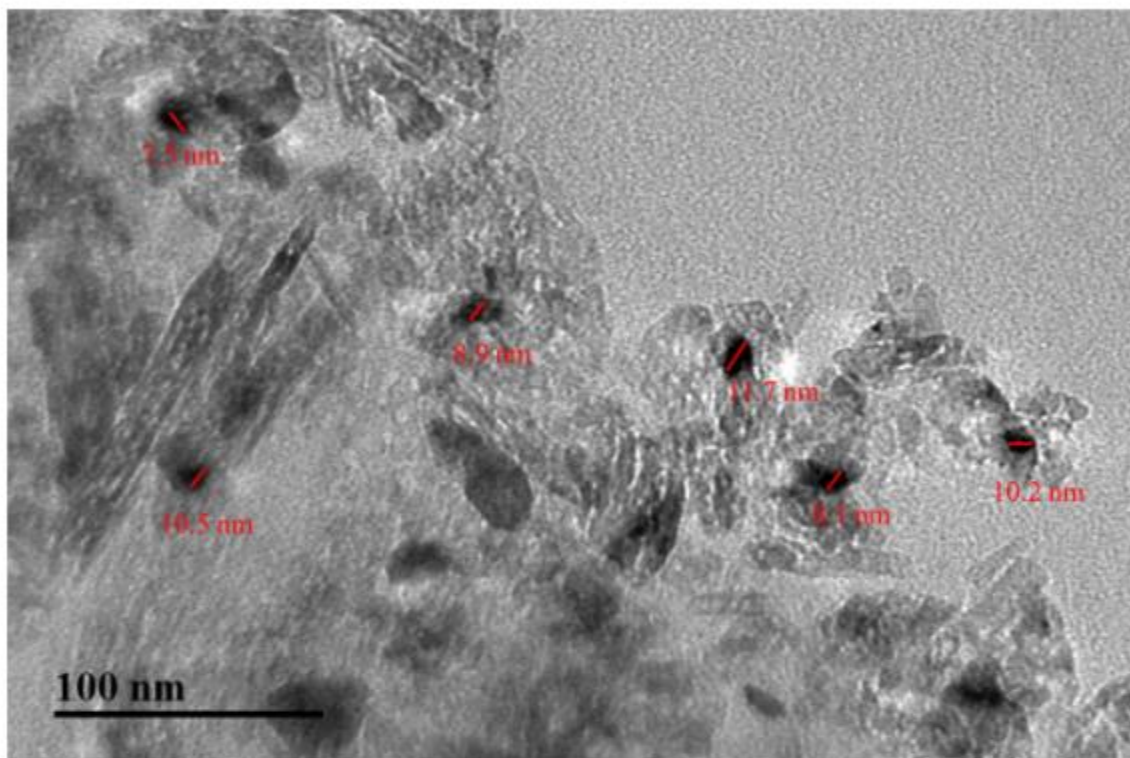


Figure 5-11: TEM image of Ce-Ni catalyst for DSR

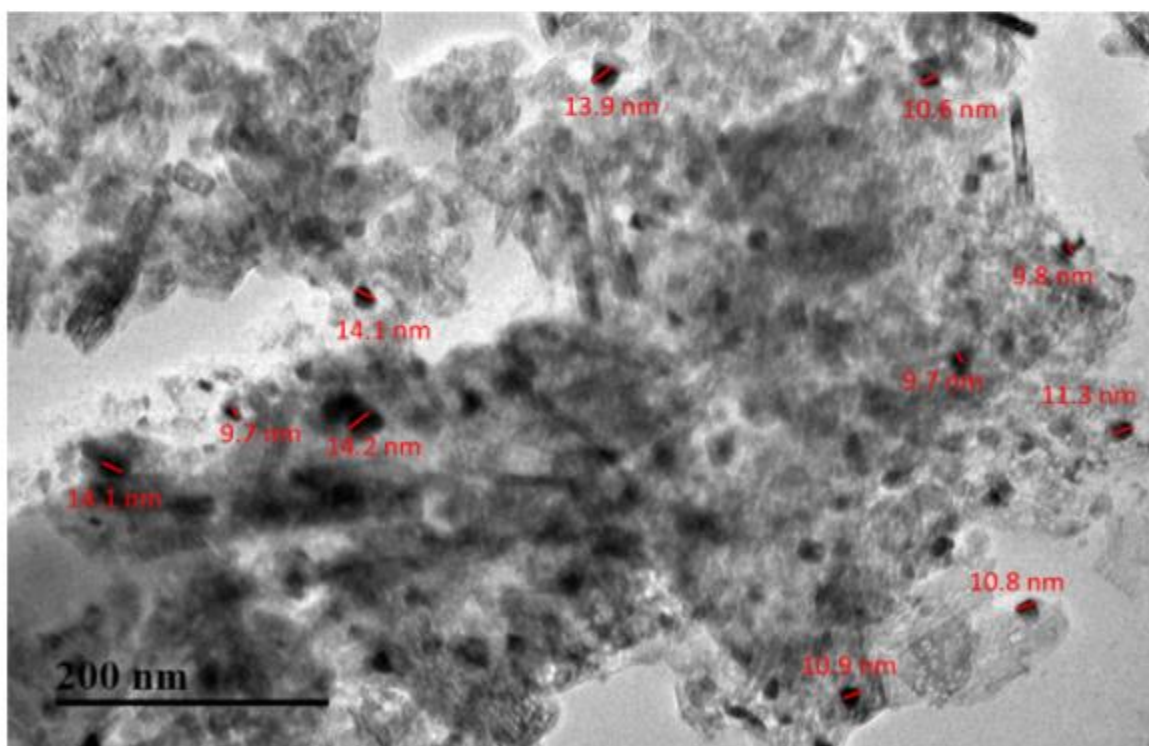


Figure 5-12: TEM image of Eu-Ni catalyst sample

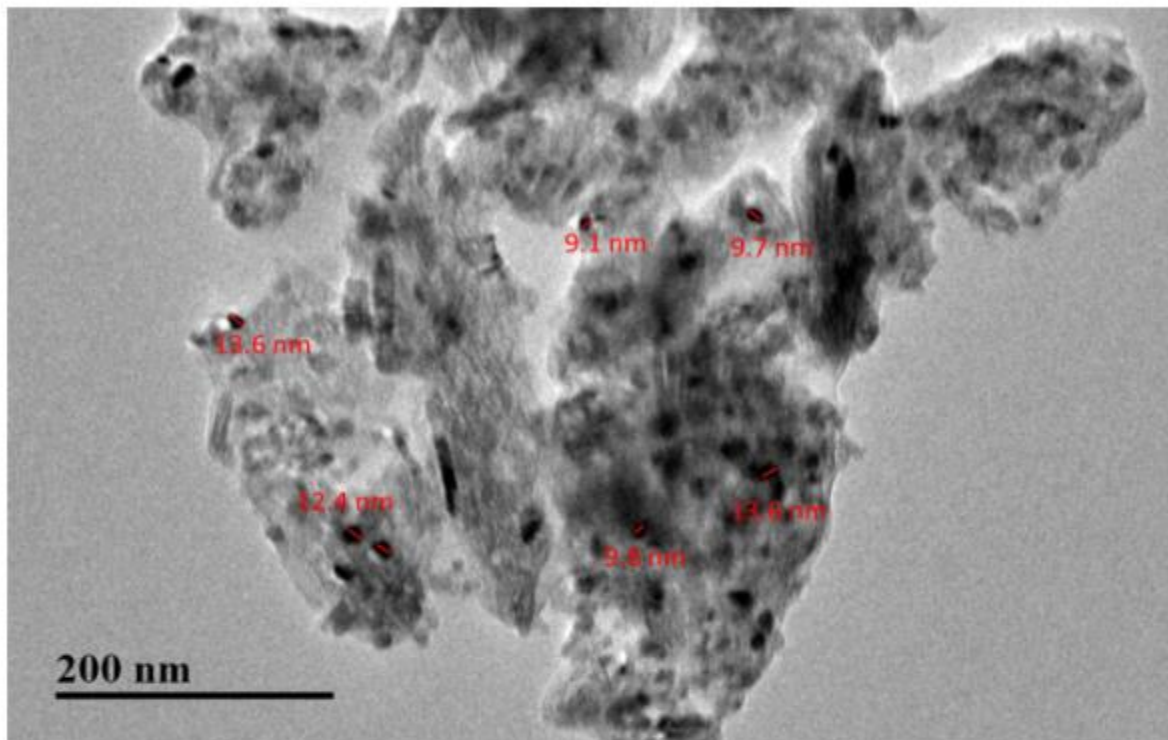


Figure 5-13: TEM image of Pr-Ni catalyst sample

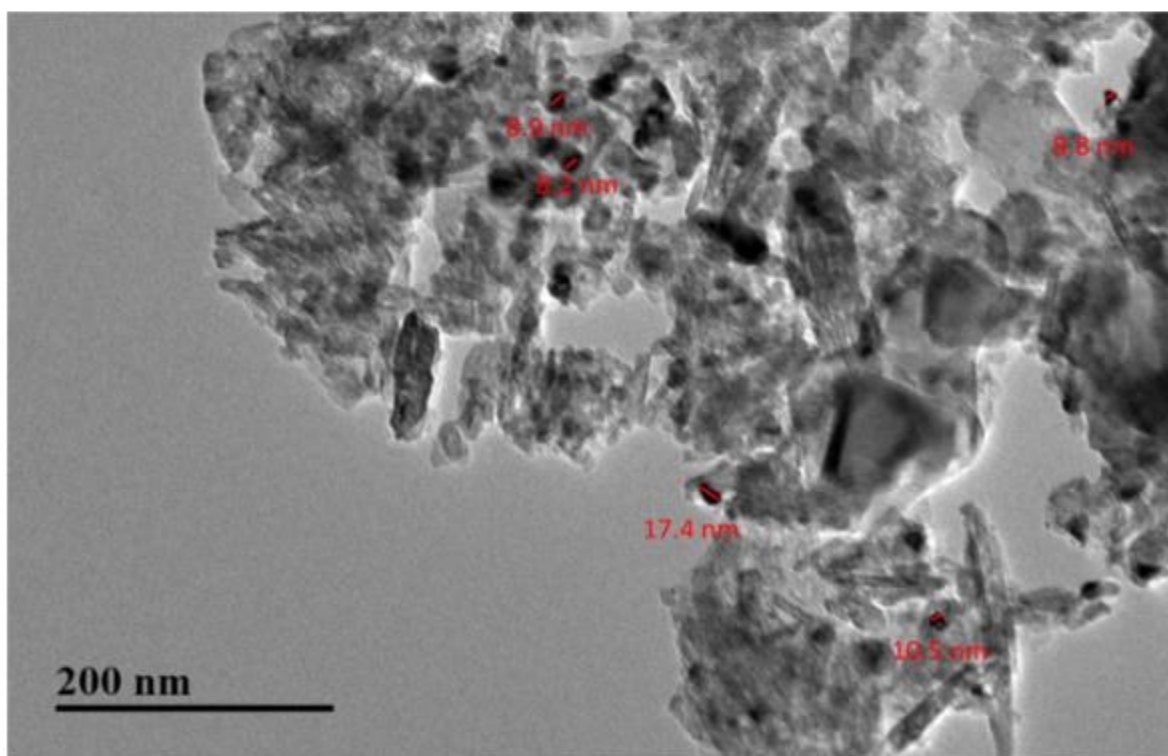


Figure 5-14: TEM image of Gd-Ni catalyst sample

5.2 Performance Evaluation of Synthesized Catalysts

Diesel steam reforming (DSR) experiments were performed in a fixed bed reactor (FBR). Reforming of diesel fuel is more difficult than other available fuels for reforming, mostly due to high contents of coke precursors. Moreover, the sulfur contents of the received diesel fuel were around 6ppm. Diesel fuel was acquired from Saudi Aramco and SimDis analysis was performed. Simulated Distillation (SimDis) is a Gas Chromatographic technique for determining the boiling point distribution of petroleum products by Flame Ionization Detection. SimDis analysis of the diesel fuel was performed and directly related to the boiling points of various hydrocarbons. A calibration curve is generated from a standard sample, where the retention time of each n-alkane is plotted against its boiling point. Figure 5-15 shows a GC-MS chromatogram of diesel. Diesel contains a very high proportion of high molecular weight hydrocarbon chains, ranging from C₁₀ to C₂₄. Along with the paraffins, various types of monocyclic and bicyclic aromatic compounds were also present in a significant amount.

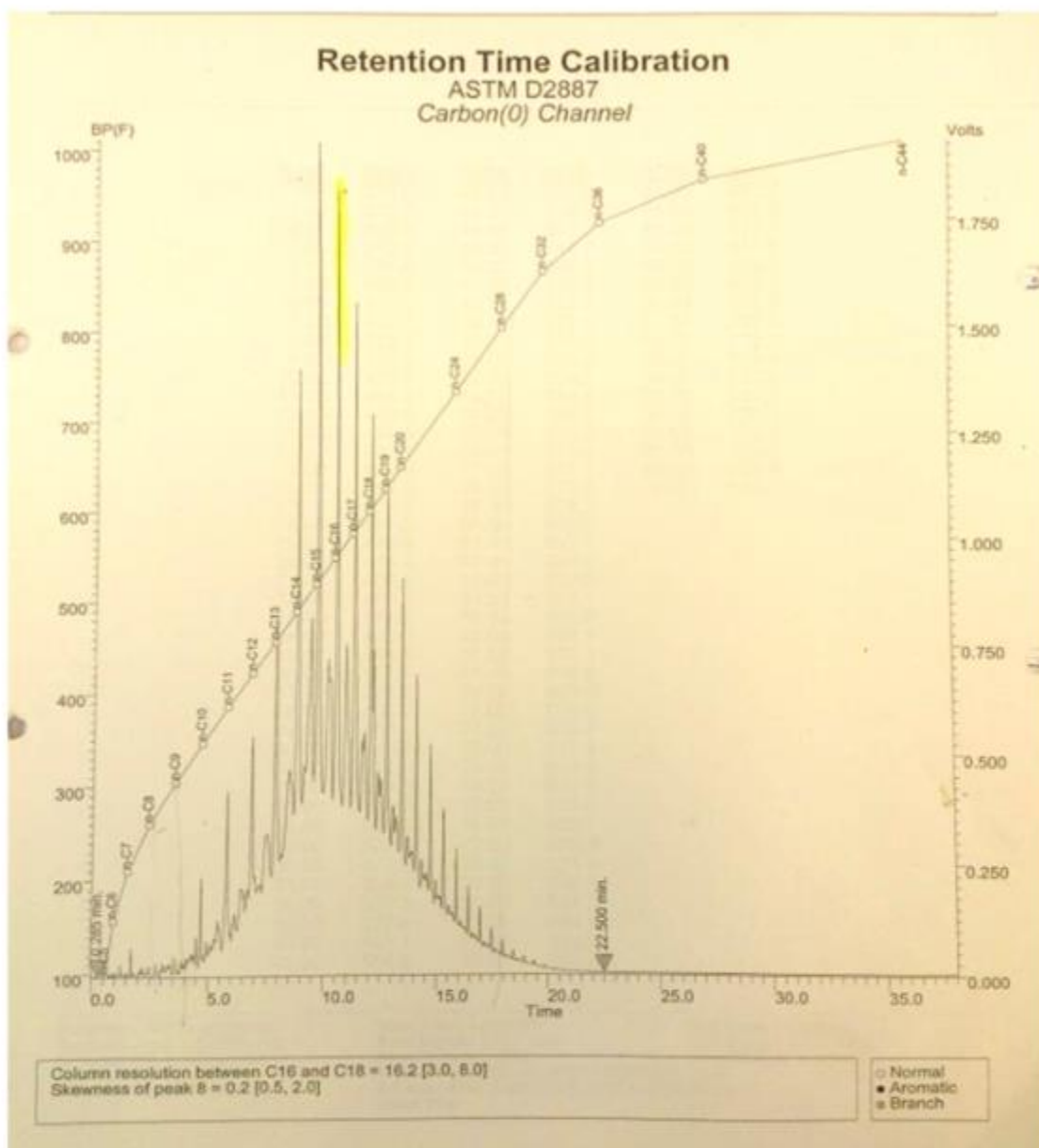


Figure 5-15: SimDis GC-MS results of Diesel used in Diesel Steam Reforming.

Table 5-6: Boiling point distribution of Diesel used in Diesel Steam Reforming by SimDis GC-MS .

Recovery (%)	Temperature (°C)
IBP	143
10	169
20	213
30	244
40	269
50	288
60	307
70	324
80	342
90	365
FBP	427

First of all, blank tests were carried out at a range of different temperatures. Later diesel steam reforming over Ni/ γ -Al₂O₃ with different Ni metal loadings of 6%, 12% and 18% were performed. The purpose of varying nickel weight percent on support was to find out the optimum nickel percent, where hydrocarbon and water conversion were maximum. The effects of varying lanthanide series promoters over non-promoted Ni-based catalysts were also studied. 5% of each Lanthanum (La), Cerium (Ce), Europium (Eu), Praseodymium (Pr) and Gadolinium (Gd) was impregnated on 12% Ni/ γ -Al₂O₃ and performance of each catalyst was separately evaluated in a fixed bed reactor. The feed mixture consisted of diluted Nitrogen, steam and diesel fuel with an average gas hourly space velocity (GHSV) of 5800 h⁻¹, steam to carbon (S/C) ratio of 3.0 and atmospheric pressure. DI (Deionized) water was used as a source of steam; and DI water was pre-

heated at 170°C and pre-mixed with a little flow of nitrogen (15NL/h or 250 ml/min) before it was introduced into the FBR.

The major products of DSR reactions are H₂, CO_x, and CH₄. The GC-17-A by Shimadzu was used to analyze the gaseous products, but to check the concentration of C1+ gases, gas samples were randomly tested in Agilent 3000 micro GC. It was observed that less than 0.5 mole percent of ethylene and propylene were part of the gas stream. Following equations have been used to calculate the conversion, H₂ yield, reforming efficiency and selectivity of different products.

$$\text{Conversion of Diesel (\%)} = \frac{M_{CO_p} + M_{CO_2p} + M_{CH_4p}}{M_{D_r}} \times 100 \quad 5-4$$

$$\text{Water Conversion (\%)} = \frac{\text{Water In} - \text{Water Out}}{\text{Water In}} \quad 5-5$$

$$S_{H_2} (\%) = \frac{M_{H_2p}}{M_{CO_2p} + M_{CO_p} + M_{CH_4p} + M_{H_2p}} \times 100 \quad 5-6$$

$$S_{CO} (\%) = \frac{M_{CO_p}}{M_{CO_2p} + M_{CO_p} + M_{CH_4p} + M_{H_2p}} \times 100 \quad 5-7$$

$$S_{CO_2} (\%) = \frac{M_{CO_2p}}{M_{CO_2p} + M_{CO_p} + M_{CH_4p} + M_{H_2p}} \times 100 \quad 5-8$$

$$S_{CH_4} (\%) = \frac{M_{CH_4p}}{M_{CO_2p} + M_{CO_p} + M_{CH_4p} + M_{H_2p}} \times 100 \quad 5-9$$

$$\text{Yield of } H_2 (\%) = \frac{M_{H_2p}}{M_{H_2T}} \times 100 \quad 5-10$$

$$\eta = \frac{h_{prod}}{h_{diesel}} = \frac{(M_{CO_p} + M_{H_2p}) \cdot h_{H_2-LHV}}{M_{Diesel} \cdot h_{diesel-LHV}} \quad 5-11$$

M_{CO_p} , M_{CO_2p} , M_{CH_4p} , M_{H_2p} are amounts (mol) of CO, CO₂, CH₄, and H₂ respectively in the products. However, M_{D_r} is the amount (mol) of diesel's carbon in reactants. M_{H_2T} is the theoretical Hydrogen production (mol) and η is the efficiency of reforming and 'h' is the enthalpy.

5.2.1 Blank Runs

Prior to diesel steam reforming over monometallic and bimetallic catalysts, blank runs were performed at different temperatures and steam to carbon ratio of 3.0. There was no significant conversion of diesel observed between 350 °C to 500 °C. A very small flow of hydrogen and methane were observed at temperatures higher than 550 °C. Cracking of diesel was observed and resulted in water production and carbon deposits were observed once the reactor was removed. Hydrogen selectivity was more than 92% at 620 °C and of methane was 8%. Selectivity of carbon monoxide and carbon dioxide was 0% and very little quantity of water was also produced.

5.2.2 Diesel Steam Reforming in a Gibbs free Reactor in Aspen HYSYS®

Equilibrium compositions were calculated by minimization of Gibb's free energy. Aspen Hysys v 7.3 software has been used for calculations. The code requires specification of the system i.e. reactor for the calculations. The Gibb's reactor has been selected for the calculations using the Peng-Robinson property method. For the purpose of simulation all the reaction conditions, S/C (3.0) ratio and flow rates were defined as in real reactions. Equilibrium conversion was calculated at three different temperatures (580°C, 600°C and 620°C), and results were compared with the results obtained from Pr-Ni catalyzed steam reforming. Aspen Hysys code also requires the definition of products. Hydrogen, CO, CO₂, CH₄, C (graphite), remaining fuel as well as water were considered as the product of reforming. Ethane, Propane, Ethylene, Propylene and various other compounds were included. The results are presented as gaseous products on dry basis. After running simulation at three different temperatures and keeping the other reaction conditions and

flow rates constant, it was found that conversion of diesel was 100%, C1+ gases were found less than 10^{-6} mol% so neglected and no coke formation was observed. So, only the four major products were further considered, hydrogen, carbon monoxide, carbon dioxide and methane.

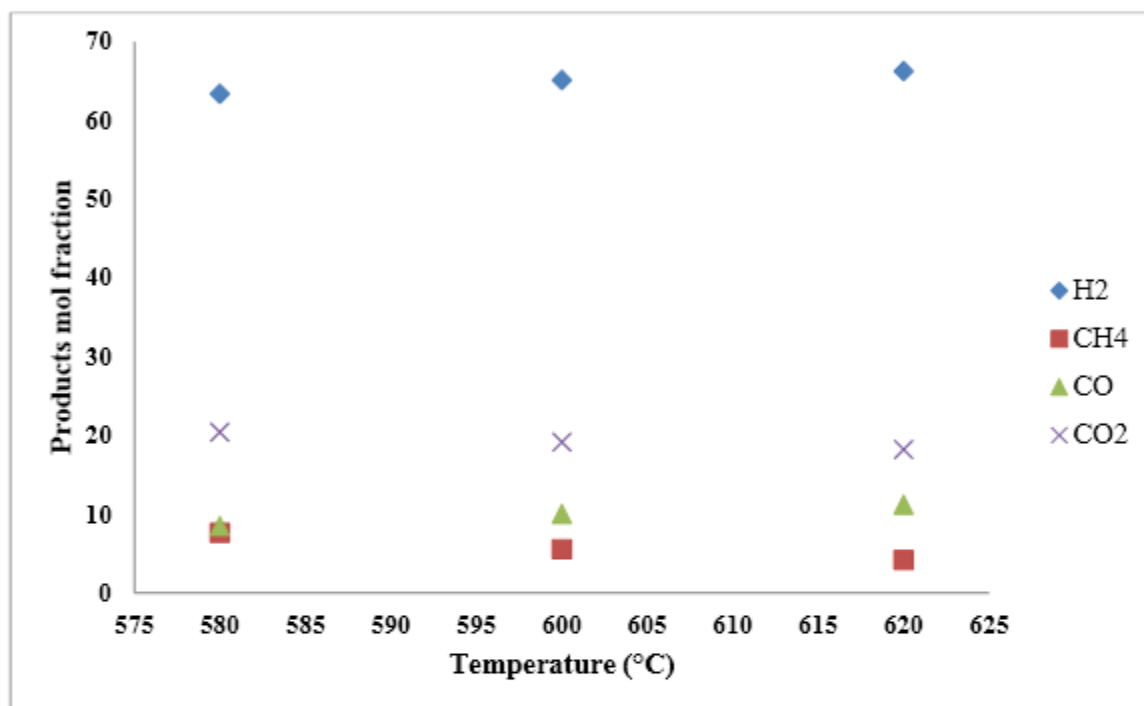


Figure 5-16: Diesel steam reforming, the effect of temperature on an equilibrium product composition at, S/C = 3.0, P = 1 atm.

5.2.3 Diesel Steam Reforming over the non-promoted Ni/ γ -Al₂O₃ Catalyst

Activity of a Ni/ γ -Al₂O₃ catalyst with different Ni metal loadings on γ -Al₂O₃ was observed in a fixed bed reactor system. Evaluations of all the catalysts were conducted at 620°C, a steam to carbon ratio of 3.0 and GHSV of 5800 h⁻¹ as mentioned in the earlier section, unless otherwise mentioned. Reaction conditions, feed streams, feed composition, catalyst position and reaction temperatures were kept constant. Using the previously mentioned formula, conversion of diesel and water has been displayed in the following

figures. By closely looking at the comparison of the diesel conversion in Figure 5-17 and selectivity in Table 5-7 of different gases in the product stream, it is easy to suggest that maximum diesel conversion was achieved with 12 % Ni metal loading. Steam reforming begins to dominate when 12%Ni catalyst was used, hence selectivity of methane was found lowest.

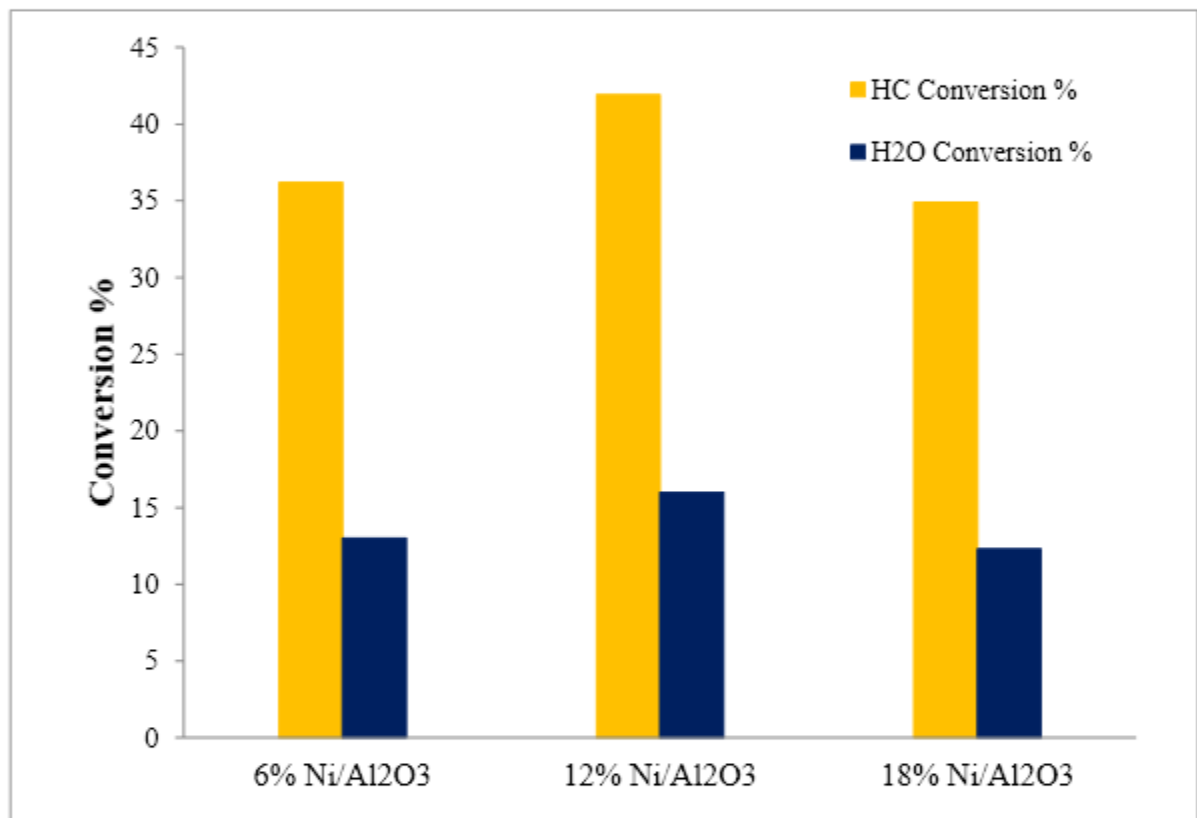


Figure 5-17: Diesel Steam reforming on the surface of Ni/Al₂O₃ catalyst with different Ni metal loading of 6% to 18% in 10 hours; at 620 °C, 1 atm, S/C = 3.0, GHSV of 5800 h⁻¹ and sulfur in fuel = 6 ppm.

Table 5-7: Conversion and selectivity of 6%Ni/ γ -Al₂O₃, 12%Ni/ γ -Al₂O₃ and 18%Ni/ γ -Al₂O₃ (Time = 10h, S/C = 3.0, GHSV = 5800 h⁻¹, pressure = 1bar, Temperature = 620 °C)

Metal Loading %	Diesel Conversion %	Water Conversion %	H ₂ Selectivity %	CO Selectivity %	CO ₂ Selectivity %	CH ₄ Selectivity %
6	36.2	13	71.0	6.2	19	3.8
12	41.7	18.5	73.2	5.7	20.1	1.0
18	34.9	12.3	72.5	7.4	18.2	1.9

5.2.4 Diesel Steam Reforming over Lanthanide promoted Ni/ γ -Al₂O₃ Catalyst

In this section all the lanthanide series promoted catalysts were subjected to time-on-stream experiments. Time-on-stream experiments for La-Ni, Ce-Ni, Eu-Ni, Pr-Ni and Gd-Ni catalysts were run at 620°C, S/C = 3.0, 1 atmospheric pressure and GHSV (Gas Hourly Space Velocity) = 5800 h⁻¹. These conditions are similar to the conditions employed during performance evaluation of non-promoted Ni-based (6%, 12% and 18%) catalysts. Diesel conversion, hydrogen percentage yield and selectivities of hydrogen, carbon monoxide, carbon dioxide, and methane were also calculated and presented.

Figure 5-18 compares the conversion of as a function of time on stream of all the lanthanide series promoted catalyst, while Table 5-8, Table 5-9, Table 5-10, Table 5-11 and Table 5-12 represents the selectivity of H₂, CO, CO₂, and CH₄ over the period of 40 h. In La-Ni activity of the catalyst was found consistent during the first 10 hours of reaction

and conversion of diesel and water was also found consistent due to its coke resistance ability [48].

Table 5-8: Conversion and selectivity of 5%La-12%Ni/ γ Al₂O₃ (Time = 40h, S/C = 3.0, GHSV = 5800 h⁻¹, pressure = 1atm, Temperature = 620 °C)

Time on stream h	Diesel Conversion %	Water Conversion %	H ₂ Selectivity %	CO Selectivity %	CO ₂ Selectivity %	CH ₄ Selectivity %
10	52.9	29.4	71.1	6.7	20.1	2.2
20	47.2	23.5	72.4	5.5	20.7	1.3
30	37.3	18.2	73.1	5.5	20.2	1.2
40	24.5	11.8	74.0	5.0	19.7	1.3

Cerium has been used as a promoter along with the nickel on the support of alumina and it helped suppressing the carbon deposition during steam reforming reactions [49] [48]. To understand and endorse the effect of cerium on diesel steam reforming; ceria supported by metallic catalyst was synthesized and evaluated for the same working conditions as mentioned previously. Figure 5-18 shows the effect of 5% cerium on 12% Ni/ γ Al₂O₃ catalyst for 40 h. Activity for the catalyst was found to decrease with increasing time on stream (TOS). It's evident from the following figure that a decline in diesel conversion was relatively low as compared to the lanthanum promoted bimetallic catalyst. A decline of 45% was found in diesel conversion and 50% decline in water

conversion was recorded in 40 h TOS. Although the conversion of diesel found declining with TOS but selectivity of hydrogen was found consistent throughout the evaluation

Table 5-9: Conversion and selectivity of 5%Ce-12%Ni/ γ -Al₂O₃ (Time = 40h, S/C = 3.0, GHSV = 5800 h⁻¹, pressure = 1atm, Temperature = 620 °C)

Time on stream h	Diesel Conversion %	Water Conversion %	H ₂ Selectivity %	CO Selectivity %	CO ₂ Selectivity %	CH ₄ Selectivity %
10	50.8	24.8	73.0	5.6	20.2	1.2
20	42.0	20.6	73.3	5.8	19.4	1.5
30	31.1	15.0	73.6	5.7	19.0	1.6
40	27.5	12.5	73.7	5.2	19.1	2.0

Europium is not a renowned promoter or catalyst used for diesel steam reforming because not much literature found stating the use of europium as promoter for the nickel supported alumina catalysts. The conversion of diesel was found very consistent during first 10 h of reaction and later a huge decline was observed after 20 h of TOS. Similarly, water conversion was found consistent during the first 20 h on TOS and later decreased to a minimum value. A decline of 40% in diesel conversion was found in 40 h of reaction and that is less than compared to lanthanum promoted bimetallic catalyst and equivalent to ceria promoted catalyst. The steam reforming reaction is selective towards hydrogen during TOS and that is evident from the Table 5-10. The conversion of diesel was found decreasing with TOS due to coke formation.

Table 5-10: Conversion and selectivity of 5%Eu-12%Ni/ γ -Al₂O₃ (Time = 40h, S/C = 3.0, GHSV = 5800 h⁻¹, pressure = 1atm, Temperature = 620 °C)

Time on stream h	Diesel Conversion %	Water Conversion %	H ₂ Selectivity %	CO Selectivity %	CO ₂ Selectivity %	CH ₄ Selectivity %
10	56.9	28.2	73.3	5.8	20.4	1.4
20	49.4	23.6	72.2	5.7	20.6	1.5
30	37.9	15.6	73.7	4.8	20.1	1.3
40	30.6	10.8	74.0	4.6	19.8	1.5

During the evaluation process of 5% praseodymium promoted 12% nickel supported γ -alumina catalyst (Figure 5-18), it was observed that the catalyst performed best among the other lanthanide promoted catalysts. Conversions of diesel and water during first ten hours were found highest and similarly the decline in diesel and water conversion during TOS was found a minimum. It is evident from the Table 5-11 that the selectivity of hydrogen is consistent during TOS. Similarly, the decline in conversion with the passage of time was found minimum comparing to all lanthanide promoted catalysts evaluated during this study, i.e. 50% and decline in diesel conversion was also found a minimum (i.e. 50%) on 5%Pr-12%Ni/ γ -Al₂O₃.

Table 5-11: Conversion and selectivity of 5% Pr-12%Ni/ γ Al₂O₃ (Time = 40h, S/C = 3.0, GHSV = 5800 h⁻¹, pressure = 1atm, Temperature = 620 °C)

Time on stream h	Diesel Conversion %	Water Conversion %	H ₂ Selectivity %	CO Selectivity %	CO ₂ Selectivity %	CH ₄ Selectivity %
10	71.8	33.4	71.4	6.1	20.5	2.0
20	62.8	30.4	71.6	6.0	20.5	2.0
30	52.0	24.0	72.3	5.7	20.3	1.7
40	35.8	16.4	72.7	5.8	19.9	1.7

Figure 5-18 shows the conversion of diesel at 5% gadolinium promoted 12% nickel supported γ alumina catalyst with TOS. It is evident that diesel conversion and hydrogen yield was constant during the first 20 h of reaction and later a significant decline in diesel conversion was observed. It is speculated that coke formation at catalyst was increased abruptly after 20 h of reaction and resulted in decline of diesel conversion however, selectivity of hydrogen remains consistent. Although percentage yield of hydrogen reduced with TOS but concentration of hydrogen in product gas remains consistent.

Table 5-12: Conversion and selectivity of 5% Gd-12%Ni/ γ -Al₂O₃ (Time = 40h, S/C = 3.0, GHSV = 5800 h⁻¹, pressure = 1atm, Temperature = 620 °C)

Time on stream h	Diesel Conversion %	Water Conversion %	H ₂ Selectivity %	CO Selectivity %	CO ₂ Selectivity %	CH ₄ Selectivity %
10	56.6	25.8	71.4	6.1	20.5	2.0
20	54.2	21.5	72.6	5.6	20.1	1.6
30	34.9	13.6	71.4	6.1	20.5	2.0
40	21.8	9.7	74.2	4.6	19.4	1.8

Figure 5-18 shows the variation in conversion of diesel (COD) over different promoted and non-promoted Ni-based (12%Ni) catalyst over time on stream (TOS). According to comparison of conversion, Pr-Ni bimetallic catalyst exhibits the highest conversion activity during the 40 h run. According to TPR of Pr-Ni catalyst, it strengthens the interaction between the active metal and support, thus it blocked the transfer and agglomeration of the active metal. On the other hand Eu-Ni and Gd-Ni also demonstrated excellent results compared to the non-promoted nickel catalyst. In case of Ce-Ni and La-Ni catalysts, conversion was lower compared to other promoted catalysts. For Ce and La promoted catalysts, the dispersion decreased to a certain value, which should be attributed to the transfer and agglomeration of the active metal [24]. Reactions (3) and (4) in section 2.1 represents the methanation reactions of CO_x during diesel steam reforming. The methanation reactions shift the equilibrium of reaction (1) to the right side and hence enhanced the diesel steam reforming reaction. Table 5-13 shows that when Pr, Gd and La

catalysts were used CH₄ selectivity was twice as compare to non-promoted catalyst. Due to heavy coke formation, choking of reactor and pressure buildup (up to 3bar) the reaction over non-promoted catalysts were stopped after 10h of reaction; however, all the promoted catalysts were successfully working for 40 hours. The speculated reason of decline in catalyst activity was later confirmed when CHNS and TGA of all the spent catalysts was performed. It is evident from the following comparison that praseodymium promoted Ni-based catalyst proved best in the study.

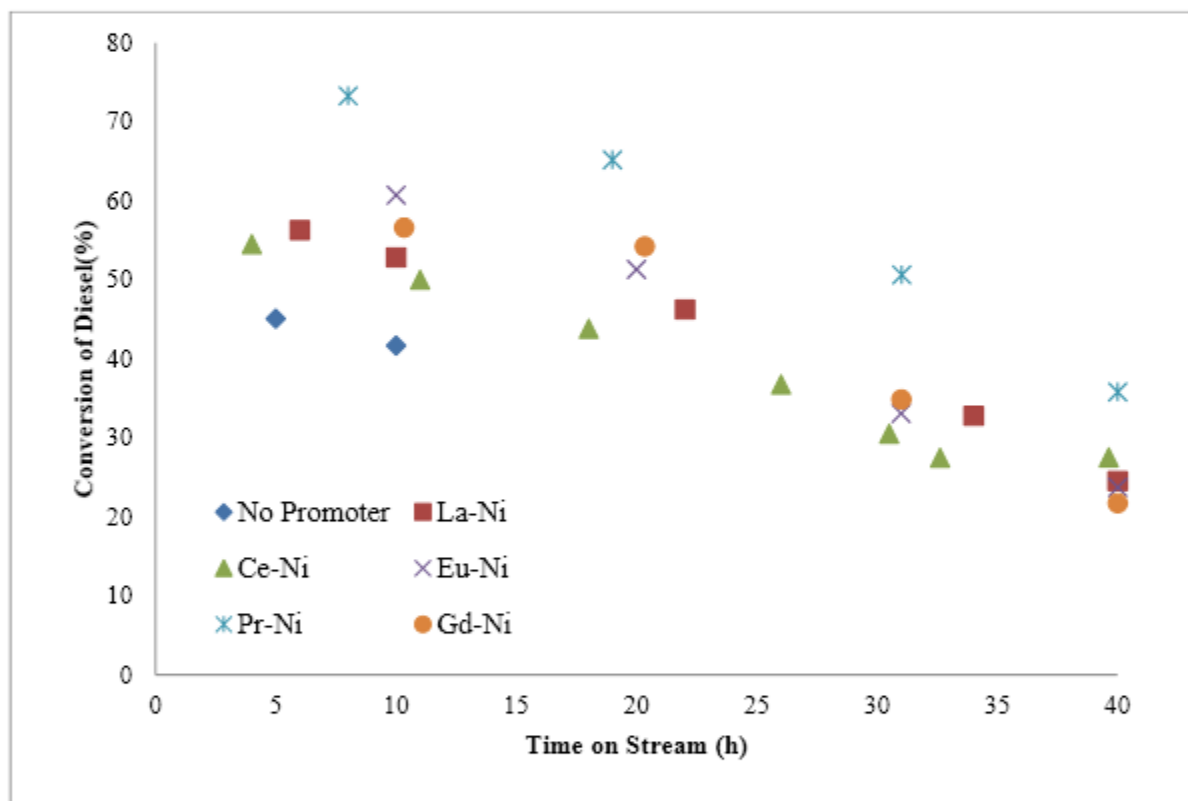


Figure 5-18: Conversion of Diesel during a 40h run over Lanthanide promoted bimetallic and non-promoted monometallic Ni-based catalysts at 620 °C, 1 atm, S/C = 3.0, GHSV of 5800 h⁻¹ and sulfur in fuel = 6 ppm

Figure 5-19 shows a comparison of the hydrogen yield of these catalysts during the 40h run at 620 °C and atmospheric pressure. From the start of the reaction the hydrogen yield of all the lanthanide promoted catalysts showed an obvious influence and once again Pr-Ni catalyst dominated other promoted and non-promoted catalysts. It was clear from the comparison that hydrogen yields were higher in lanthanide promoted catalysts than that over non-promoted catalysts; similarly, there were significant differences between the hydrogen yields obtained from different promoters. Although difference of the hydrogen yield of La-Ni, Ce-Ni and Gd-Ni promoted catalysts from non-promoted catalyst was not significant in the start of the reaction but Eu-Ni and Pr-Ni showed very good performance in the first 10 h of the reaction with Pr-Ni produced more than 75% H₂ (yield) (calculated at the 10h time). It was also observed that the yield of H₂ in Gd-Ni catalyst was consistent for the first 20 hours of reaction and that shows it's better coke formation resistance than the La-Ni and Ce-Ni or non-promoted catalyst. The decline in yield with TOS is either due to coke formation and the blockage of active sites or this behavior occurs mainly due to the oxidation of active sites (due to excessive steam) [49]. The efficiency of the reforming process was calculated for all the promoted catalysts (after 40h of reaction) by

$$\text{using equation } \eta = \frac{h_{prod}}{h_{diesel}} = \frac{(M_{CO_p} + M_{H_2p}) \cdot h_{H_2-LHV}}{M_{Diesel} \cdot h_{diesel-LHV}}$$

5-11 and results are shown in Figure 5-20. The reforming efficiency of Pr-Ni catalyst was best amongst all the promoted catalysts. It was also observed that, although the conversion of diesel and the H₂ %Yield for Eu-Ni was better compared to Gd-Ni catalyst but overall reforming efficiency was higher in case of Gd-Ni compared to Eu, Ce and La promoted catalysts.

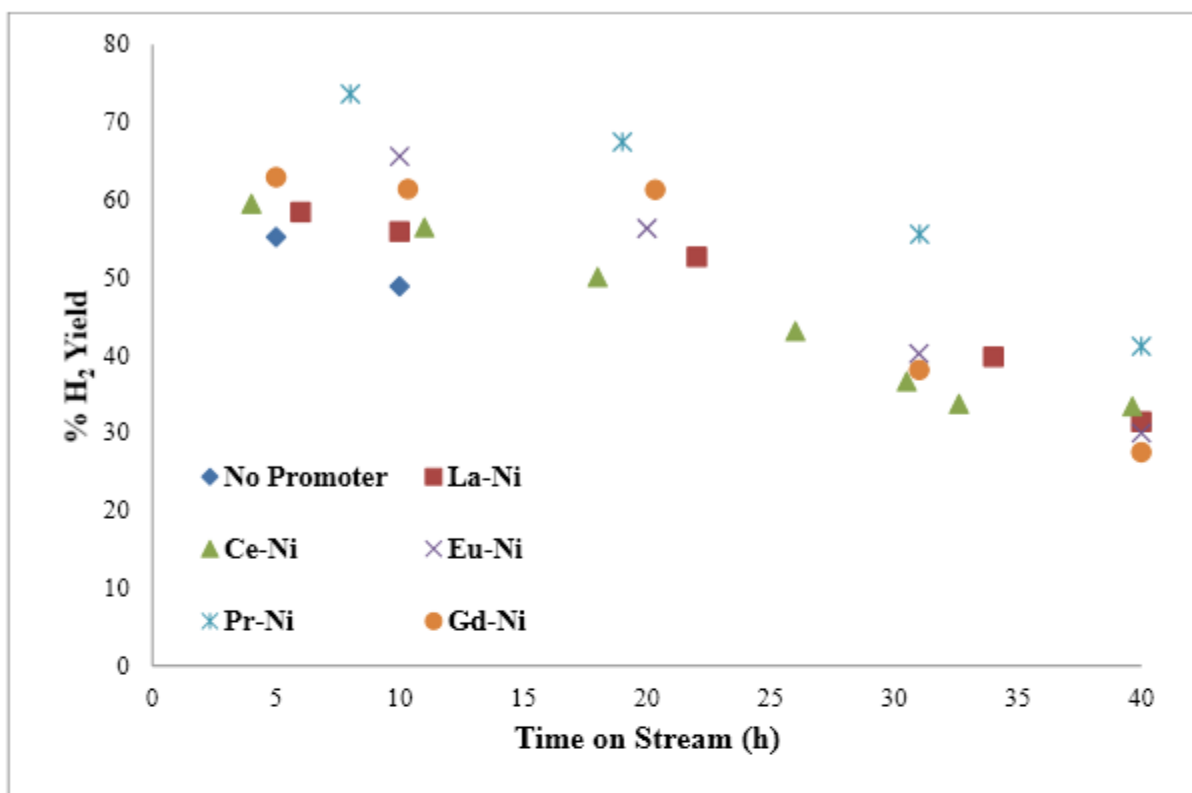


Figure 5-19: % Yield of H₂ during a 40h run over Lanthanide promoted bimetallic and non-promoted monometallic Ni-based catalysts at 620 °C, 1 atm, S/C = 3.0, GHSV of 5800 h⁻¹ and sulfur in fuel =6 ppm

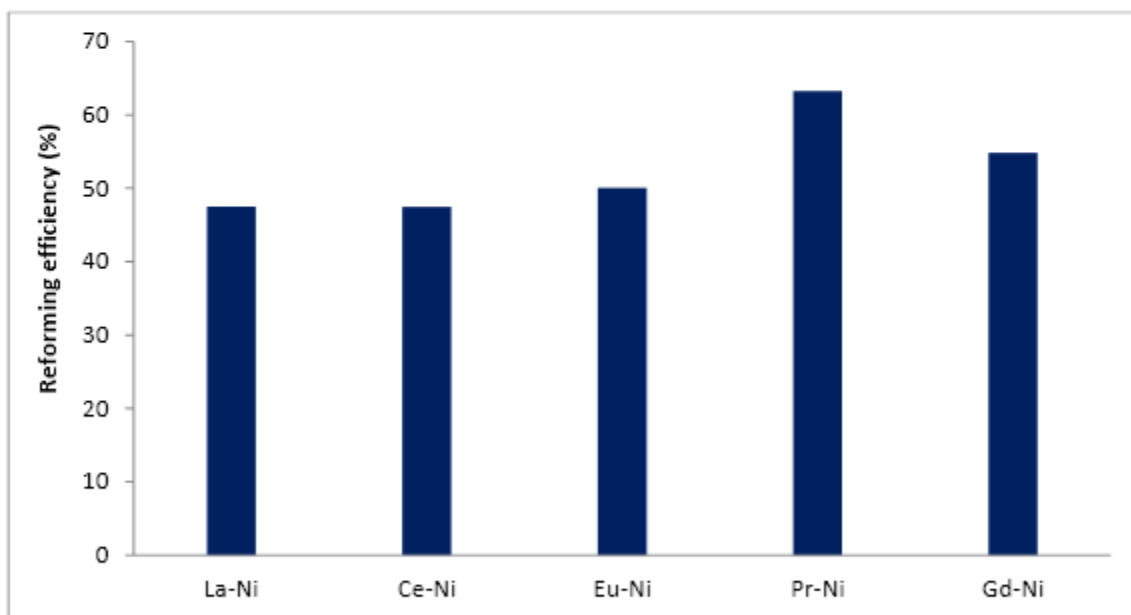


Figure 5-20: Reforming efficiency during a 40h run over Lanthanide promoted bimetallic Ni-based catalysts at 620 °C, 1 atm, S/C = 3.0, GHSV of 5800 h⁻¹ and sulfur in fuel = 6 ppm.

Table 5-13: Comparison of selectivities of different products over Lanthanide promoted bimetallic and non-promoted monometallic Ni-based catalysts at 620 °C, 1 atm, S/C = 3.0, GHSV of 5800 h⁻¹ and sulfur in fuel = 6 ppm.

Catalyst	Selectivity			
	H ₂ (%)	CO (%)	CO ₂ (%)	CH ₄ (%)
Un-Promoted	73.22	5.69	20.08	1.01
La-Ni	71.10	6.66	20.06	2.19
Ce-Ni	73.00	5.59	20.22	1.20
Eu-Ni	72.32	5.82	20.44	1.43
Pr-Ni	71.39	6.13	20.46	2.02
Gd-Ni	71.39	6.13	20.46	2.02

5.2.5 Thermo Gravimetric Analysis (TGA)

Figure 5-21 presents the weight loss curves of the used promoted and non-promoted catalysts. TGA of the catalysts were performed in the dry air atmosphere and the temperature range for TGA was 95 °C to 1000 °C. The initial mass reduction in some cases was due to the result of moisture evaporation. A quick weight loss was observed at 400 °C, 470 °C, 425 °C, 360 °C, 380 °C and 450 °C in non-promoted, La-Ni, Ce-Ni, Eu-Ni, Pr-Ni and Gd-Ni catalysts respectively. The weight increment due to coke formation measured in non-promoted catalyst after 10 h run was 4.61%. All the promoted catalysts were evaluated for 40 hours and percentage weight increment due to coke formation were 3.05%, 5.07%, 2.59%, 2.45% and 2.82% in La-Ni, Ce-Ni, Eu-Ni, Pr-Ni and Gd-Ni

respectively. For all the spent catalysts, coke gasification can be divided into three different sections. 1st section ranges from 420°C to 500°C and this part coke gasified could be of polymerized form; however, the quantity of coke gasified before this temperature is monoatomic carbon. 2nd section represents the whisker type of carbon and this type of coke is hard to gasify, its range could be from 500°C to 560°C [50]. Most of the carbon whiskers formed is hard to gasify and some of them encapsulate the Ni metal particles. Gasification of carbon whiskers could start from 600°C onward and this type of coke is usually converted into graphite [30]. TGA analysis revealed that all the promoted catalysts helped increasing the resistance towards the coke formation of catalyst, however, Eu, Pr and Gd performed better than the other promoters. CHNS analyses of all the spent promoted and non-promoted catalysts were performed in the presence of dilute oxygen in helium at very high temperature and results are shown in Figure 5-28.

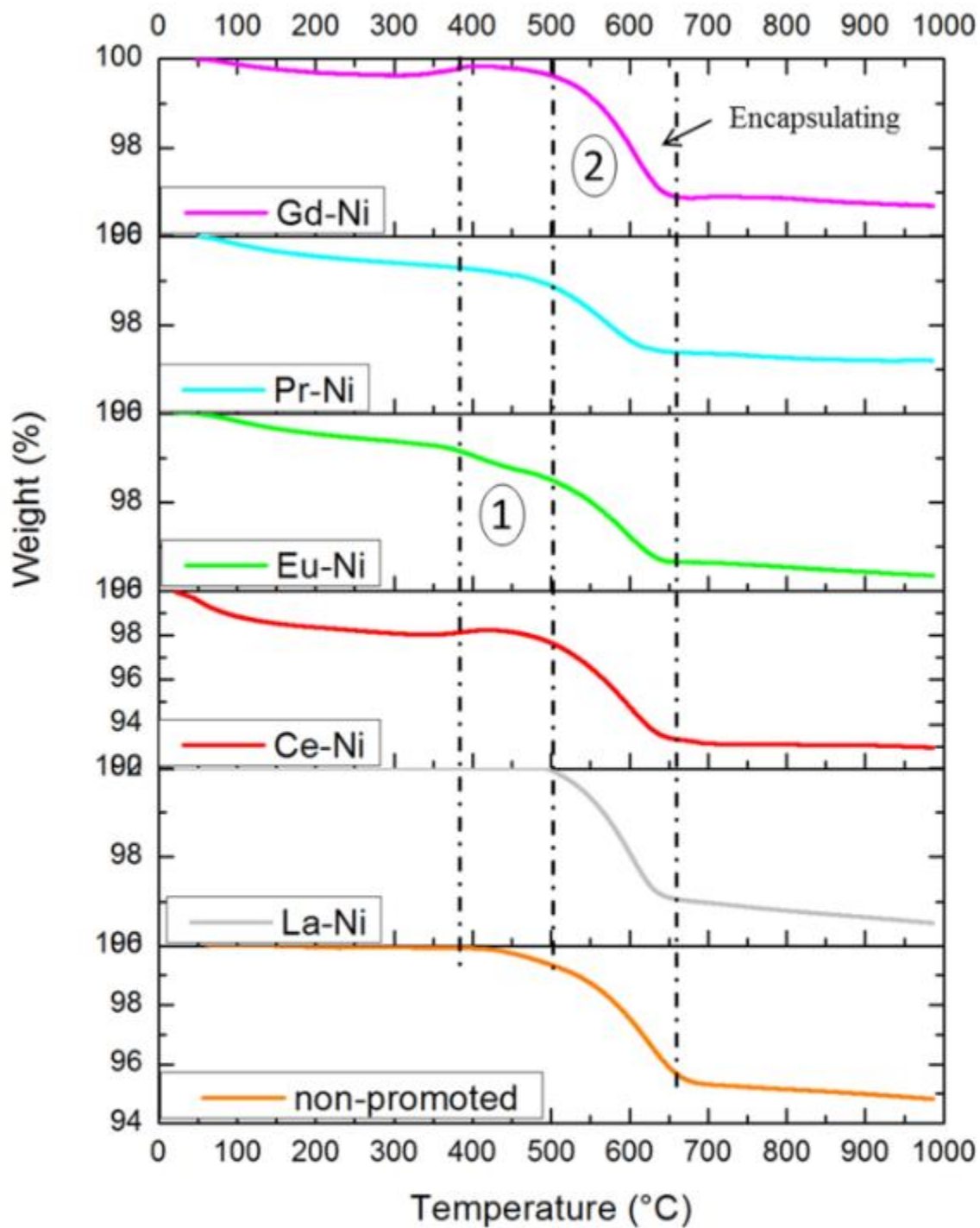


Figure 5-21: TGA results of non-promoted and promoted catalysts. Zone 1 represents gasification of polymerized carbon, zone 2 represents weight loss due to carbon whiskers and the zone 3 represents weight loss due to gasification of encapsulated carbon.

Table 5-14: %Weight loss results of all the spent catalysts from TGA.

Catalyst	Weight loss (%)
Non-Promoted	††4.61
Ce-Ni	5.07
La-Ni	3.05
Gd-Ni	3.24
Eu-Ni	2.59
Pr-Ni	2.45

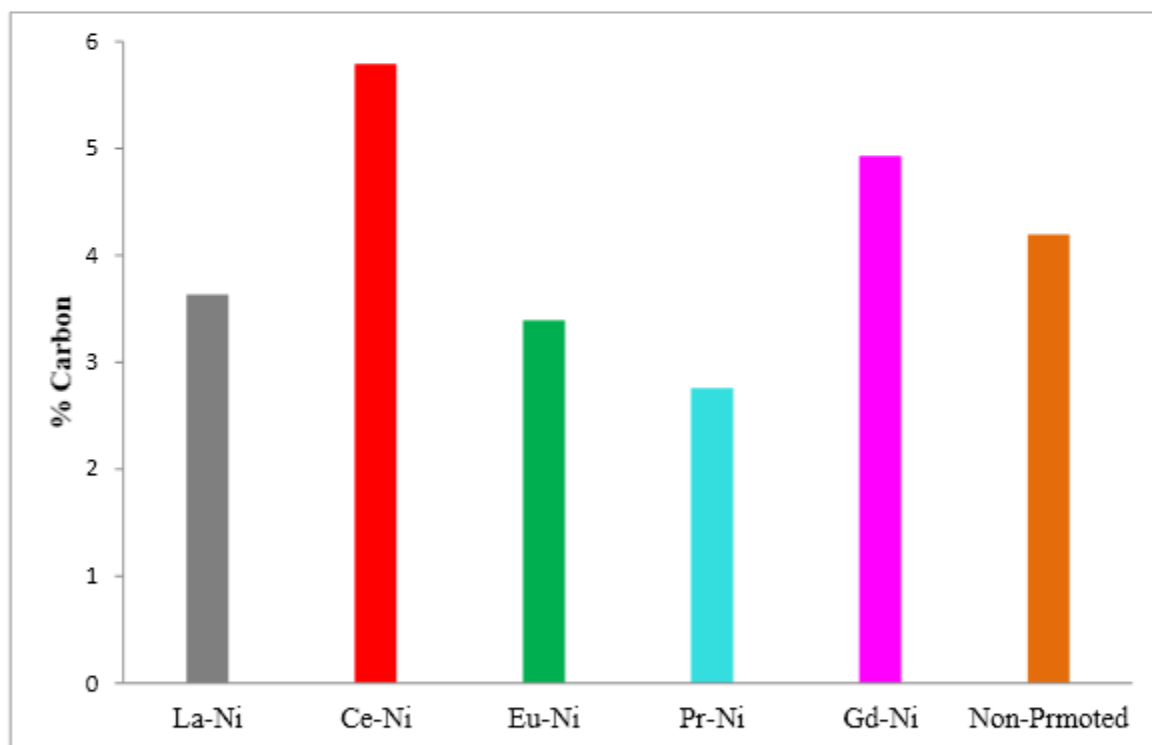


Figure 5-22: CHNS results of Coke formed (%) on non-promoted and promoted catalysts.

†† Non-promoted catalyst last only 10 hours due to heavy coke formation and pressure buildup, reaction was stopped.

5.2.6 Effect of Temperature on Diesel Steam Reforming over 5%Pr-12%Ni/ γ Al₂O₃ Catalyst

Since the praseodymium promoted nickel based catalyst performed best when tested against non-promoted, La-Ni, Ce-Ni, Eu-Ni and Gd-Ni, so it was further evaluated at three different temperatures. All the remaining reaction conditions were kept constant to check the effect of temperature on diesel conversion, % yield and H₂ selectivity. Figure 5-23 shows the effect of temperature on activity of Pr-Ni catalyst. It is quite evident that in the start of evaluation catalyst performed best at 620 °C but with the passage of time catalyst working at 600 °C showed consistency in its reactivity. Only advantage of testing at low temperature was better stability with TOS; however conversion of diesel was low when catalyst was tested at 580 °C. Consistency in the activity of catalyst at low temperature was due to low coke formation at low temperatures and that was found in agreement when CHNS and TGA of the catalyst were performed.

Percentage yield of hydrogen is shown in Figure 5-25. It is clear from the figure that yield of H₂ was found highest at 620 °C in first 10 h, but after that the Ni-Pr evaluated at 600 °C exhibited consistency and further decline in yield of H₂ was observed after 25 h of reaction. % Yield of H₂ was found almost constant when the catalyst was evaluated at 580 °C but the reactivity of the catalyst was very low. Similarly, the reforming efficiency of Pr-Ni at three different temperatures was calculated for 40 hours of reaction and shown in Figure 5-24. Selectivity of CO increased with an increase in temperature as shown in Figure 5-26 that suggests the shift in equilibrium of reaction 1. The conversion of diesel increased from 42% to 66% with an increase of just 20°C in reaction temperature. One

reason for increase in percentage yield of hydrogen with change in temperature was because of more water conversion at high temperature (increase in water conversion from 22% to 32%).

Figure 5-27 shows the comparison of the results obtained at equilibrium conversion (from HYSYS) to the %yield of hydrogen at three different temperatures when steam reforming was performed in the presence of Pr-Ni catalyst. Pr-Ni showed very promising results at high temperatures and results were almost equal to equilibrium values.

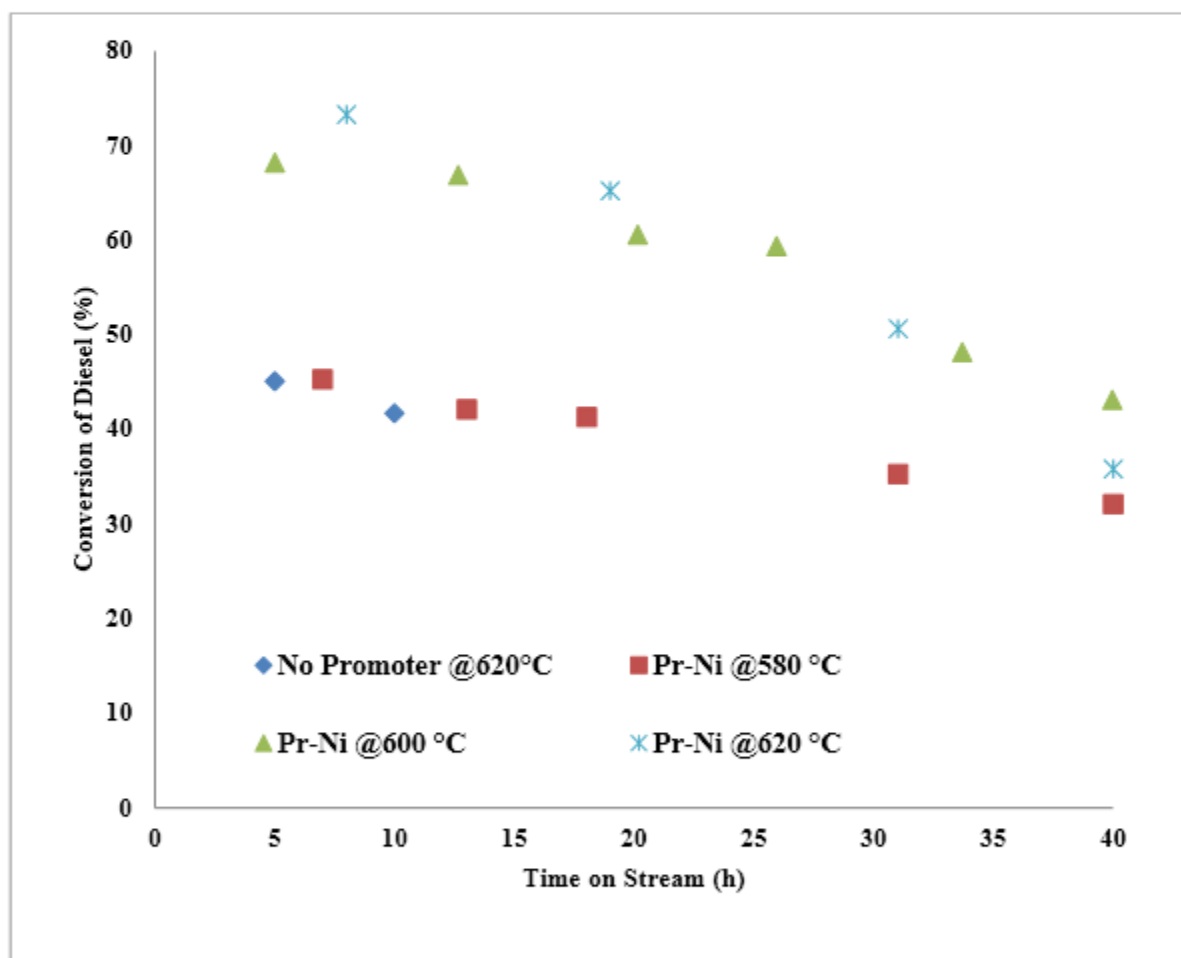


Figure 5-23: The effect of temperature on conversion of Diesel during a 40h run over Pr-Ni bimetallic and non-promoted monometallic Ni-based catalysts at 1 atm, S/C = 3.0, GHSV of 5800 h⁻¹ and sulfur in fuel = 6 ppm

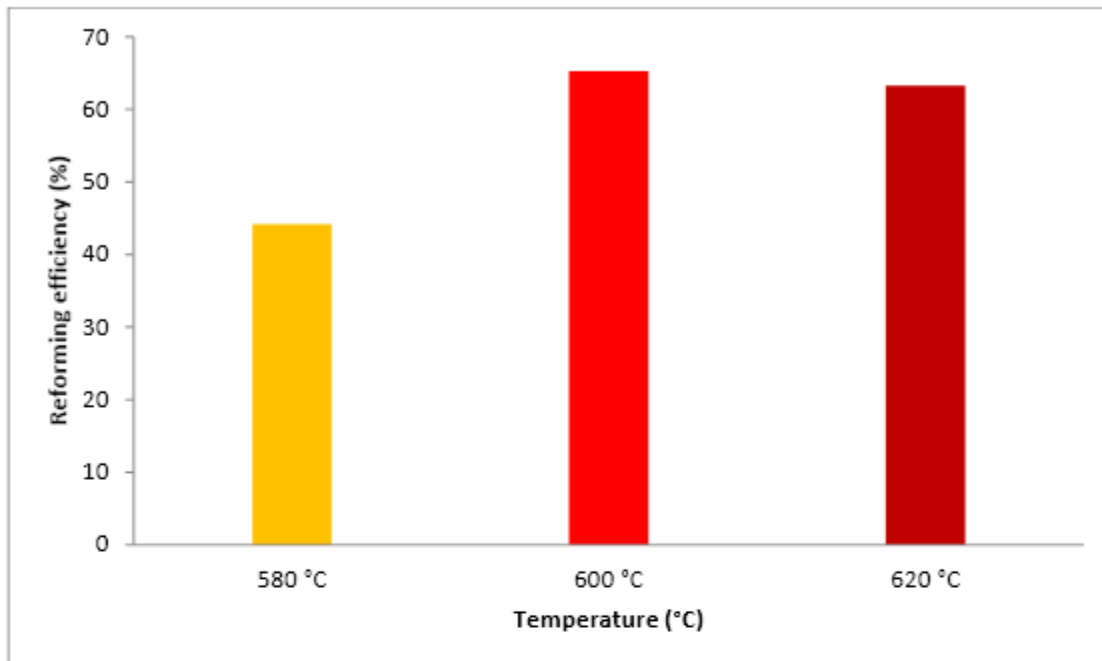


Figure 5-24: The effect of temperature on the reforming efficiency of Diesel during a 40h run over Pr-Ni bimetallic Ni-based catalysts at 1 atm, S/C = 3.0, GHSV of 5800 h⁻¹ and sulfur in fuel = 6 ppm.

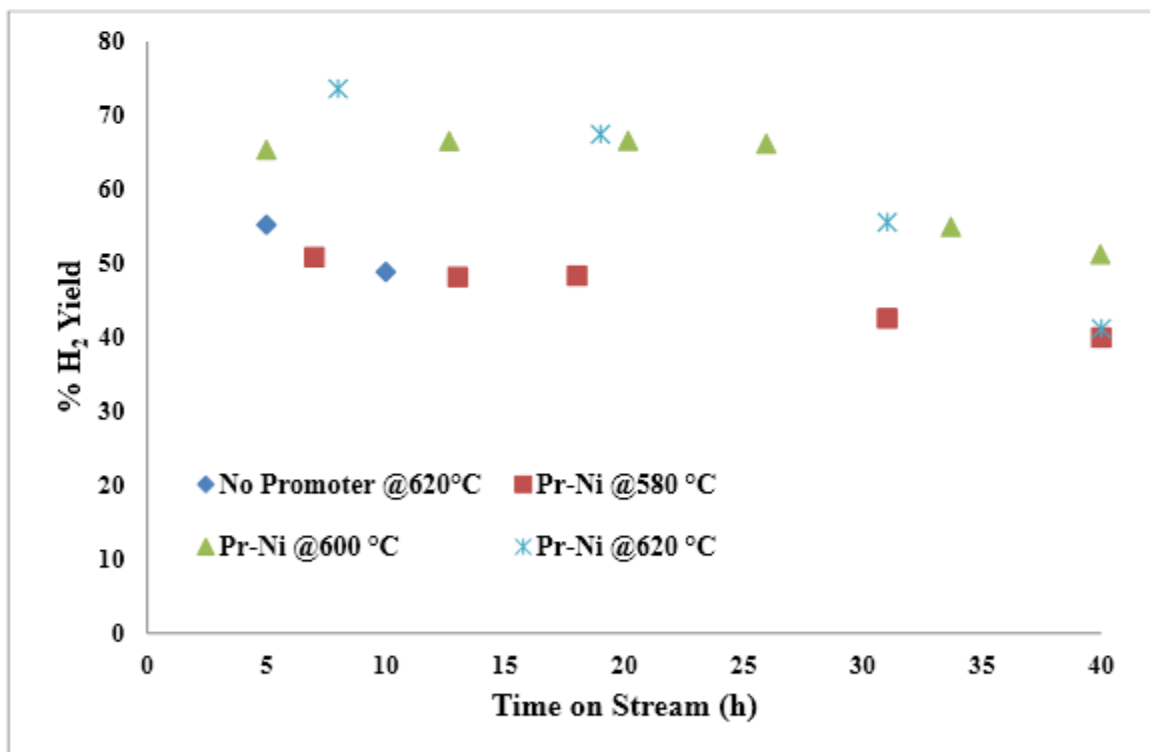


Figure 5-25: The effect of temperature on the % Yield of H₂ during a 40h run over Pr-Ni bimetallic and non-promoted monometallic Ni-based catalysts at 620 °C, 1 atm, S/C = 3.0, GHSV of 5800 h⁻¹ and sulfur in fuel = 6 ppm

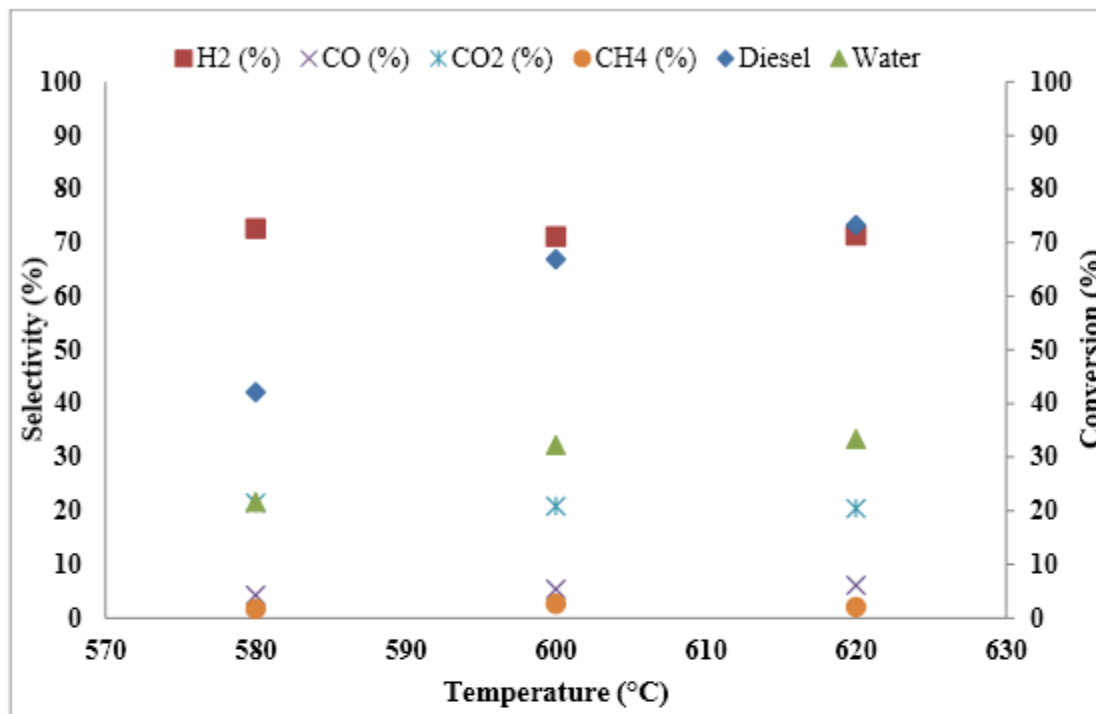


Figure 5-26: The effect of temperature on conversion of Diesel and water, selectivity of H₂, CO, CO₂ and CH₄ after 10h of reaction, over Pr-Ni catalysts at 1 atm, S/C = 3.0, GHSV of 5800 h⁻¹ and sulfur in fuel = 6 ppm

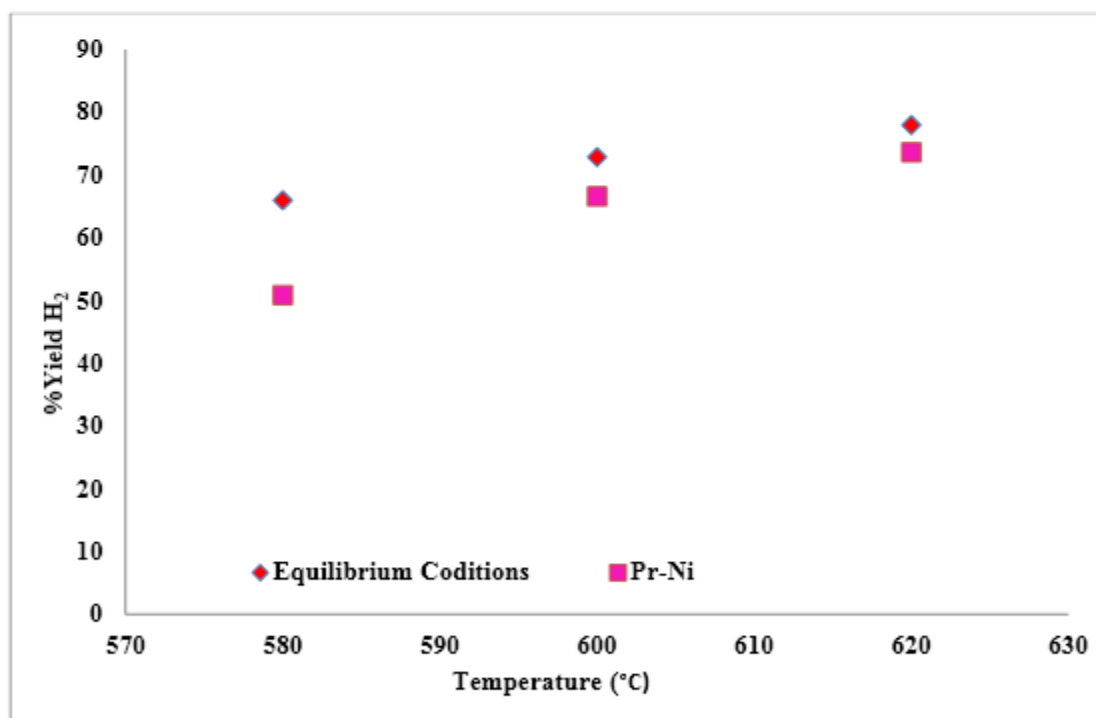


Figure 5-27: Comparison of the %H₂ Yield at three different temperatures for data obtained at equilibrium conversion with results from Pr-Ni catalyst, at 1 atm and S/C = 3.0.

Diesel steam reforming of Pr-Ni catalyst was performed at three different temperatures of 580°C, 600°C and 620°C. All three experiments were performed for 40 hours. Figure 5-28 presents the TGA of all these spent catalysts and percentage coke formed was 1.5%, 1.79% and 2.45% of spent catalysts evaluated at 580°C, 600°C and 620°C respectively.. This shows us when diesel steam reforming was carried out at low temperature; it helped decreasing the total coke formed on the catalyst, but at the cost of drop in catalyst activity. TGA of Pr-Ni catalysts revealed that praseodymium have provided very good resistance towards metal encapsulation, and hence type of coke form is easy to gasify. Similarly total coke formation was counterchecked using another technique called CHNS and its results are shown in Figure 5-29. CHNS analyses of the promoted and non-promoted catalysts were performed in the presence of dilute oxygen in helium at very high temperature.

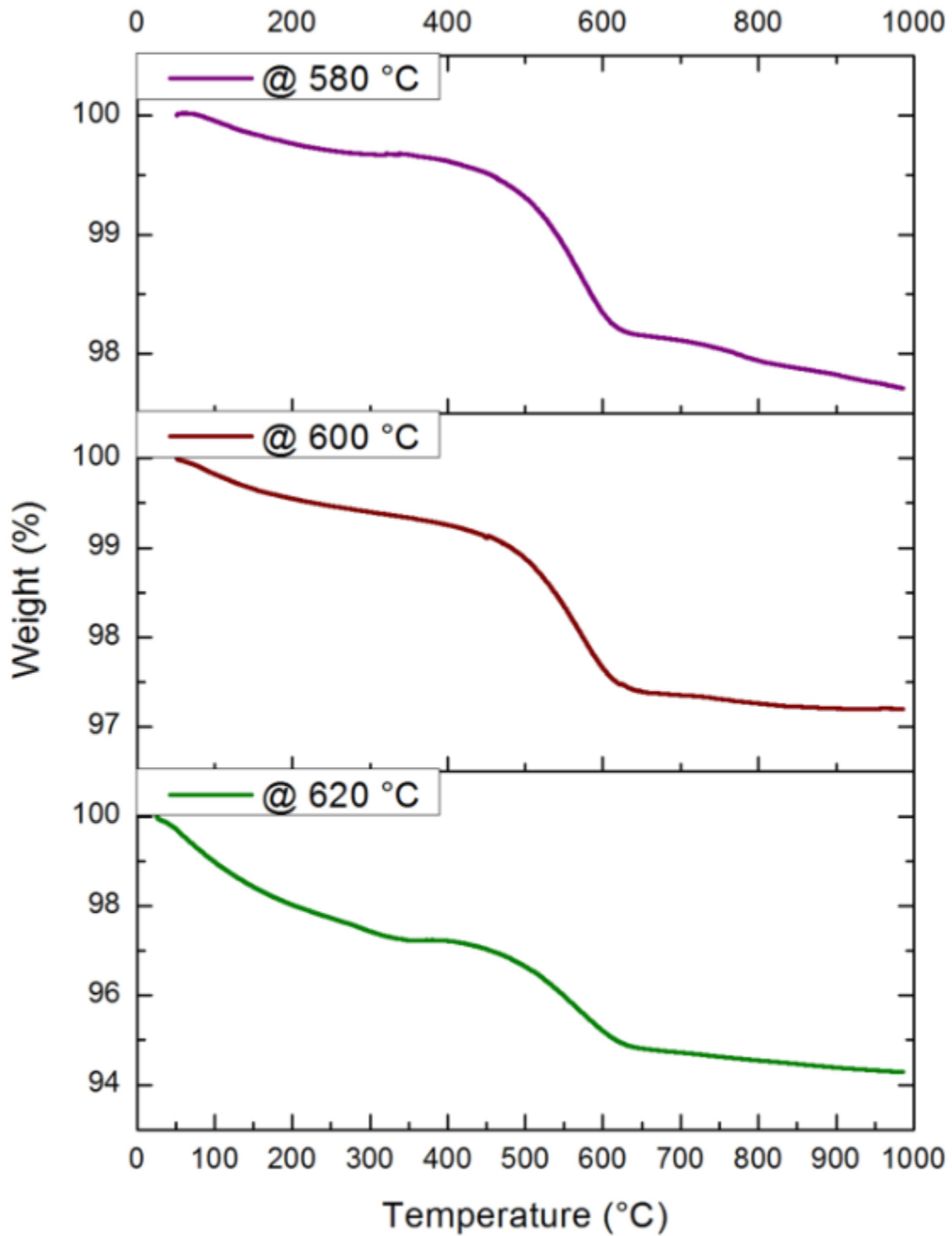


Figure 5-28: TGA results of Pr-Ni catalyst (the effect of temperature on coke formation).

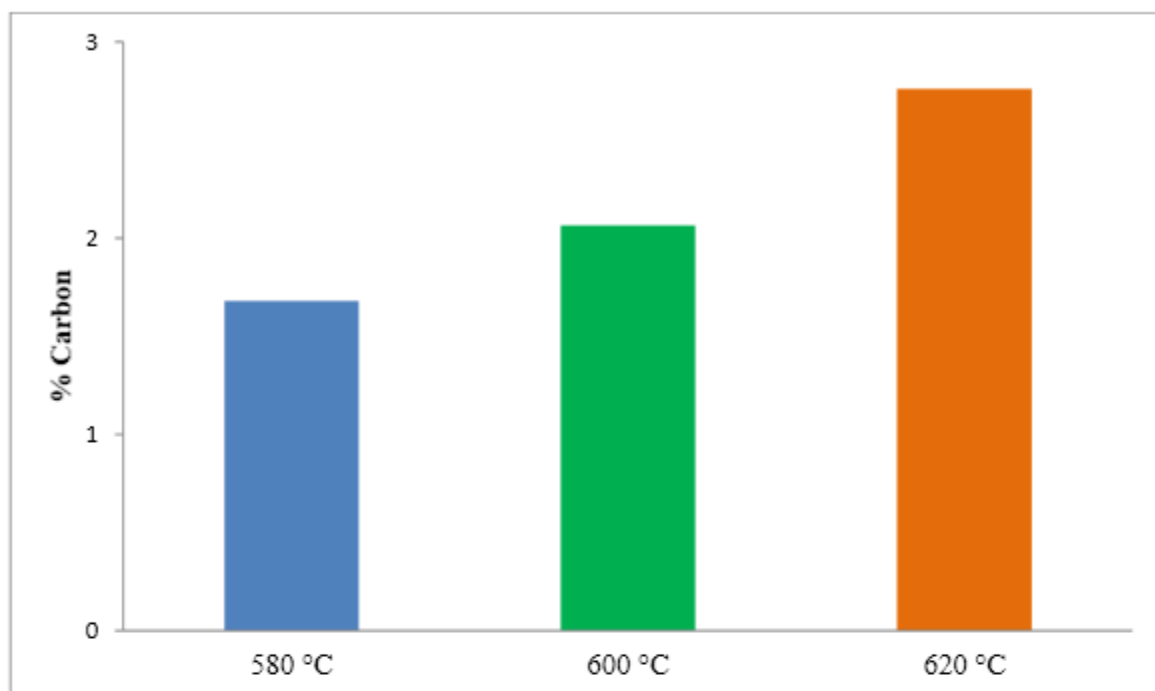


Figure 5-29: CHNS results of Pr-Ni catalyst (the effect of temperature on coke formation).

Chapter 6

CONCLUSION AND RECOMMENDATIONS

6.1 Conclusion

In this investigation promoted and non-promoted nickel over gamma alumina catalysts were prepared, characterized and evaluated. The following are the conclusions drawn from this research.

- i. XRD, SEM, EDX and TEM techniques revealed that the presence of metals enhanced the uniform metal dispersion over the surface of support. The point EDX of different catalyst performed revealed that the nickel impregnation and promoters was also very uniform. TEM of the catalysts revealed that particles size was also in accordance with XRD results and there was no agglomeration of metal.
- ii. TPR analyses of all the promoted and non-promoted catalysts were performed and the addition of promoters strengthened the interaction between active metal and support. A single reduction peak of Pr-Ni suggested better bonding between metal and support.
- iii. Evaluation of the promoted and non-promoted catalyst in a Fixed Bed Reactor showed that 12%Ni/ γ -Al₂O₃ catalyst performed best among non-promoted

catalysts and Pr-Ni catalysts performed best among all the lanthanide promoted catalysts in terms of diesel conversion and % yield of H₂.

- iv. Performance evaluation of Pr-Ni catalyst was observed at three different temperatures and best stability was observed at 600 °C.
- v. TGA and CHNS of all the spent catalysts were performed to find out the percent increase in the weight of catalyst due to carbon formation after 40 h of operation. The gain in % weight of catalyst was lowest in Eu-Ni, Pr-Ni and Gd-Ni catalysts. Similarly, the lowest coke formation in Pr-Ni was observed at 580 °C.

6.2 Recommendations

Following suggestions will be very useful to continue this work in a more improved and productive way in the future.

- i. For better understanding of dispersion and metal loading of a lanthanide series on support material, the variation in percentage of lanthanide promoters and modification of support material should be employed to get maximum activity and better performance.
- ii. All the lanthanide promoted catalyst can be tested at a wide range of temperatures to better understand the reaction mechanism and reaction kinetics.
- iii. The effect of contaminants in fuel may be investigated for long term stability of the catalyst.

REFERENCES

- [1] Dushyant, J. Shekhawat, D. J. Spivey and A. Berry, *Fuel Cells: Technologies for fuel processing*, Elsevier, 2011.
- [2] Y. Jamal and M. Wyszynski, "On-board generation of hydrogen-rich gaseous fuels. A review,," *International journal of Hydrogen Energy*, vol. 19, no. 7, pp. 557-572, 1994.
- [3] F.-L. Clémence, A. Nicolas, B. Jasmin and G. François, "Steam reforming of liquid hydrocarbons over a nickel-alumina spinel catalyst," *Journal of Power Sources*, vol. 195, no. 10, pp. 3275-3283, 2010.
- [4] A. Naidja, C. Krishna, T. Butcher and D. Mahajan, "Cool flame partial oxidation and its role in combustion and reforming of fuels for fuel cell systems,," *Progress in Energy and Combustion Science*, vol. 29, no. 2, pp. 155-191, 2003.
- [5] B. Jeffrey R., P. Michael B. and O. Norman K., "An economic survey of hydrogen production from conventional and alternative energy sources," *International Journal of Hydrogen Energy*, vol. 35, no. 16, pp. 8371-8384, 2010.
- [6] J. Sheffield, "World population growth and the role of annual energy use per

- capita.," *Technological Forecasting and Social Change*, vol. 59, no. 1, pp. 55-87, 1998.
- [7] R. Joyeux and R. Ripple, "Household energy consumption versus income and relative standard of living: a panel approach," *Energy Policy*, vol. 35, no. 1, pp. 50-60, 2007.
- [8] G. Erdmann, "Future economics of the fuel cell housing market.," *International Journal of Hydrogen Energy*, vol. 28, no. 7, pp. 685-694, 2003.
- [9] P. Agnolucci, "Economics and market prospects of portable fuel cells.," *International Journal of Hydrogen Energy*, vol. 32, no. 17, pp. 4319-4328, 2007.
- [10] M. Ball and W. M., "The future of hydrogen-Opportunities and challenges.," *International Journal of Hydrogen Energy*, vol. 34, pp. 615-627, 2009.
- [11] O. G.A., G. A. and P. G.K.S., *Beyond Oil and Gas:Methanol Economy.*, Weinheim: Wiley-VCH, 2006.
- [12] C. Rice, "Direct formic acid fuel cells," *Journal of Power Sources*, vol. 111, no. 1, pp. 83-89, 2002.
- [13] A. Aricò, B. V. and A. V., "Direct Methanol Fuel Cells: History, Status and Perspectives," *Electrocatalysis of Direct Methanol Fuel Cells*, pp. 1-78, 2009.

- [14] C. Oloman and L. H., "Electrochemical Processing of Carbon Dioxide.," *ChemSusChem*, vol. 1, no. 5, pp. 385-391, 2008.
- [15] M. Aresta and D. A., "Utilisation of CO₂ as a chemical feedstock: opportunities and challenges.," *Dalton Transactions*, vol. 28, pp. 2975-2992, 2007.
- [16] B. Lindström, J. Karlsson, P. Ekdunge, L. De Verdier, B. Häggendal, J. Dawody, M. Nilsson and L. Pettersson, "Diesel fuel reformer for automotive fuel cell applications.," *International Journal of Hydrogen Energy*, vol. 34, no. 8, pp. 3367-3381, 2009.
- [17] h. Lui and z. j., *Electrocatalysis of Direct Methanol Fuel Cells.*, Wiley-VCH., 2009.
- [18] W. Viestich, L. A. and H. A.G., *Fuel Cell Handbook.*, Wiley., 2003.
- [19] F.-L. Clémence, A. Nicolas, B. Nadi and E. A. Ines, "Diesel steam reforming with a nickel–alumina spinel catalyst for solid oxide fuel cell application," *Journal of Power Sources*, pp. 7673-7680, 2011.
- [20] B. Schädel and M. D. O. Duisberg, "Steam reforming of methane, ethane, propane, butane, and natural gas over a rhodium-based catalyst," *Catalysis Today*, vol. 142, no. 1-2, pp. 42-51, 2009.
- [21] S. Goud, W. Whittenberger, S. Chattopadhyay and M. Abraham, "Steam reforming of n-hexadecane using a Pd / ZrO₂ catalyst: Kinetics of catalyst deactivation,"

International Journal of Hydrogen Energy, vol. 32, no. 14, pp. 2868-2874, September 2007.

- [22] X. Lihao, M. Wanliang and S. Qingquan, "Hydrogen production through diesel steam reforming over rare-earth promoted Ni/ γ -Al₂O₃ catalysts," *Journal of Natural Gas Chemistry*, vol. 202, pp. 287-293, 2011.
- [23] D. H. Kim, J. S. Kang, Y. J. Lee, N. K. Park, Y. C. Kim, S. I. Hong and D. Moon, "Steam reforming of n-hexaadecane over noble metal-modified Ni-based catalysts," *Catalyst Today*, vol. 136, no. 3-4, pp. 228-234, 2008.
- [24] X. Lihao, M. Wanliang and S. Qingquan, "Hydrogen production through diesel steam reforming over rare-earth promoted Ni/ γ -Al₂O₃ catalysts," *Journal of Natural Gas Chemistry*, vol. 20, no. 3, pp. 287-293, 2011.
- [25] Granlund, J. Moa Z., N. Kjell, D. Marita, P. Jazaer and Lars J., "Evaluation of Co, La, and Mn promoted Rh catalysts for autothermal reforming of commercial diesel," *Applied Catalysis B: Environmental*, Vols. 154-155, pp. 389-394, 2014.
- [26] Ines, N. Esma Achouri, C. Abatzoglou, N. Fauteux-Lefebvre and Braidy, "Diesel steam reforming: Comparison of two nickel aluminate catalysts prepared by wet-impregnation and co-precipitation," *Catalysis Today*, vol. 207, pp. 13-20, 2013.
- [27] L. Guohui, H. Linjie, M. H. Josephine and I., "Comparison of reducibility and stability of alumina-supported Ni catalysts prepared by impregnation and co-

- precipitation," *Applied Catalysis*, pp. 16-24, 2006.
- [28] Hernández, L. W.Y., C. O.H., O. M.A. and J.A., "Structural and catalytic properties of lanthanide (La, Eu, Gd) doped ceria," *Journal of Solid State Chemistry*, vol. 184, no. 11, pp. 3014-3020, 2011.
- [29] Jones, J. Glenn, S. Jon Geest, K. Signe S., A. Jesper, R. Martin P. and J. Jan, "First principles calculations and experimental insight into methane steam reforming over transition metal catalysts," *Journal of Catalysis*, vol. 259, pp. 147-160, 2008.
- [30] C. H. Bartholomew and R. J. Farrauto, *Fundamentals of Industrial Catalytic Processes*, 2nd ed., Wiley, 2005.
- [31] J. Anderson and M. Boudart, "Catalytic steam reforming," *Catalysis, Science and Technology*, vol. 5, 1984.
- [32] L. Wang, K. Murata and M. Inaba, "Development of novel highly active and sulphur-tolerant catalysts for steam reforming of liquid hydrocarbons to produce hydrogen," *Applied Catalysis A: General*, vol. 257, pp. 43-47, 2004.
- [33] G. Li, L. Hu and J. Hill, "Comparison of reducibility and stability of alumina supported Ni catalysts prepared by impregnation and co-precipitation," *Applied Catalysis*, vol. 301, pp. 16-24, 2006.
- [34] L. Feio, C. Hori, S. Damyanova, F. Noronha, W. Cassinelli, C. Marques and J.

- Bueno, "The effect of ceria content on the properties of Pd/CeO₂/Al₂O₃ catalysts for steam reforming of methane.," *Applied Catalysis A: General*, vol. 316, no. 1, pp. 107-116, 2007.
- [35] M. Sugisawa, K. Takanabe, M. Harada, J. Kubota and K. Domen, "Effects of La addition to Ni/Al₂O₃ catalysts on rates and carbon deposition during steam reforming of n-dodecane," *Fuel Processing Technology*, vol. 92, no. 1, pp. 21-25, January 2011.
- [36] M. Pacheco, J. Sira and J. Kopasz, "Reaction kinetics and reactor modeling for fuel processing of liquid hydrocarbons to produce hydrogen: isooctane reforming," *Applied Catalysis A: General*, vol. 250, no. 1, pp. 161-175, 2003.
- [37] J. Agrell, H. Birgersson and M. Boutonnet, "Steam reforming of methanol over a Cu/ZnO/Al₂O₃ catalyst: a kinetic analysis and strategies for suppression of CO formation," *Power Sources*, vol. 106, no. 1-2, pp. 249-257, 2002.
- [38] J. Nowotny and L. Sheppard, "International Conference on Materials for Hydrogen Energy: Solar Hydrogen," in *ICMHE*, 2004.
- [39] D. Depeyre, C. Filcoteaux and C. Chardaire, "Pure n-Hexadecane Thermal Steam Cracking," *Industrial & Engineering Chemistry Process Design and Development*, vol. 24, no. 4, pp. 1251-1258, 1985.

- [40] J. J. Strohm, J. Zheng and C. Song, "Low-temperature steam reforming of jet fuel in the absence and presence of sulfur over Rh and Rh–Ni catalysts for fuel cells," *Journal of Catalysis*, vol. 238, pp. 309-320, 2006.
- [41] Z. O. Malaibari, A. Amin, E. Croiset and W. Epling, "Performance characteristics of MoNi/Al₂O₃ catalysts in LPG oxidative steam reforming for hydrogen production," *international journal of hydrogen energy*, vol. 39, pp. 10061-10073, 2014.
- [42] Gobaraa, M. H.M., K. R.S., E.-S. F.H., H. M.S. and S.A., "Various characteristics of Ni and Pt–Al₂O₃ nanocatalysts prepared by microwave method to be applied in some petrochemical processes," *Egyptian Journal of Petroleum*, vol. 23, no. 1, pp. 105-118, 2014.
- [43] G. Seo, Y. Jeong, P. Min Hye, S. Sunyoung and In Kyu, "Effect of calcination temperature of mesoporous alumina xerogel (AX) supports on hydrogen production by steam reforming of liquefied natural gas (LNG) over Ni/AX catalysts," *international journal of hydrogen energy*, vol. 33, pp. 7427-7434, 2008.
- [44] K. Christensen, D. Chen, R. Lødengb and A. Holmen, "Effect of supports and Ni crystal size on carbon formation and sintering during steam methane reforming," *Applied Catalysis A: General*, vol. 314, no. 1, pp. 9-22, 2006.
- [45] J. Gil Seo, M. H. Youn, S. Park and I. K. Song, "Effect of calcination temperature of

mesoporous alumina xerogel (AX) supports on hydrogen production by steam reforming of liquefied natural gas (LNG) over Ni/AX catalysts," *International Journal of Hydrogen Energy*, vol. 33, no. 24, pp. 7427-7434, 2008.

- [46] L. Zhang, X. Q. Wang, B. Tan and U. S. Ozkan, "Effect of preparation method on structural characteristics and propane steam reforming performance of Ni–Al₂O₃ catalysts," *Journal of Molecular Catalysis A: Chemical*, vol. 297, no. 1, pp. 26-34, 2009.
- [47] Katta, S. Lakshmi, T. Putla, R. Gode and Benjaram M., "Doped nanosized ceria solid solutions for low temperature soot oxidation: Zirconium versus lanthanum promoters," *Applied Catalysis B: Environmental*, vol. 101, pp. 101-108, 2010.
- [48] Laosiripojana, S. N., A. W. and S., "Catalytic steam reforming of ethane and propane over CeO₂-doped Ni/Al₂O₃ at SOFC temperature: Improvement of resistance toward carbon formation by the redox property of doping CeO₂," *Fuel*, vol. 85, no. 3, pp. 323-332, 2006.
- [49] Lucre'cio, F. Alessandra Fonseca, A. Germano Tremiliosi and E. Moreira, "Co/Mg/Al hydrotalcite-type precursor, promoted with La and Ce, studied by XPS and applied to methane steam reforming reactions," *Applied Surface Science*, vol. 255, pp. 5851-5856, 2009.
- [50] D. L. and Trimm, "Catalysts for the control of coking during steam reforming."

Catalysis Today, vol. 49, pp. 3-10, 1999.

[51] D. Trimm, "Coke formation and minimisation during steam reforming reactions,"

Catalysis Today, vol. 37, no. 3, pp. 233-238, 1997.

[52] T. K. R. K. M. K. H.H. Dobbs Jr., "4th European Solid Oxide Fuel Cell Forum," in

Proceedings of the 4th European Solid Oxide Fuel Cell Forum, Switzerland, 2000.

[53] P. Cheekatamarla and W. Thomson, "Catalytic activity of molybdenum carbide for hydrogen generation via diesel reforming," *Journal of Power Sources*, vol. 158, no.

1, pp. 477-484, 2006.

Appendix A

DETAILS OF COMPOSITION, CONVERSION, % H₂ YIELD AND SELECTIVITY OF LANTHANIDE SUPPORTED Ni/ γ Al₂O₃ CATALYSTS

Following figures represents the conversion of diesel and water, % yield of H₂, selectivity of H₂, CO, CO₂ and CH₄ and gas product composition of all the promoted and non-promoted catalysts:

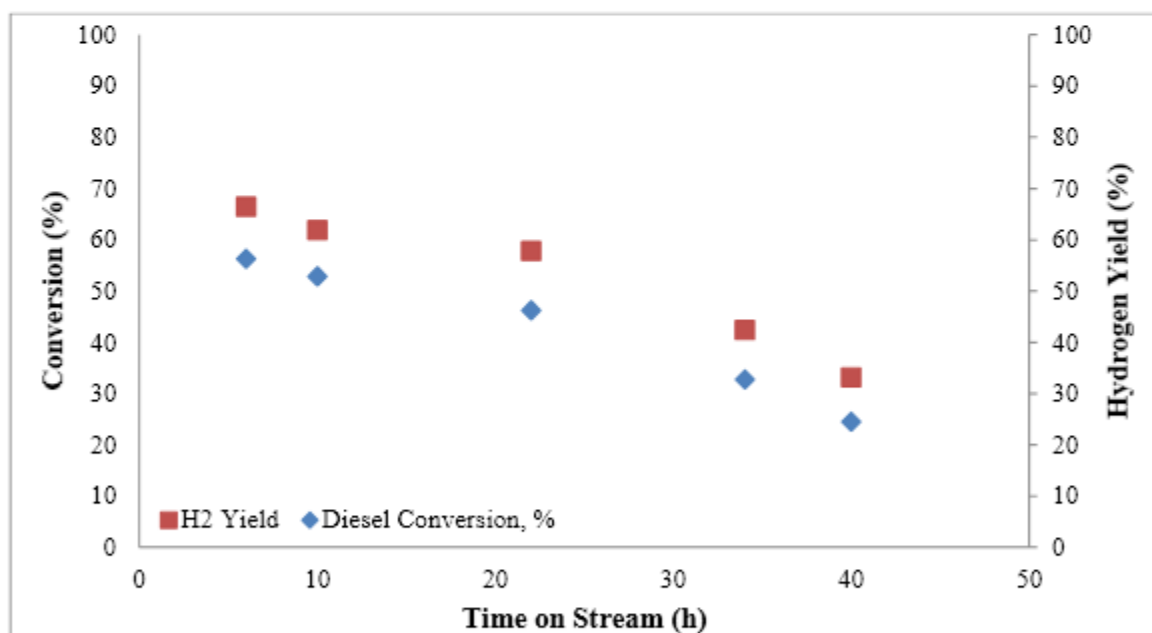


Figure A- 1: Effect of time on diesel conversion and hydrogen yield; for steam reforming of 5%La-12%Ni/ γ Al₂O₃ catalyst for 40 hours; at 620 °C, 1 atm, S/C = 3.0, GHSV of 5800 h⁻¹ and sulfur in fuel = 6 ppm.

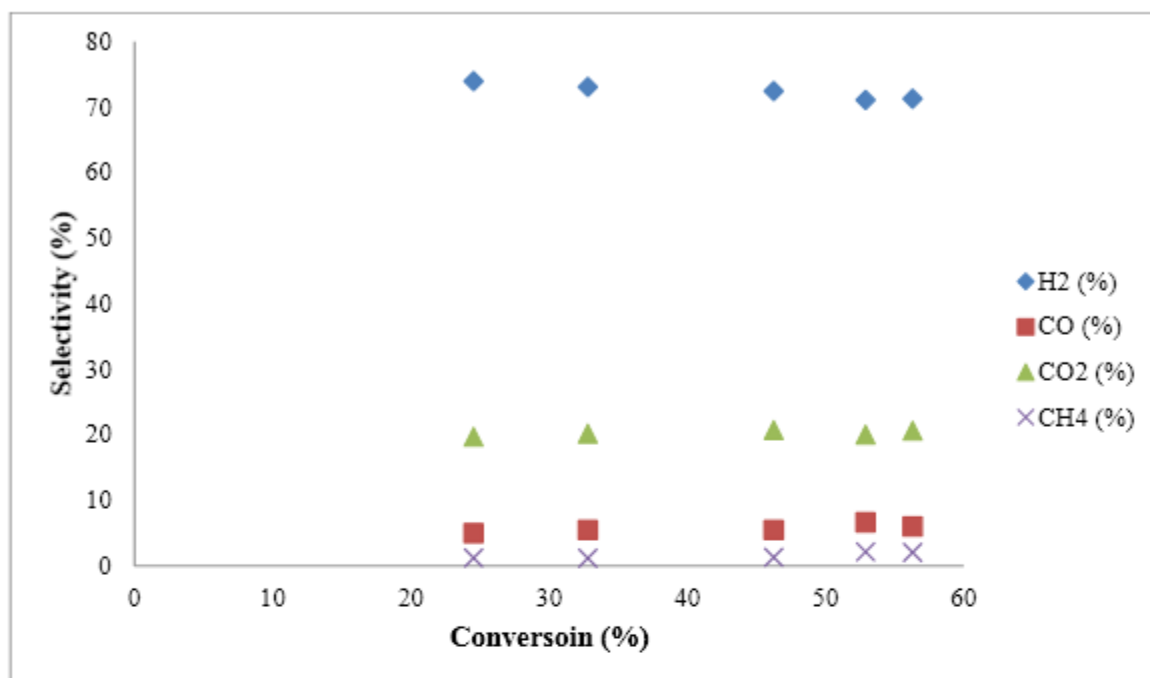


Figure A- 2: Selectivity of diesel Steam reforming products against the Diesel conversion on of 5%La-12%Ni/ γ -Al₂O₃ catalyst for 40 hours; at 620 °C, 1 atm, S/C = 3.0, GHSV of 5800 h⁻¹ and sulfur in fuel = 6 ppm

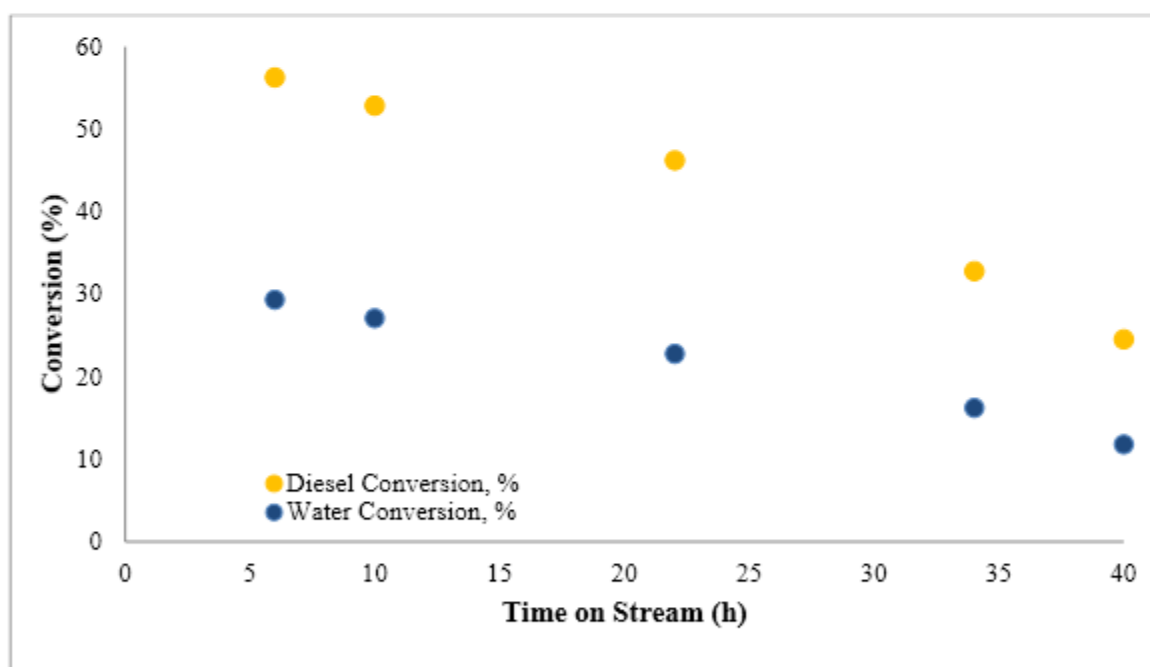


Figure A- 3: Diesel Steam reforming on 5%La-12%Ni/ γ -Al₂O₃ catalyst for 40 hours; at 620 °C, 1 atm, S/C = 3.0, GHSV of 5800 h⁻¹ and sulfur in fuel = 6 ppm

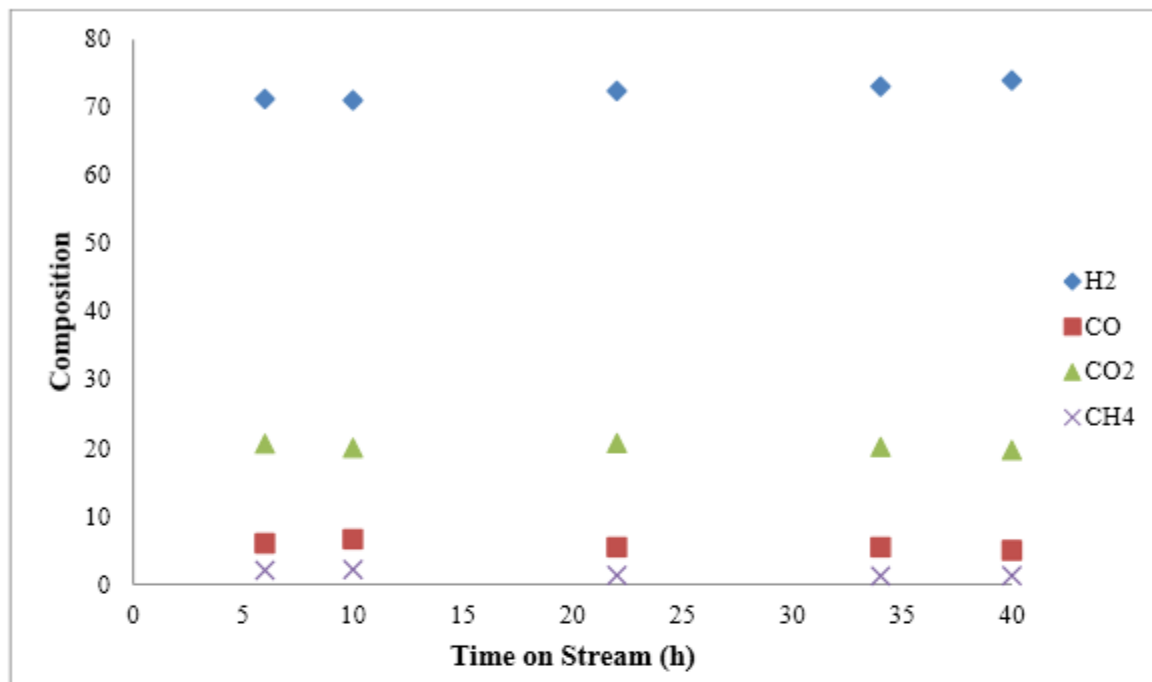


Figure A- 4: Gas product composition variation for steam reforming of diesel on 5%La-12%Ni/ γ -Al₂O₃ catalyst for 40 hours; at 620 °C, 1 atm, S/C = 3.0, GHSV of 5800 h⁻¹ and sulfur in fuel = 6 ppm

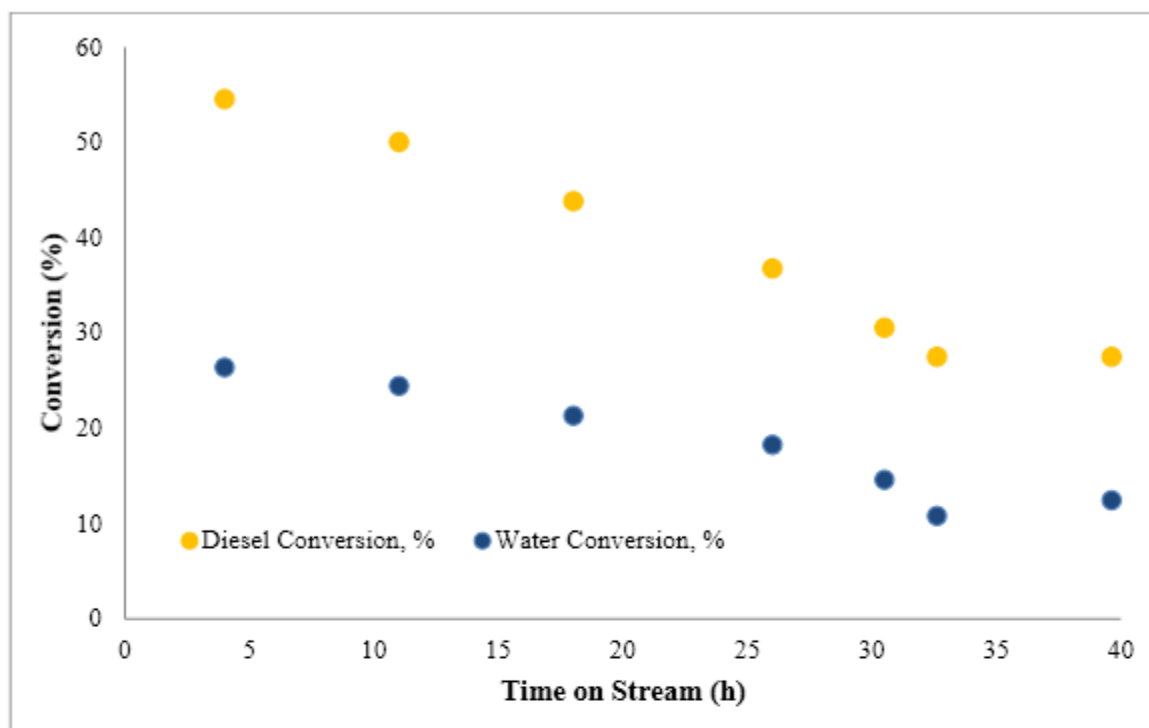


Figure A- 5: Diesel Steam reforming on 5%Ce-12%Ni/ γ Al₂O₃ catalyst for 40 hours; at 620 °C, 1 atm, S/C = 3.0, GHSV of 5800 h⁻¹ and sulfur in fuel = 6 ppm

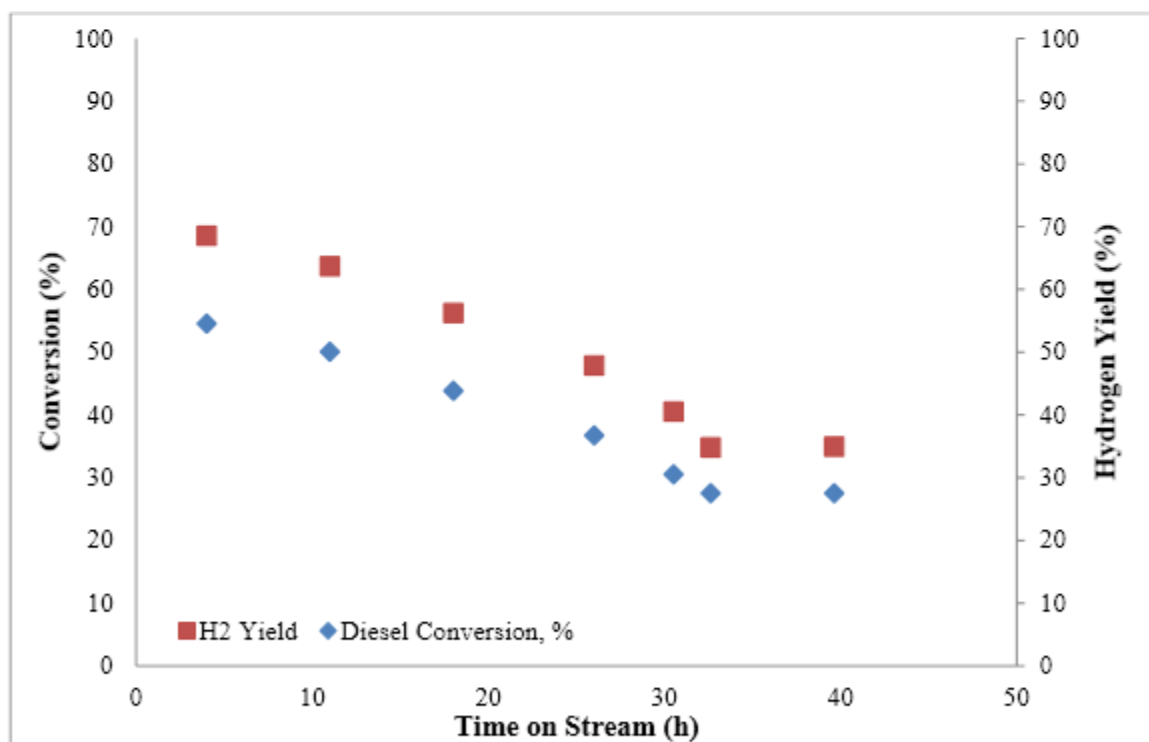


Figure A- 6: Effect of time on diesel conversion and hydrogen yield for steam reforming on 5%Ce-12%Ni/ γ Al₂O₃ catalyst for 40 hours; at 620 °C, 1 atm, S/C = 3.0, GHSV of 5800 h⁻¹ and sulfur in fuel = 6 ppm.

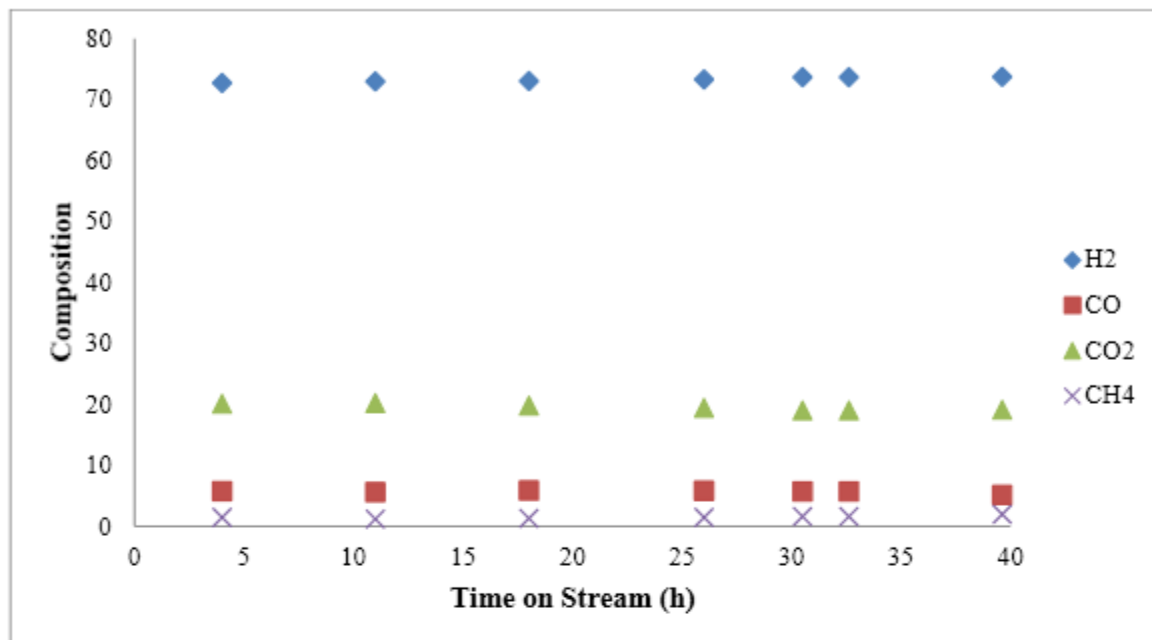


Figure A- 7: Gas product composition variation for steam reforming of diesel on 5%Ce-12%Ni/ γ Al₂O₃ catalyst for 40 hours; at 620 °C, 1 atm, S/C = 3.0, GHSV of 5800 h⁻¹ and sulfur in fuel = 6 ppm

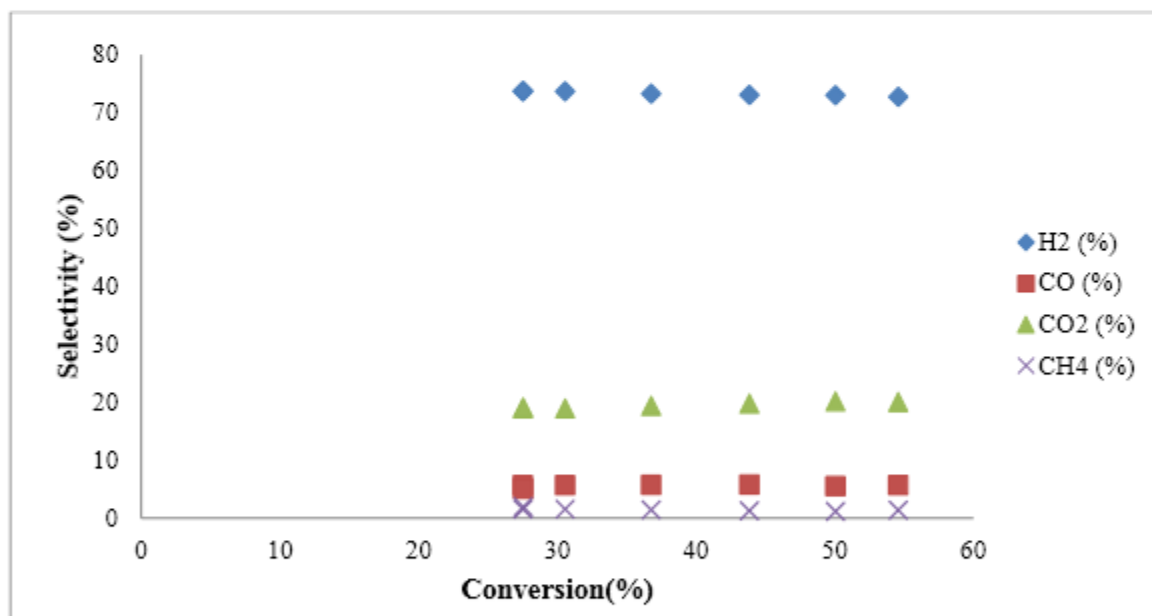


Figure A- 8: Selectivity of diesel Steam reforming products against the Diesel conversion on 5%Ce-12%Ni/ γ Al₂O₃ catalyst for 40 hours; at 620 °C, 1 atm, S/C = 3.0, GHSV of 5800 h⁻¹ and sulfur in fuel = 6 ppm

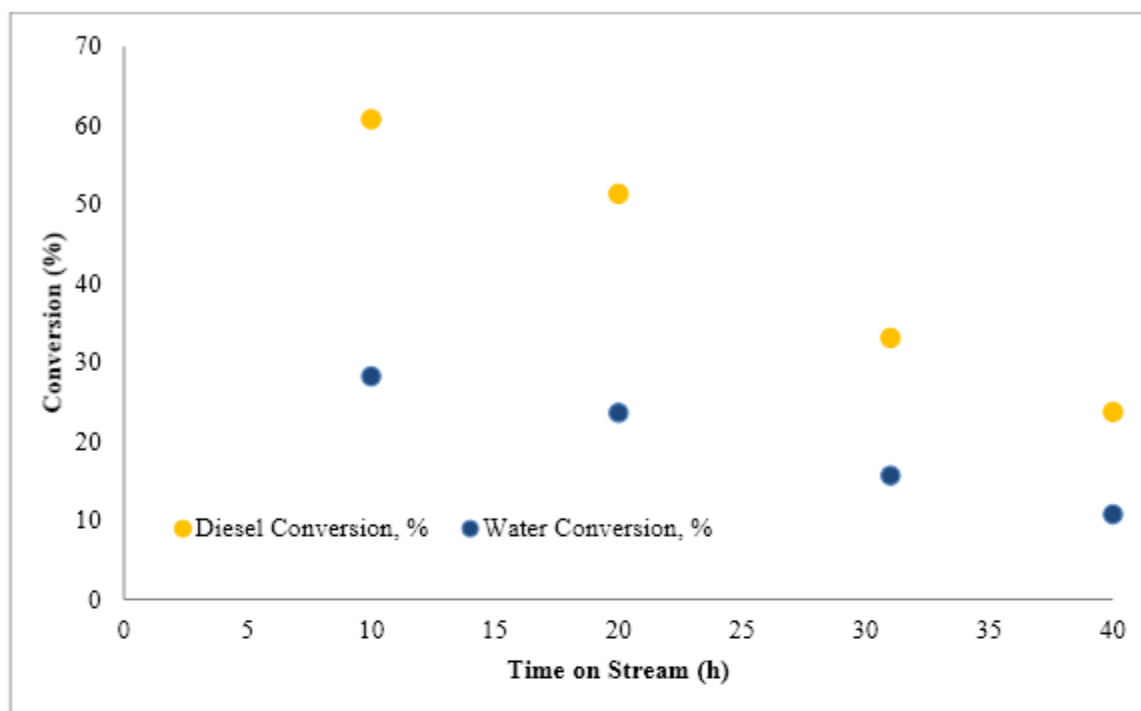


Figure A- 9: Diesel Steam reforming on 5%Eu-12%Ni/ γ -Al₂O₃ catalyst for 40 hours; at 620 °C, 1 atm, S/C = 3.0, GHSV of 5800 h⁻¹ and sulfur in fuel = 6 ppm

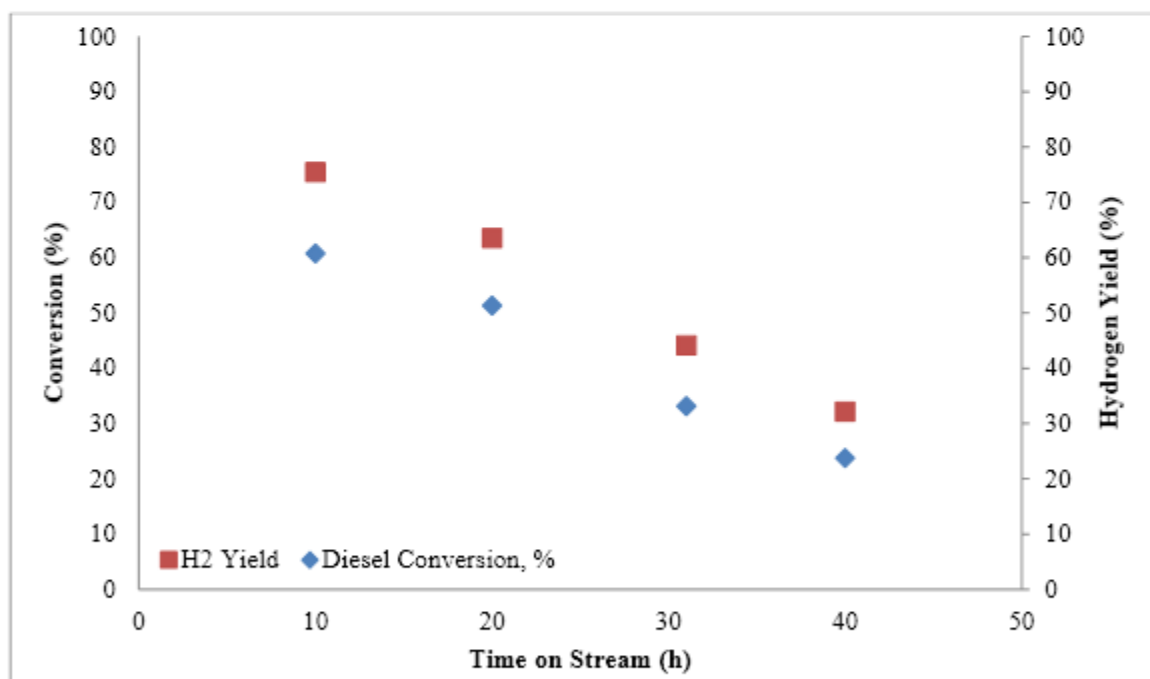


Figure A- 10: Effect of time on diesel conversion and hydrogen yield for steam reforming on 5%Eu-12%Ni/ γ -Al₂O₃ catalyst for 40 hours; at 620 °C, 1 atm, S/C = 3.0, GHSV of 5800 h⁻¹ and sulfur in fuel = 6 ppm.

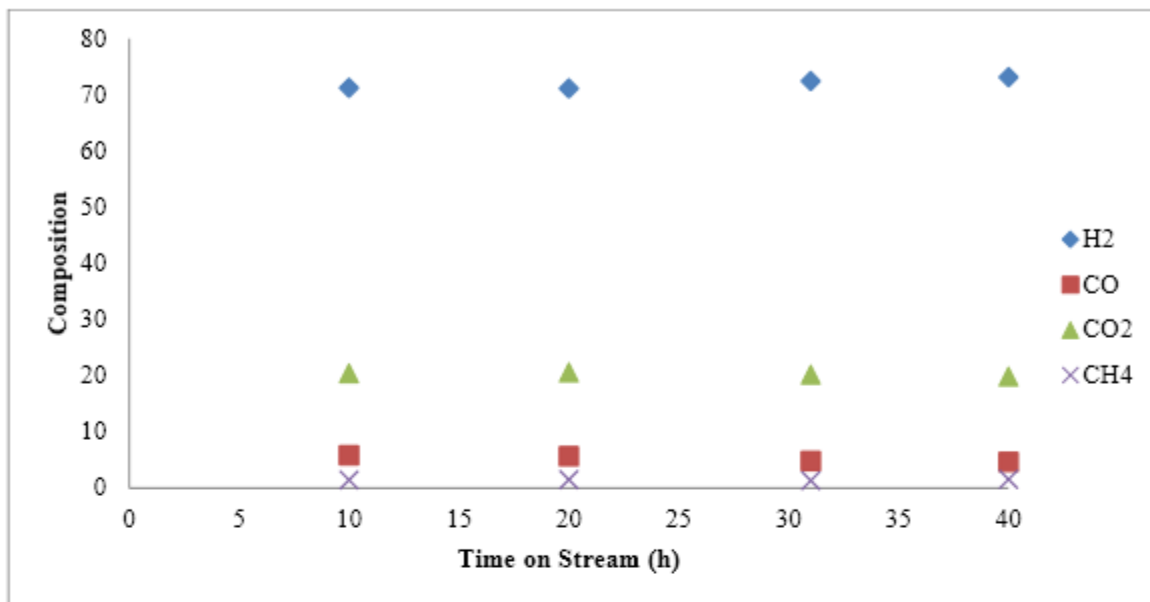


Figure A- 11: Gas product composition variation for steam reforming of diesel on 5%Eu-12%Ni/ γ -Al₂O₃ catalyst for 40 hours; at 620 °C, 1 atm, S/C = 3.0, GHSV of 5800 h⁻¹ and sulfur in fuel = 6 ppm

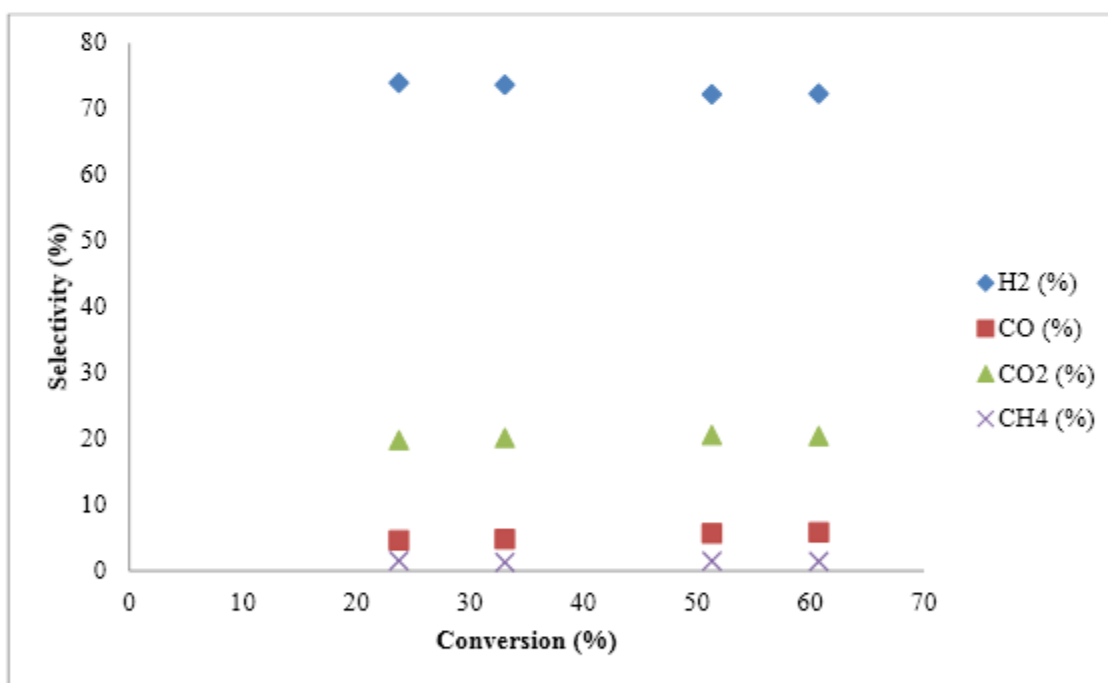


Figure A- 12: Selectivity of diesel Steam reforming products against the Diesel conversion on 5%Eu-12%Ni/ γ -Al₂O₃ catalyst for 40 hours; at 620 °C, 1 atm, S/C = 3.0, GHSV of 5800 h⁻¹ and sulfur in fuel = 6 ppm

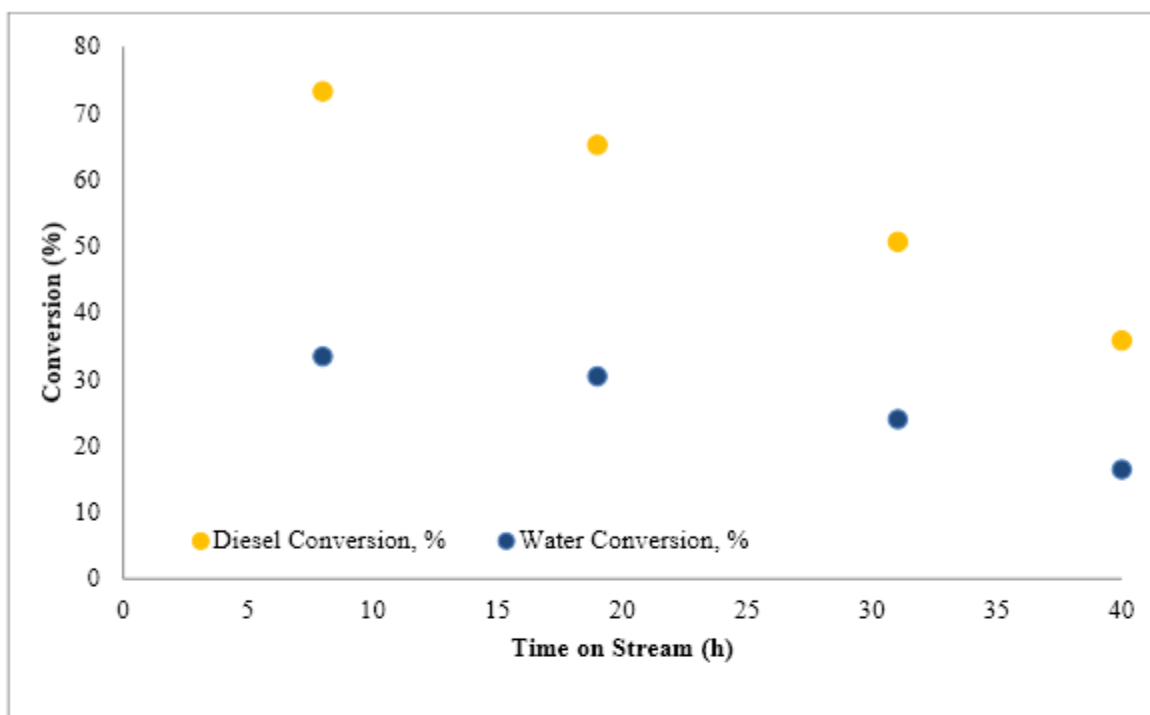


Figure A- 13: Diesel Steam reforming on 5%Pr-12%Ni/ γ -Al₂O₃ catalyst for 40 hours; at 620 °C, 1 atm, S/C = 3.0, GHSV of 5800 h⁻¹ and sulfur in fuel = 6 ppm

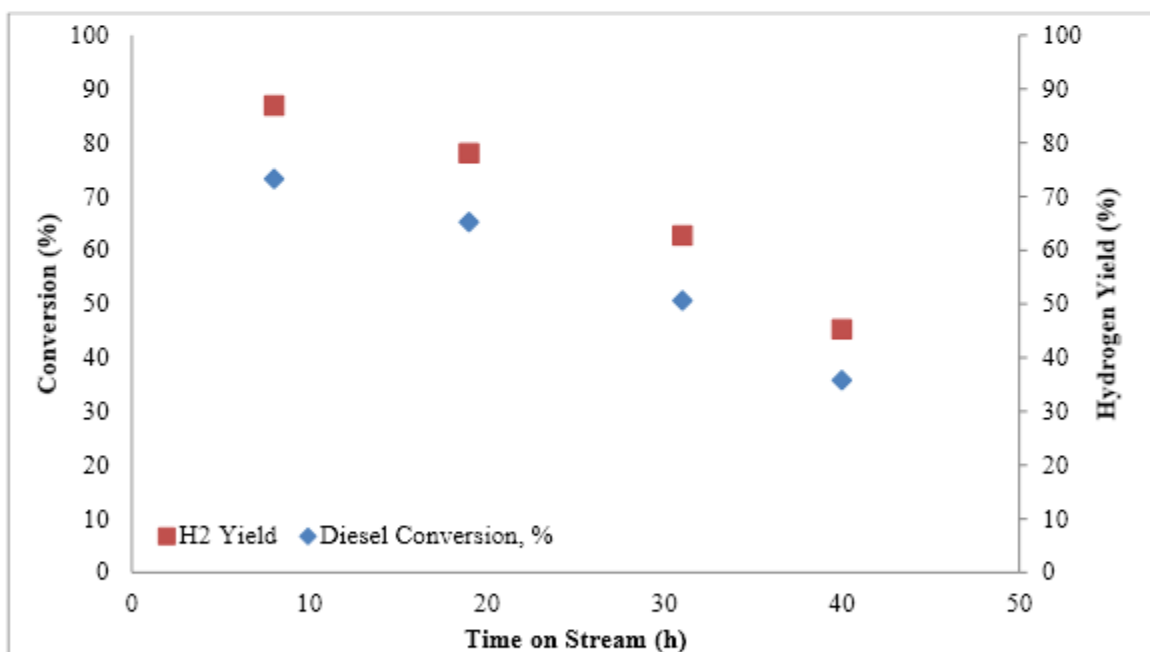


Figure A- 14: Effect of time on diesel conversion and hydrogen yield for steam reforming on 5%Pr-12%Ni/ γ -Al₂O₃ catalyst for 40 hours; at 620 °C, 1 atm, S/C = 3.0, GHSV of 5800 h⁻¹ and sulfur in fuel = 6 ppm.

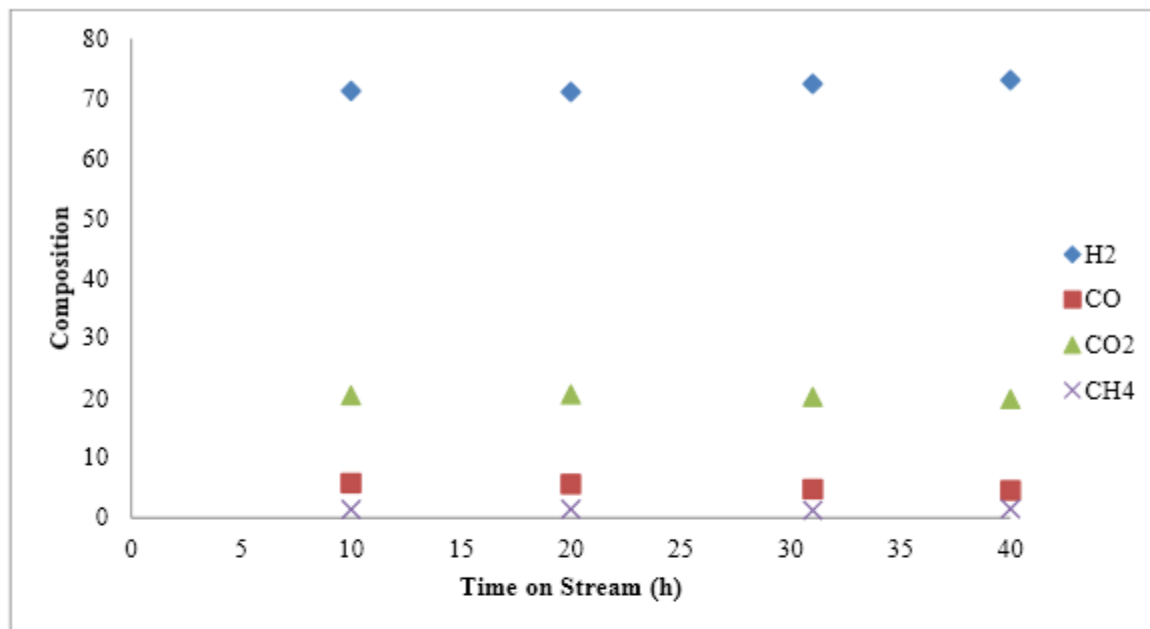


Figure A- 15: Gas product composition variation for steam reforming of diesel on 5%Pr-12%Ni/ γ Al₂O₃ catalyst for 40 hours; at 620 °C, 1 atm, S/C = 3.0, GHSV of 5800 h⁻¹ and sulfur in fuel = 6 ppm

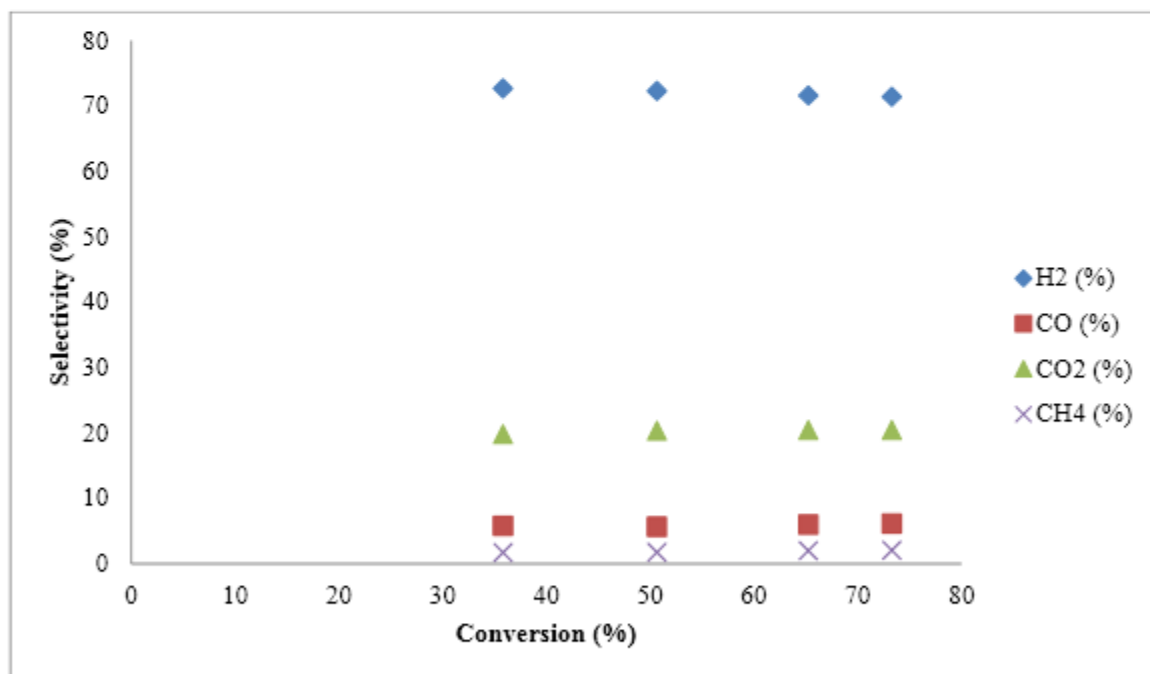


Figure A- 16: Selectivity of diesel Steam reforming products against the Diesel conversion on 5%Pr-12%Ni/ γ Al₂O₃ catalyst for 40 hours; at 620 °C, 1 atm, S/C = 3.0, GHSV of 5800 h⁻¹ and sulfur in fuel = 6 ppm

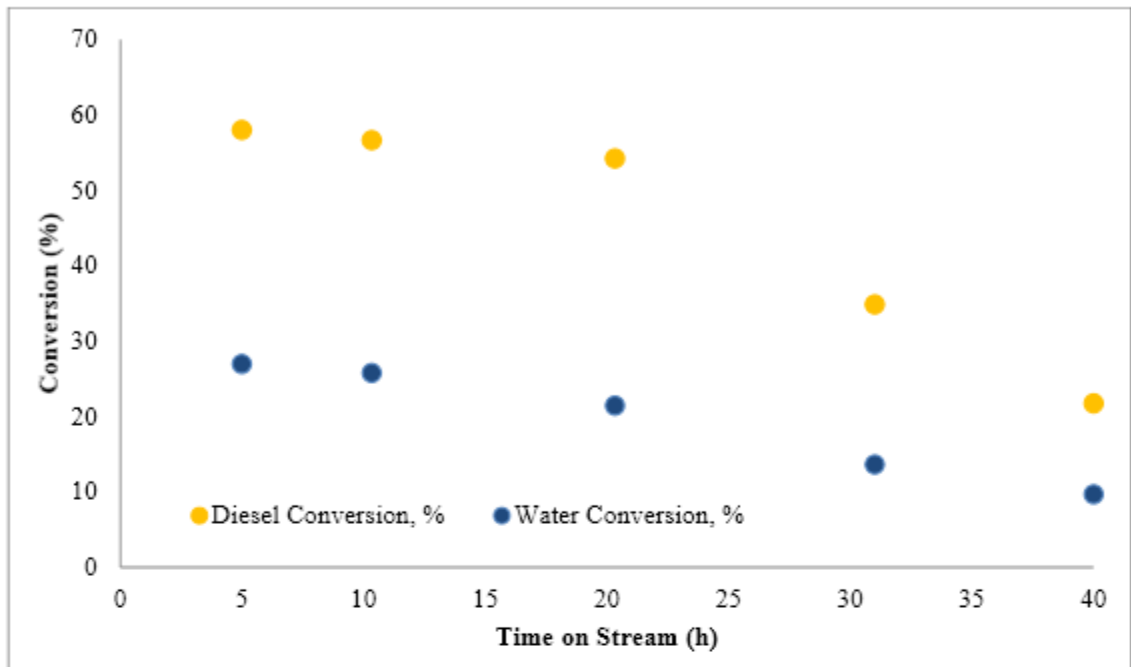


Figure 0-1

Figure A- 17: Diesel Steam reforming on 5%Gd-12%Ni/ γ Al₂O₃ catalyst for 40 hours; at 620 °C, 1 atm, S/C = 3.0, GHSV of 5800 h⁻¹ and sulfur in fuel = 6 ppm

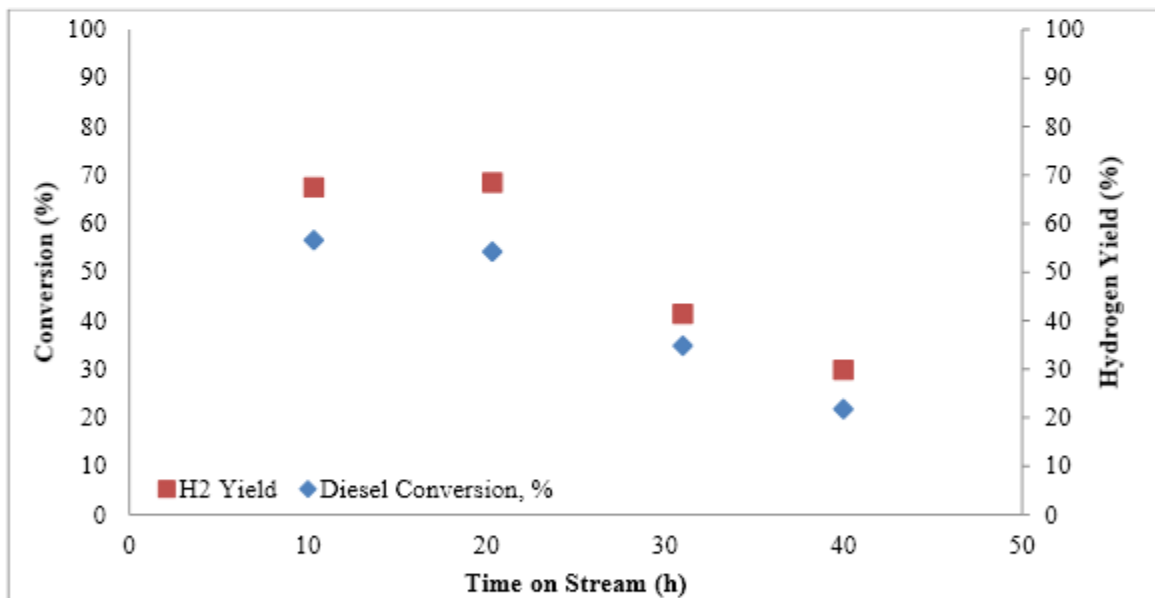


Figure A- 18: Effect of time on diesel conversion and hydrogen yield for steam reforming on 5%Gd-12%Ni/ γ Al₂O₃ catalyst for 40 hours; at 620 °C, 1 atm, S/C = 3.0, GHSV of 5800 h⁻¹ and sulfur in fuel = 6 ppm.

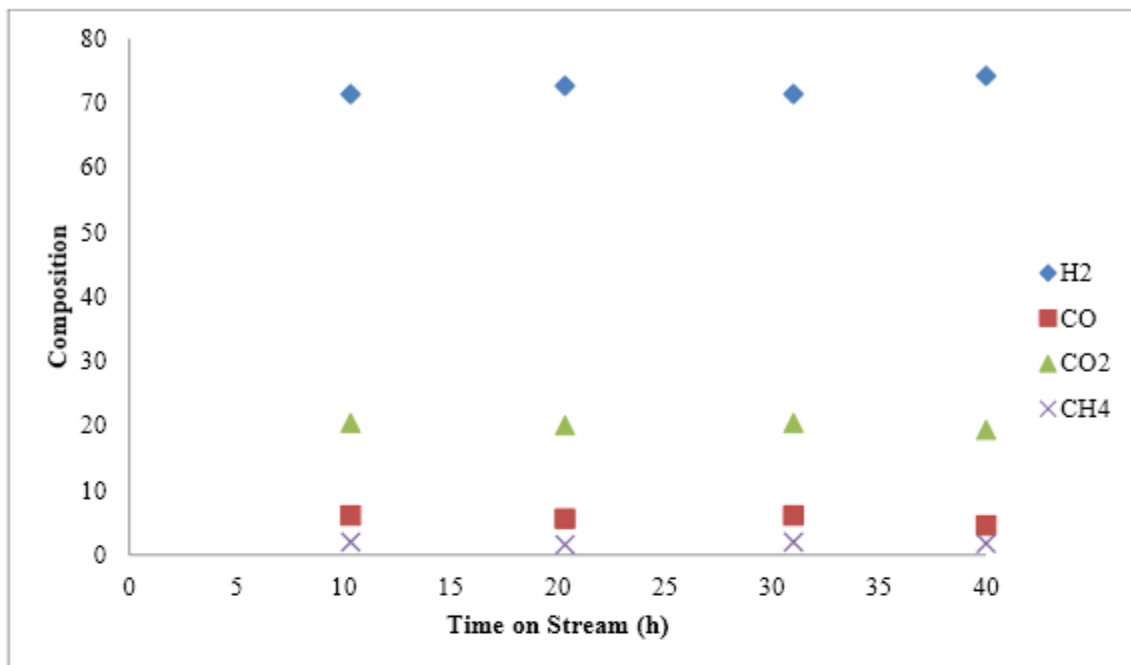


Figure A- 19: Gas product composition variation for steam reforming of diesel on 5%Gd-12%Ni/ γ Al₂O₃ catalyst for 40 hours; at 620 °C, 1 atm, S/C = 3.0, GHSV of 5800 h⁻¹ and sulfur in fuel = 6 ppm

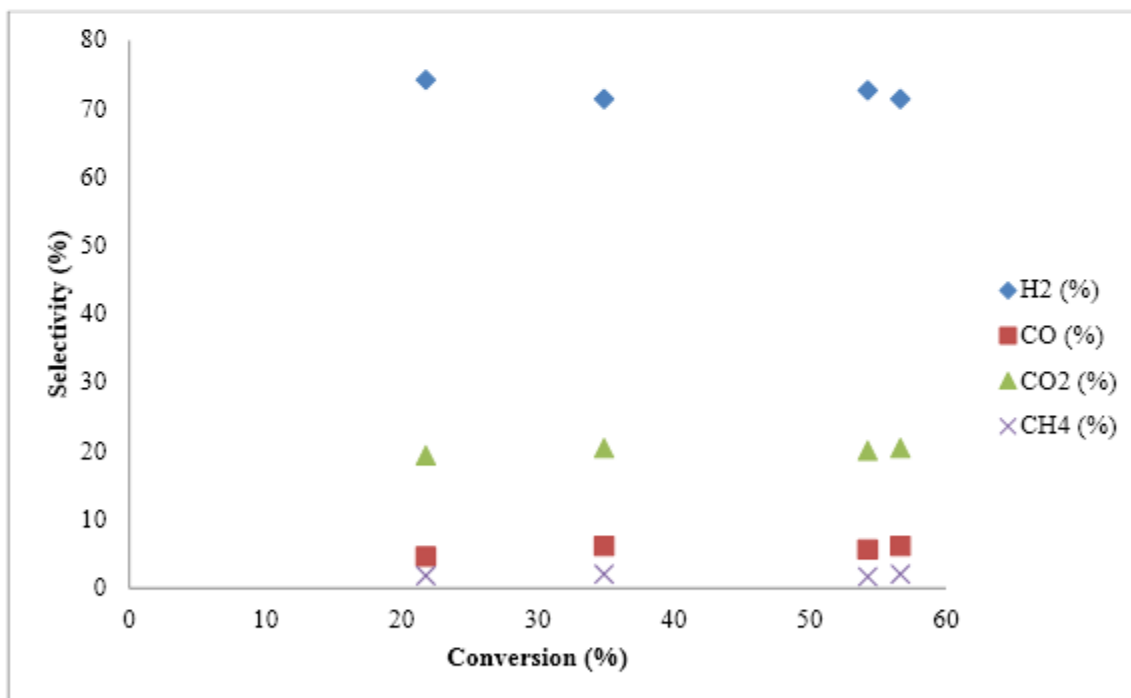


Figure A- 20: Selectivity of diesel Steam reforming products against the Diesel conversion on 5%Gd-12%Ni/ γ Al₂O₃ catalyst for 40 hours; at 620 °C, 1 atm, S/C = 3.0, GHSV of 5800 h⁻¹ and sulfur in fuel = 6 ppm

Appendix B

SUPPLEMENTARY CHARACTERIZATION

RESULTS

SEM Results:

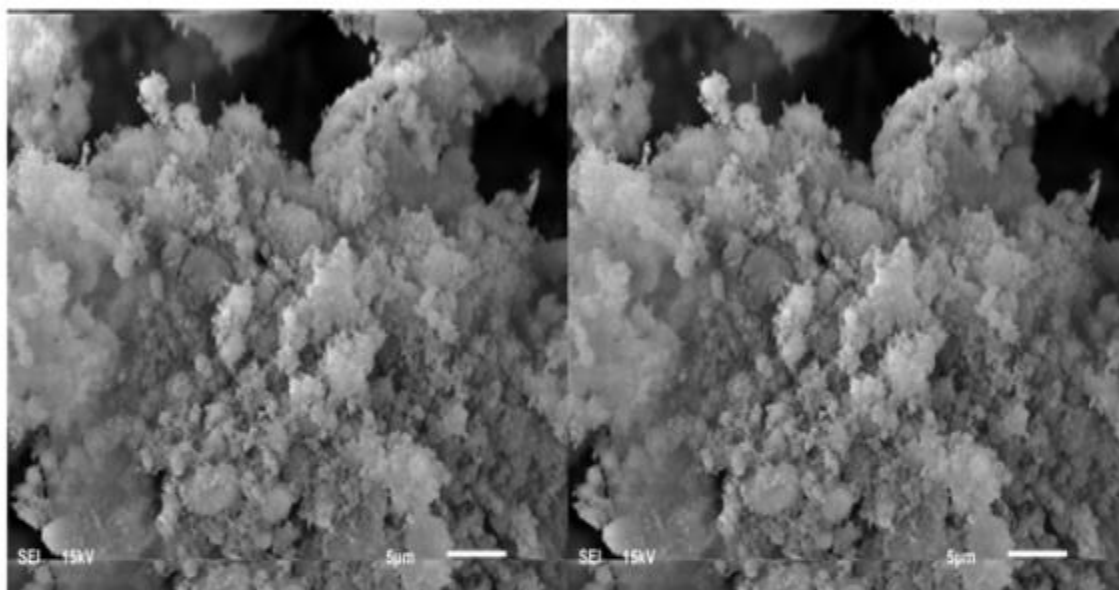


Figure B- 1: The SEM image of 12%Ni/Al₂O₃ catalyst

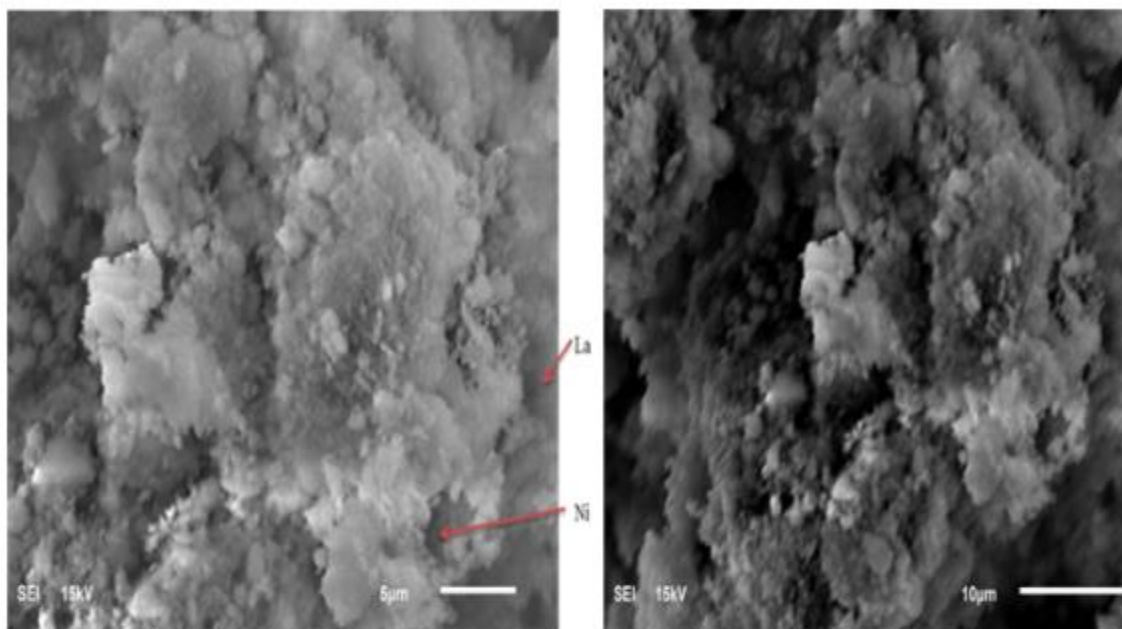


Figure B- 2: The SEM image of 5%La-12%Ni/ γ -Al₂O₃

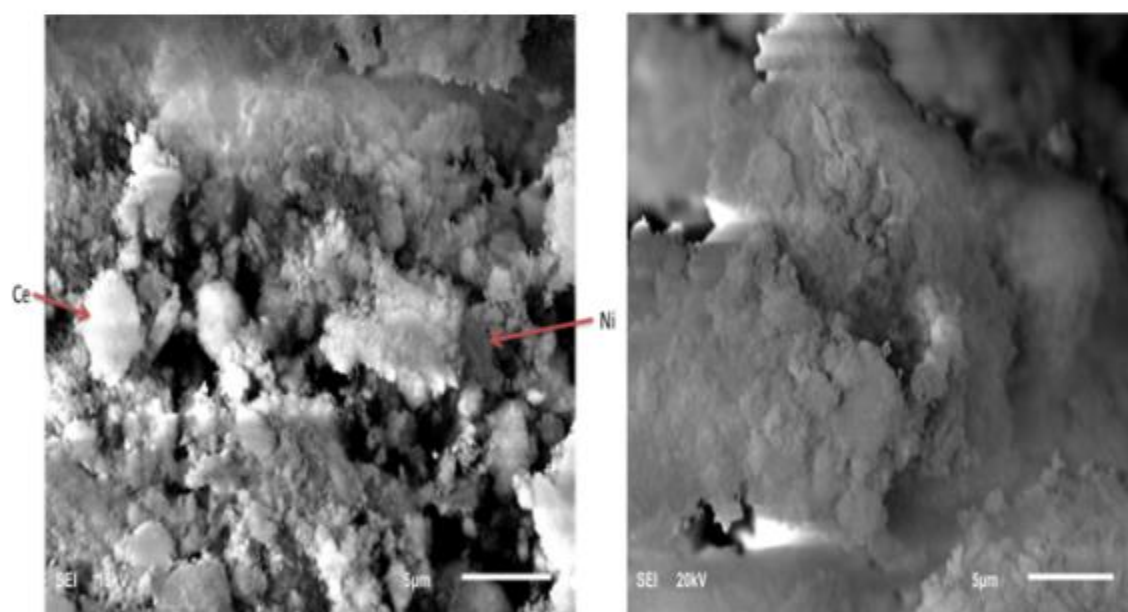


Figure B- 3: The SEM image of Ce-Ni catalyst.

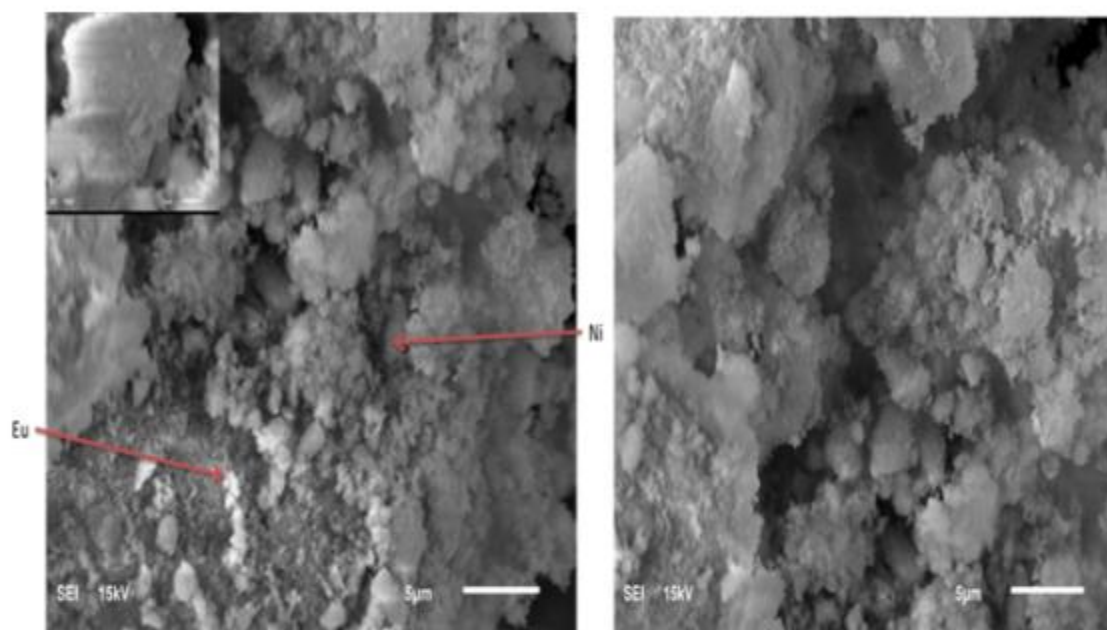


Figure B- 4: The SEM image of Eu-Ni catalyst .

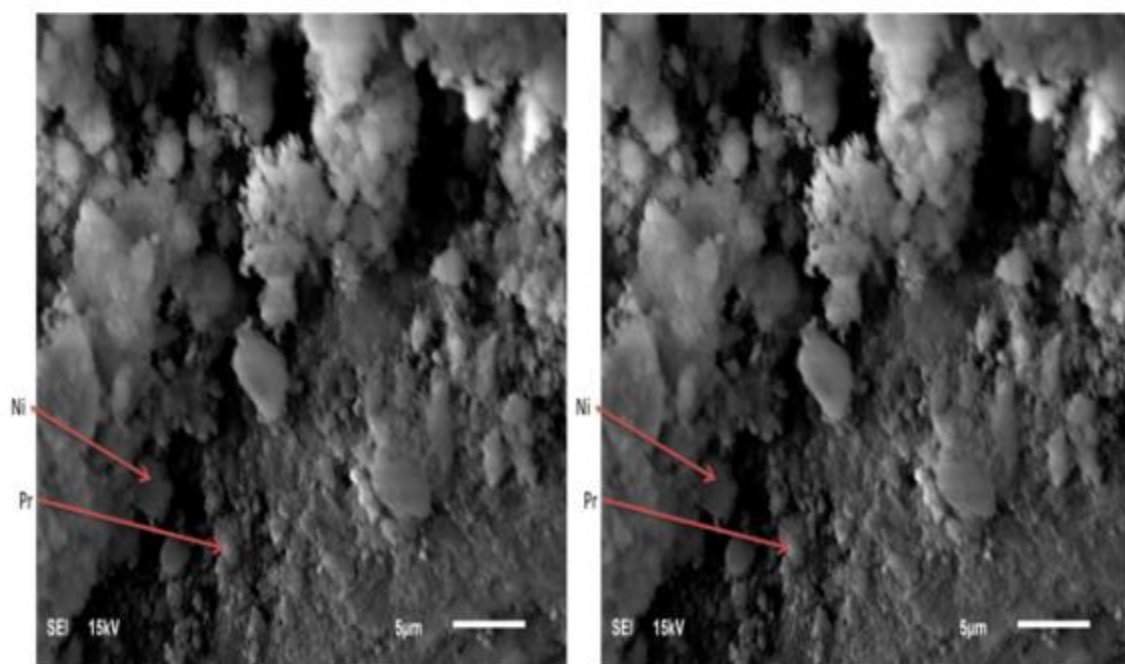


Figure B- 5: The SEM image of Ni-Pr catalyst.

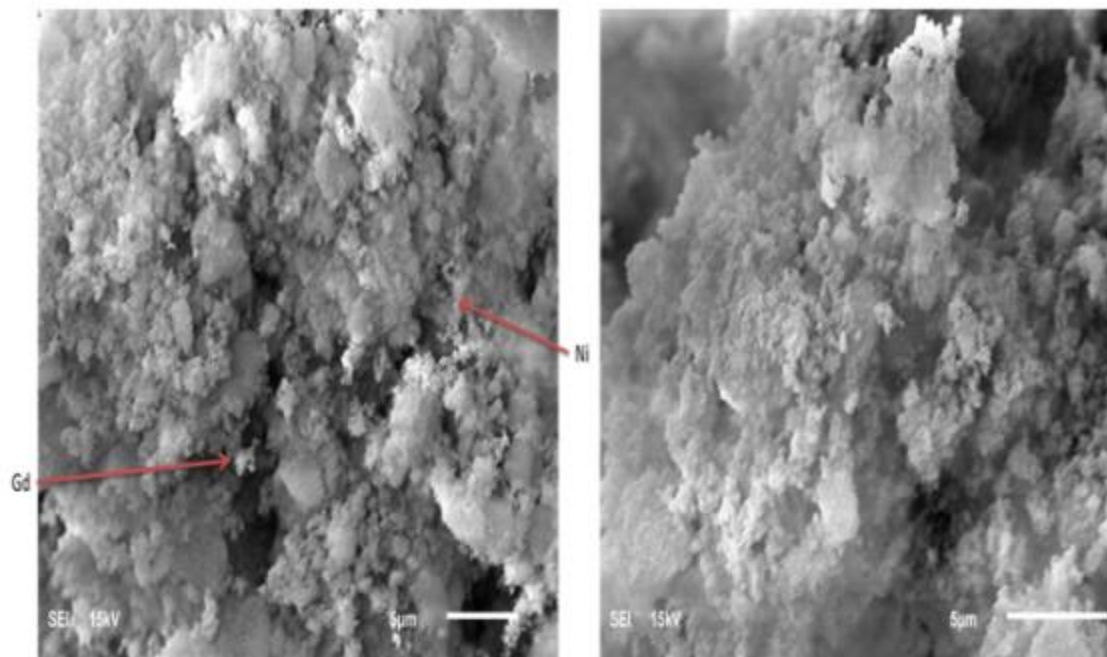


Figure B- 6: The SEM image of Gd-Ni catalyst.

Vitae

Name : Muhammad Naeem Younis

Nationality : Pakistani

Date of Birth : 4/18/1987

Email : mnaeem772@gmail.com

Address : 446-Neelam Block, Allama Iqbal Town, Lahore, Pakistan.

Academic Background : Chemical Engineering

List of publications :

- Article written and published on “Adsorption of organic chemicals on graphene coated biochars and its environmental implications” in “Green Processing and Synthesis”(October 2014)
- 247th ACS National Meeting & Exposition, which held on March 16-20, 2014, Dallas, Texas. Title of the paper presented “Ni:-based mixed metal oxide catalysts for oxidative dehydrogenation: reduction kinetics and catalytic activity”
http://abstracts.acs.org//chem/247nm/program/view.php?pub_num=207&par=CATL

- CHEMINDEX 2013, dated 4th Nov' 2013 held in Bahrain, title of the work presented (Oral): "Diesel Steam Reforming: Prospects, Challenges and Opportunities".
- Article written and published on "Production and Characterization of Biodiesel from Waste and Vegetable Oils" in "Journal of Quality and Technology Management" (June 2009).